AD

AD714981

REPORT NO. RR-TR-70-22

ANALYSIS OF A CYLINDRICAL LASER RESONATOR HAVING A ZONED OUTPUT MIRROR

by

George A. Emmons

September 1970

This document has been approved for public release and sale; its distribution is unlimited.

U.S. ARMY MISSILE COMMAND
Redstone Arsenal, Alabama

165

DISPOSITION INSTRUCTIONS

Destroy this report when it is no longer needed. Do not return it to the originator.

DISCLAIMER

The findings in this report are not to be construed as an official Department of the Army position unless so designated by other authorized documents.

TRADE NAMES

Use of trade names or manufacturers in this report does not constitute an official indorsement or approval of the use of such commercial hardware or software.

16 September 1970 Report No. RR-TR-70-22

ANALYSIS OF A CYLINDRICAL LASER RESONATOR HAVING A ZONED OUTPUT MIRROR

by

George A. Emmons

DA Project No. 1T262303A308

AMC Management Structure Code No. 522C.11.47300

Applied Physics Branch
Physical Sciences Laboratory
Research and Engineering Directorate
U.S. Army Missile Command
Redstone Arsenal, Alabama 35809

ABSTRACT

A theoretical analysis was performed on a zoned resonator to determine whether both resonator feedback and a focused output could be achieved with a single optical element. It was found that under certain conditions that well-defined modes do exist and that a focused output could be obtained.

This resonator was formed by two parallel mirrors (circular, plane, and equal sized) symmetrically placed about a common axis. One mirror had a uniform reflectivity of unity. The other mirror was zoned. It consisted of alternately transmitting and totally reflecting concentric zones. The reflecting zones provided the resonator feedback and the transmitting zones provided the output coupling. The transmission zones were arranged in a manner similar to the transmission zones on a Freznel zone plate. Thus, the zoned mirror tended to focus the field coupled out of the resonator.

For a zoned resonator in which the output mirror consisted of alternately totally reflecting and totally transmitting zones of equal area the following results were obtained:

1) When the focal length of the zoned mirror was less than the resonator length, stable resonator modes were obtained and sharp focusing of the output was achieved.

2) When the focal length was approximately equal to the resonator length, stable resonator modes were not obtained.

3) When the focal length was greater than the resonator length, stable modes were obtained but sharp focusing of the output could not be achieved.

Based on these findings it was concluded that a focused output was possible but that focusing at large distances was not feasible.

The mode structures of zoned resonators were more irregular than the corresponding mode structures of unzoned resonators. It was found that the mode structures could be made more regular by increasing the reflectivity of the transmission zones and/or decreasing the area of these zones. The irregularity of these fields was more pronounced for resonators having large Fresnel numbers than for those having small Fresnel numbers.

For resonators having small Fresnel numbers, the maximum focused intensity was achieved when the reflectivity of the transmitting zones was zero and the transmitting and reflecting zones were equal

in area. However, maximum focused intensity per unit output power was achieved when the area of the transmitting zones was reduced and the area of the reflection zones correspondingly increased. The optimum transmission area was about 74 percent of the area of the half-period zones. Because their field structures are strongly dependent on the characteristics of the zoned mirror, the optimum values of reflectivity and area for resonators having large Fresnel numbers are almost impossible to predict. However, optimum values do exist, and for a given configuration they could be found.

Some of the zoned resonators analyzed had focused intensities several times greater than the maximum intensity of the resonator field. However, the power passing through the main lobe in the focal plane was only about 20 percent of the total output power.

ACKNOWLEDGMENTS

I wish to express my sincere appreciation to Dr. William E. Webb and Dr. George J. Dezenberg for their comments and helpful criticisms and Mr. Billy Gibbs for his assistance in computer programming.

This work was sponsored by the U.S. Army Missile Command, Redstone Arsenal, Alabama.

CONTENTS

LIST OF ILLUSTRATIONS

LIST OF ILLUSTRATIONS (Continued)

LIST OF ILLUSTRATIONS (Continued)

LIST OF ILLUSTRATIONS (Continued)

LIST OF ILLUSTRATIONS (Continued)

LIST OF ILLUSTRATIONS (Concluded)

LIST OF TABLES

CHAPTER I

INTRODUCTION

A theoretical analysis was performed on a zoned resonator to determine whether both resonator feedback and a focused output could be achieved with a single optical element. It was found that under certain conditions that well-defined modes do exist and that a focused output could be achieved.

The zoned resonator was formed by two parallel mirrors symmetrically placed about a common axis. These mirrors were circular, plane, and equal sized. One mirror had a uniform reflectivity of unity. The other mirror was a zoned mirror; it consisted of alternately totally reflecting and transmitting concentric zones. The reflecting zones provided the resonator feedback and the transmitting zones provided the output coupling. The transmission zones were arranged in a manner similar to the transmission zones on a Fresnel zone plate.[1] This zoned mirror tended to focus the portion of the field coupled out of the resonator.

A mode of this resonator is a field configuration which satisfies Maxwell's equations and the boundary conditions at the mirrors. However,

---

[1]Jenkins, Francis A., and Harvey E. White, Fundamentals of Optics, McGraw-Hill Book Company, Inc., p. 360 (1957).

because of the lack of boundary conditions on the walls of the resonator, approximations are required in order to obtain the modes of the resonator. One of the most successful approximate methods of obtaining resonator modes is based on scalar diffraction theory.[2-7]

This theory utilizes a scalar formulation of Huygen's principle to relate the field on each mirror in terms of the field on the other mirror. Solutions obtained represent resonator modes. These modes are field configurations such that, except for a change in magnitude and phase, they are reproduced after a double pass through the resonator. With each double pass the resonator modes decrease in amplitude. This decrease in amplitude results from transmission losses through the mirrors and diffraction losses through the open side

---

[2]Fox, A. G., and Tingye Li, "Resonant Modes in a Maser Interferometer" Bell System Technical Journal, Volume 40, pp. 453-488 (1961).

[3]Boyd, G. D., and J. P. Gordon, "Confocal Multimode Resonator for Millimeter Through Optical Wavelength Masers" Bell System Technical Journal, Volume 40, pp. 389-508 (1961).

[4]Boyd, G. D., and H. Kogelnik, "Generalized Confocal Resonator Theory" Bell System Technical Journal, Volume 41, pp. 1347-1369 (1962).

[5]Fox, A. G., and Tingye Li, "Modes in a Maser Interfoermeter with Curved and Tilted Mirrors" Proceedings of the IEEE, Volume 51, pp. 80-89 (1963).

[6]Li, Tingye, "Diffraction Loss and Selection of Modes in Maser Resonators with Circular Mirrors" Bell System Technical Journal, Volume 44, pp. 917-932 (1965).

[7]Fox, A. Gardner, and Tingye Li, "Computation of Optical Resonator Modes by the Method of Resonance Excitation" IEEE Journal of Quantum Electronics, Volume QE-4, pp. 460-465 (1968).

walls. In an active laser resonator these losses would be compensated for by stimulated emission and steady-state oscillations could then occur.

The usual form of the scalar diffraction theory for resonators assumes a constant resonator gain. It does not account for either saturable gain or nonuniform gain distributions. However, Statz and Tang[8] and Fox and Li[9] modified the theory so that saturable gain could be considered. They found, that if the small signal gain were not too large, the resonator modes had essentially the same configuration as those obtained when uniform gain was assumed. Li and Skinner[10] considered a resonator having nonuniform gain. They also found that the resonator modes were very similar to those obtained for resonators having uniform gain.

It should also be mentioned that field configurations obtained from scalar diffraction theory have been compared to experimentally determined

---

[8]Statz, H., and C. L. Tang, "Problem of Mode Deformation in Optical Resonators" Journal of Applied Physics, Volume 36, pp. 1817-1819 (1965).

[9]Fox, A. G., and Tingye Li, "Effect of Gain Saturation on the Oscillating Modes of Optical Masers" IEEE Journal of Quantum Electronics, Volume QE-2, pp. 774-783 (1966).

[10]Li, Tingye, and J. G. Skinner, "Oscillating Modes in Ruby Lasers with Nonuniform Energy Distributions" Journal of Applied Physics, Volume 36, pp. 2595-2596 (1965).

modes. It was found that the theory quite accurately predicted the measured mode structure.[11,12]

Thus, because of its general applicability, the scalar theory of optical resonators was utilized in analyzing the zoned resonator, and since gain has little effect on the resonator mode structure, a uniform gain was assumed. Recently, this method of resonator mode analysis was used to obtain the modes of a confocal resonator having a single output coupling aperture,[13] and it has previously been used to obtain the modes of a Fabry-Perot resonator having coupling apertures in both mirrors.[14]

This paper is divided into five main chapters. In Chapter II the basic resonator equations are presented. Also in Chapter II the equations expressing the output fields of the resonator are derived. In Chapter III the characteristics of the zoned mirror are discussed. The focusing properties of the zoned mirror and the optimization of the focused output are considered in detail. In Chapter IV the numerical method used to solve the resonator equations is

---

[11]Kogelnik, H., and W. W. Rigrod, "Visual Display of Isolated Optical-Resonator Modes" Proceedings of the IRE, Volume 50, p. 220 (1962).

[12]Rosenberger, D., "Mode Spectrum in the He-Ne Maser" Quantum Electronics — Paris 1963 Conference, by P. Grivet and N. Bloembergen, Volume 2, Columbia University Press, pp. 1301-1304 (1964).

[13]McNice, Garner T., and Vernon E. Derr, "Analysis of the Cylindrical Confocal Laser Resonator Having a Single Circular Coupling Aperture" IEEE Journal of Quantum Electronics, Volume QE-5, pp. 569-575 (1969).

[14]Li, Tingye, and H. Zucker, "Modes of a Fabry-Perot Laser Resonator with Output Coupling Apertures" Journal of the Optical Society of America, Volume 57, pp. 984-986 (1967).

presented. It is basically a power method; this is the method referred to by Fox and Li[15] as the method of successive approximations. In Chapter V resonator mode control is discussed. In Chapter VI the results of the analysis of the zoned resonator are presented.

In Chapter VII characteristics of the zoned resonator are briefly summarized and conclusions presented.

---

[15]Fox, A. G., and Tingye Li, "Resonant Modes in a Maser Interferometer" Bell System Technical Journal, Volume 40, pp. 453-488 (1961).

CHAPTER II

INTEGRAL FORMULATION OF THE RESONATOR PROBLEM

This chapter is divided into three sections. In the first, the integral form of the resonator equations is presented. These equations express the field at a point on one mirror in terms of the integral of the field over the other mirror. Solutions to these equations represent resonator modes.

In the second section an expression for the output power from the resonator is developed. This expression is given in terms of the resonator fields and the characteristics of the output mirror.

In the last section an expression for the fields transmitted through the output mirror is determined. This expression is valid for the Fresnel region of the resonator.

A. Resonator Equations

A diagram showing the pertinent geometry of the self-focusing resonator is given in Figure 1. This resonator is formed by two circular plane mirrors symmetrically located about the resonator axis. The mirrors have equal radii, a_p, and they are separated a distance (d). One of the mirrors, designated the input mirror, has a uniform reflectivity; the other mirror, the zoned mirror, has a reflectivity that is a function of mirror radius. The polar

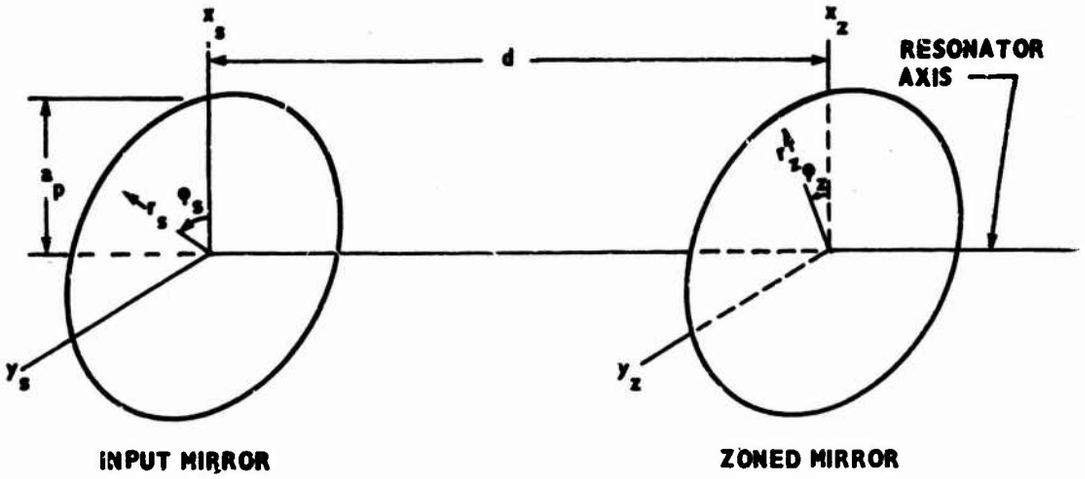

Figure 1. Resonator Geometry

coordinates $\left(r_s, \phi_s\right)$ and $\left(r_z, \phi_z\right)$ are used to describe positions on the input and the zoned mirrors respectively.

The modes of this resonator can be described by the integral equations first established by Fox and Li.[1] They used a scalar formulation of Huygens principle to relate the field on one mirror in terms of the integral of the field on the other mirror. Their equations are valid for resonators whose mirror dimensions are large compared to a wavelength and whose fields are essentially transverse electromagnetic and plane polarized in a single direction.

The fields on the resonator mirrors can be written in the forms given below.[2] On the input mirror the field is given by

---

[1]Fox, A. G., and Tingye Li, "Resonant Modes in a Maser Interferometer" Bell System Technical Journal, Volume 40, pp. 453-488 (1961).

[2]Li, Tingye, "Diffraction Loss and Selection of Modes in Maser Resonators with Circular Mirrors" Bell System Technical Journal, Volume 44, pp. 917-932 (1965).

$$E_{mn}\left(r_s, \phi_s\right) = R_{ns}\left(r_s\right)e^{-jm\phi_s} , \qquad \text{(II-1)}$$

and on the zoned mirror the field is given by

$$E_{mn}\left(r_z, \phi_z\right) = R_{nz}\left(r_z\right)e^{-jm\phi_z} . \qquad \text{(II-2)}$$

The terms (m) and (n) are nonnegative integers, $R_{ns}\left(r_s\right)$ and $R_{nz}\left(r_z\right)$ represent the radial variations of the fields, and $\exp\left(-jm\phi_s\right)$ and $\exp\left(-jm\phi_z\right)$ represent the azimuthal variations of the fields. The azimuthal field variations are sinusoidal and have a degeneracy of (m). For a given angular degeneracy, the radial variations of the fields are related to each other by the following integral equations:

$$R_{ns}\left(r_s\right) = \int_0^1 \rho_z NK_m\left(r_z, r_s\right)\bar{R}_{nz}\left(r_z\right)r_z dr_z \qquad \text{(II-3)}$$

and

$$R_{nz}\left(r_z\right) = \int_0^1 \rho_s NK_m\left(r_z, r_s\right)\bar{R}_{ns}\left(r_s\right)r_s dr_s . \qquad \text{(II-4)}$$

These equations are a normalized form of the usual resonator equations. They have been normalized with respect to the radii of the mirrors in such a way that the mirror apertures are equal to one. In this normalization the resonator Fresnel number was introduced. This Fresnel number is given by

$$N = \frac{a_p^2}{\lambda d} \qquad \text{(II-5)}$$

where λ is the wavelength of the fields within the resonator medium. Also included in these resonator equations are the terms ρ_z and ρ_s; they represent the amplitude reflectivity of the zoned mirror and the input mirror respectively. These reflectivities, expressed as a function of normalized mirror radius, allow one to introduce the selective reflection characteristics of the zoned mirror into the resonator equations. The term $K_m\left(r_z, r_s\right)$ is given by

$$K_m\left(r_z, r_s\right) = 2\pi (j)^{m+1} J_m\left(2\pi N r_z r_s\right) \exp\left[-j\pi N\left(r_z^2 + r_s^2\right)\right], \quad \text{(II-6)}$$

where (j) is the imaginary number $\sqrt{-1}$, (m) is the order of the angular degeneracy, and J_m is the Bessel function of the first kind and m^{th} order.

The bars over the fields, inside the integrals of equations (II-3) and (II-4), also represent a normalization. This normalization is expressed as

$$\bar{R}_{ns}\left(r_s\right) = \frac{R_{ns}\left(r_s\right)}{\gamma_{ns}} \quad \text{(II-7)}$$

and

$$\bar{R}_{nz}\left(r_z\right) = \frac{R_{nz}\left(r_z\right)}{\gamma_{nz}} . \quad \text{(II-8)}$$

The terms γ_{ns} and γ_{nz} represent the values of the fields on the input and zoned mirrors, respectively, where the magnitudes of the fields are maximum.

A resonator mode is a field distribution such that, after a double pass through the resonator, the field reproduces itself except for a change in amplitude and phase.[3] As an example, suppose that $\bar{R}_{ns}\left(r_s\right)$ is a resonator mode.

---

[3]Fox, A. G., and Tingye Li, op. cit.

By using equations (II-3), (II-4), (II-7), and (II-8), one can show that the field after a double pass through the resonator is given by $\left[\gamma_{ns}\gamma_{nz}\bar{R}_{ns}\left(r_s\right)\right]$. In mode terminology, Γ_n, as given by

$$\Gamma_n = \gamma_{ns}\gamma_{nz} \quad , \tag{II-9}$$

represents the eigenvalue of the eigenfunction $\bar{R}_{ns}\left(r_s\right)$. Separately, γ_{ns} and γ_{nz} do not have real significance; they are merely by-products of the analytical procedure. On the other hand, Γ_n has physical meaning. It represents the change in amplitude and phase of a resonator mode caused by a double pass in the resonator.

Each resonator is described by a particular field distribution, and each distribution has a distinct eigenvalue. Because of this uniqueness the double pass power loss of a resonator mode is also unique. This loss is given by the expression

$$L_{dp} = 1 - |\Gamma_n|^2 \quad , \tag{II-10}$$

and it includes both diffraction and transmission losses. As was stated above, the mirrors have amplitude reflectivities given by ρ_z and ρ_s; transmission losses are introduced by having mirror reflectivities with amplitudes less than unity.

It has been shown that the resonator modes are orthogonal over both mirrors.[4] This suggests that any arbitrary field distribution can be decomposed into orthogonal modes. This is a standard technique which often

---

[4]Fox, A. G., and Tingye Li, "Modes in a Maser Interferometer with Curved and Tilted Mirrors" Proceedings of the IEEE, Volume 51, pp. 80-89 (1963).

facilitates not only the mathematical treatment of the problem, but also offers some insight into the physical processes involved. Fourier analysis is an example where it is usual to think of the individual components as having physical meaning; action on the composite field can be thought of as a redistribution of the energy among the components.

The resonator modes are denoted by the usual symbology of TEM_{mn}. This represents a transverse electromagnetic field with an angular mode number of m and a radial mode number of n. An arbitrary field distribution, $\xi(r, \phi)$, can thus be written as the sum of all possible modes. For fields on the input mirror, the total field is given by

$$\xi\left(r_s, \phi_s\right) = \sum_{m=0}^{\infty} \sum_{n=0}^{\infty} A_{mn} \bar{R}_{ns}\left(r_s\right) \cos m\phi_s \quad , \tag{II-11}$$

where the constants A_{mn}, because of the orthogonality of the modes over the surface of the mirror, are given by

$$A_{mn} = \left[\frac{\int_0^{2\pi} \int_0^1 \bar{R}_{ns}\left(r_s\right) \cos m\phi_s \, \xi\left(r_s, \phi_s\right) r_s \, dr_s \, d\phi_s}{\pi \int_0^1 \bar{R}_{ns}\left(r_s\right) \bar{R}_{ns}\left(r_s\right) r_s \, dr_s} \right] . \tag{II-12}$$

B. Output Power

The output power of the self-focusing resonator is due to a portion of the resonator field being transmitted through the zoned mirror. Consider the situation where the resonator is operating with a TEM_{mn} field distribution. The normalized field incident on the zoned mirror can be written as

$$\bar{E}_{mn}\left(r_z, \phi_z\right) = \bar{R}_{nz}\left(r_z\right) \cos m\phi_z \quad . \tag{II-13}$$

The transmitted field is given by the product of this equation and the amplitude transmission coefficient of the zoned mirror. If absorption is neglected, this transmission coefficient is related to the reflection coefficient by

$$\tau_z = \left(1 - \rho_z^2\right)^{1/2} \quad . \tag{II-14}$$

The total power transmitted through the zoned mirror is proportional to the square of the absolute value of the transmitted field integrated over the zoned mirror. Defining P_T to be this output power, one can write

$$P_T = C_T \int_0^{2\pi} \int_0^{1} |\tau_z \bar{E}_{mn}\left(r_z, \phi_z\right)|^2 r_z \, dr_z \, d\phi_z \quad , \tag{II-15}$$

where C_T is the proportionality constant. By using equations (II-13) and (II-14) in equation (II-15) and separating the variables, the output power can be written as

$$P_T = C_T \int_0^{1} \left(1 - \rho_z^2\right) |\bar{R}_{nz}\left(r_z\right)|^2 r_z \, dr_z \int_0^{2\pi} \cos^2 m\phi_z \, d\phi_z \quad . \tag{II-16}$$

The second integral has the value of (2π) for an angular degeneracy of zero, and it has the value of (π) for higher-order angular degeneracies. Therefore, for an angular degeneracy of zero the output power is given by

$$P_T(m = 0) = 2\pi C_T \int_0^{1} \left(1 - \rho_z^2\right) |\bar{R}_{nz}\left(r_z\right)|^2 r_z \, dr_z \quad , \tag{II-17}$$

and for all other angular degeneracies the output power is given by

$$P_T(m \neq 0) = \pi C_T \int_0^{1} \left(1 - \rho_z^2\right) |\bar{R}_{nz}\left(r_z\right)|^2 r_z \, dr_z \quad . \tag{II-18}$$

The output power, as given in equations (II-17) and (II-18), is based on a maximum field amplitude of unity inside the resonator. This measure of output power is a convenient term for comparing some resonator characteristics.

C. External Fields

The Fresnel region outside the resonator is of particular importance as it is there that the focused output is established. The geometry of this region is shown in Figure 2. The field of interest is located in a plane perpendicular to the resonator axis and located F distance from the output mirror; this plane is designated the F-plane, and the polar coordinates of a point in this plane are denoted by $\left(r_f, \phi_f\right)$.

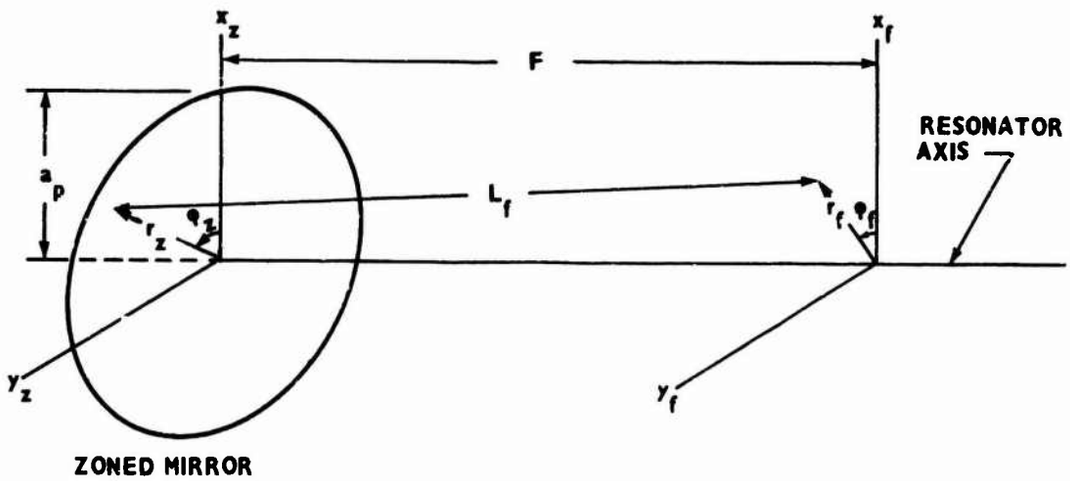

Figure 2. Geometry of Fresnel Region Outside Resonator

The source field is that portion of the resonator field transmitted through the output mirror; thus, by using a cosine dependence for the angular variation of the resonator field, the source field is given by

$\left[\tau_z \bar{R}_{nz}\left(r_z\right) \cos m\phi_z\right]$. The field in the F-plane, $E_f\left(r_f, \phi_f\right)$, resulting from this source field can be expressed as[5]

$$E_f\left(r_f, \phi_f\right) = \frac{j}{2\lambda} \int_0^{2\pi} \int_0^{a_p} \tau_z \bar{R}_{nz}\left(r_z\right) \cos m\phi_z \frac{e^{-jkL_f}}{L_f} (1 + \cos\theta) \cdot r_z dr_z d\phi_z \ , \qquad \text{(II-19)}$$

where k is the wave number, $(2\pi/\lambda)$, and where θ is the angle between the surface normal of the source and the line segment between $\left(r_z, \phi_z\right)$ and $\left(r_f, \phi_f\right)$. The cases of interest occur where both r_z and r_f are much smaller than F. In this region θ is small; therefore, if the term $(\cos\theta)$ is set equal to one, equation (II-19) can be written as

$$E_f\left(r_f, \phi_f\right) = \frac{j}{\lambda} \int_0^{2\pi} \int_0^{a_p} \tau_z \bar{R}_{nz}\left(r_z\right) \cos m\phi_z \frac{e^{-jkL_f}}{L_f} r_z dr_z d\phi_z \ . \qquad \text{(II-20)}$$

In this region of validity of this equation, that is, where θ is small, the usual Fresnel approximations concerning L_f can also be made. The term representing the change in amplitude as a function of distance is approximated by

$$\frac{1}{L_f} \approx \frac{1}{F} \ , \qquad \text{(II-21)}$$

and in the phase term L_f is approximated by

$$L_f \approx \left[F + \frac{r_z^2 + r_f^2 - 2r_z r_f \cos\left(\phi_z - \phi_f\right)}{2F}\right] \ . \qquad \text{(II-22)}$$

By using equations (II-21) and (II-22) in equation (II-20) and expanding the cosine term, the following form for the Fresnel field can be obtained:

---

[5]Silver, Samuel, Microwave Antenna Theory and Design, McGraw-Hill Book Company, Inc., New York, p. 167 (1949).

$$E_f\left(r_f, \phi_f\right) = \left(\frac{j2\pi e^{-jkF}}{\lambda F}\right) \int_0^{a_p} \tau_z \bar{R}_{nz}\left(r_z\right) \exp\left[-jk\left(\frac{r_z^2 + r_f^2}{2F}\right)\right]$$

$$\cdot \left(\frac{1}{2}\right)\left\{\frac{1}{2\pi}\int_0^{2\pi} \exp\left\{j\left[\frac{kr_z r_f}{F}\cos\left(\phi_f - \phi_z\right) + m\phi_z\right]\right\} d\phi_z\right.$$

$$\left. + \frac{1}{2\pi}\int_0^{2\pi} \exp\left\{j\left[\frac{kr_z r_f}{F}\cos\left(\phi_z - \phi_f\right) - m\phi_z\right]\right\} d\phi_z\right\} r_z dr_z \,. \quad \text{(II-23)}$$

By making use of the relations[6]

$$\exp\left[jm\left(\frac{\pi}{2} + \beta\right)\right] J_m(xy) = \frac{1}{2\pi}\int_0^{2\pi} \exp\left\{j[xy\cos\left(\beta - \beta'\right) + m\beta']\right\} d\beta' \quad \text{(II-24)}$$

and

$$\exp\left[jm\left(\frac{\pi}{2} - \beta\right)\right] J_m(xy) = \frac{1}{2\pi}\int_0^{2\pi} \exp\left\{j[xy\cos\left(\beta' - \beta\right) - m\beta']\right\} d\beta' \,, \quad \text{(II-25)}$$

equation (II-23) can be reduced to

$$E_f\left(r_f, \phi_f\right) = \cos m\phi_f \left[\frac{(j)^{m+1} 2\pi e^{-jkF}}{\lambda F}\right] \int_0^{a_p} \tau_z \bar{R}_{nz}\left(r_z\right)$$

$$\cdot \exp\left[-j\pi\left(\frac{r_z^2 + r_f^2}{\lambda F}\right)\right] J_m\left(\frac{2\pi r_z r_f}{\lambda F}\right) r_z dr_z \,. \quad \text{(II-26)}$$

As expected, the angular variation of the field is preserved, and $E_f\left(r_f, \phi_f\right)$ can be separated as

---

[6]Stratton, J. A., Electromagnetic Theory, McGraw-Hill Book Company, Inc., New York, p. 373 (1941).

$$E_f\left(r_f, \phi_f\right) = R_{nf}\left(r_f\right)\cos m\phi_f \ . \qquad \text{(II-27)}$$

Thus, by neglecting the geometrical phase term, the radial variation of the field in the F-plane can be written as

$$R_{nf}\left(r_f\right) = \left[\frac{(j)^{m+1}2\pi}{\lambda F}\right]\int_0^{a_p} \tau_z \bar{R}_{nz}\left(r_z\right) \cdot \exp\left[-j\pi\left(\frac{r_z^2 + r_f^2}{\lambda F}\right)\right] J_m\left(\frac{2\pi r_z r_f}{\lambda F}\right) r_z dr_z \ . \qquad \text{(II-28)}$$

To facilitate numerical computations the radial distances can be normalized to unit output mirror radius by replacing r_z by $a_p r_z$ and r_f by $a_p r_f$. Then equation (II-28) can be written as

$$R_{nf}\left(r_f\right) = \int_0^1 \tau_z M_p K_{mf}\left(r_z, r_f\right)\bar{R}_{nz}\left(r_z\right) r_z dr_z \ , \qquad \text{(II-29)}$$

where

$$M_p = \frac{a_p^2}{\lambda F} \qquad \text{(II-30)}$$

and

$$K_{mf}\left(r_z, r_f\right) = 2\pi(j)^{m+1} J_m\left(2\pi M_p r_z r_f\right) \exp\left[-j\pi M_p\left(r_z^2 + r_f^2\right)\right] . \qquad \text{(II-31)}$$

It must be remembered in using equation (II-29) that the radial distance is normalized to a_p; for example, if $r_f = 2$, the actual distance is $\left(2a_p\right)$.

The transmitted field along the resonator axis can be obtained from equation (II-29) by setting r_f equal to zero. For the case where m is zero this axial field can be written as

$$E_f\left(0, \phi_f\right) = 2\pi j \int_0^1 \tau_z M_p \exp\left[-j\pi M_p r_z^2\right] \bar{R}_{nz}\left(r_z\right) r_z dr_z \quad . \quad \text{(II-32)}$$

For cases where m is not equal to zero the axial field is zero.

CHAPTER III

CHARACTERISTICS OF THE ZONED MIRROR

The focused output from the self-focusing resonator is established by the selective transmission characteristics of the output mirror. This mirror is divided into alternately reflecting and transmitting zones. The reflecting zones provide resonator feedback and the transmitting zones provide output coupling. All of these zones are concentric and are symmetrically located about the resonator axis.

In this chapter the characteristics of this zoned mirror and its effects on the focusing properties of the self-focusing laser resonator are considered in detail. The first section of this chapter is used to describe the method in which the output mirror is divided into half-period zones. Following this, the basic focusing properties of the zoned mirror are established by considering the condition of uniform illumination of the mirror.

The field structure of a laser resonator is more accurately described by a Gaussian distribution than a uniform distribution. Because of this, a section of this chapter considers the focusing achievable with Gaussian illumination of the zoned mirror.

In the last section, the optimization of the zoned mirror is considered from the viewpoint of maximizing the intensity at the focal point per unit

output power. It was found that by decreasing the areas of the transmission zones, and correspondingly increasing the areas of the reflection zones, optimum conditions existed. Also discussed in this last section are some details concerning the maximum number of zones that can be placed on a mirror and the maximum focal distance.

A. Half-Period Zones

Suppose that the output mirror represents a constant phase surface for an incident wave. At the point F on the resonator axis, F distance from the output mirror, the wave can be viewed as consisting of circular, concentric half-period zones. These zones are determined by the criterion that the radius separating the i^{th} and the $(i + 1)^{th}$ zones, where $i = 1, 2, 3, \ldots$, is such that the distance from the outer edge of the i^{th} zone to F is greater than F by $(i\lambda/2)$. For the usual resonator configuration such that

$$a_p \gg \lambda$$

and a distance F such that

$$F \gg a_p ,$$

the path difference is given approximately by

$$\Delta = \frac{r_z^2}{2F} .$$

The geometry depicting this path difference is shown in Figure 3. The radius r_{zi}, corresponding to a path difference of $(i\lambda/2)$, is therefore given by

$$r_{zi} = (i\lambda F)^{1/2} .$$

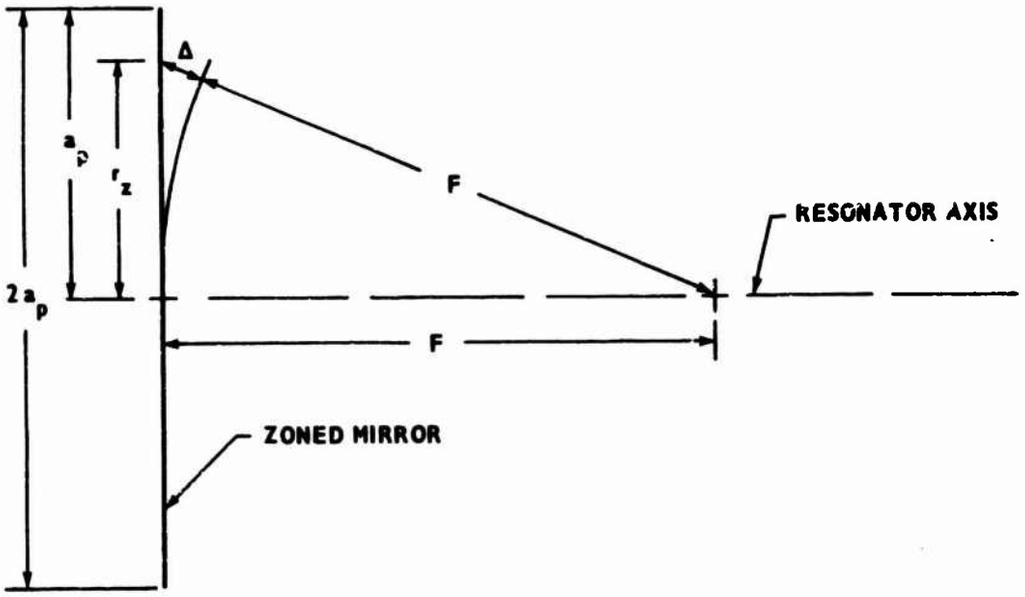

Figure 3. Path Difference Δ for Radius of r_z

In calculations the normalized radius, obtained by dividing the radius by the radius of the output mirror, is generally used. This normalized radius is given by

$$r_{zi} = \left(\frac{i\lambda F}{a_p^2}\right)^{1/2} . \qquad \text{(III-1)}$$

From the point F on the resonator axis, the incident field presents a phase difference of π across each half-period zone. This means, of course, that at F the fields resulting from adjacent zones tend to subtract and the fields resulting from alternate zones tend to add. This effect is utilized in obtaining a focused output from the laser resonator. Output focusing will be clearly illustrated in the following sections.

B. Uniform Illumination of the Zoned Mirror

In Chapter II, equation (II-32), it was shown that the field at F could be written as

$$E_f\left(0, \phi_f\right) = 2\pi j \int_0^1 \tau_z M_p \exp\left(-j\pi M_p r_z^2\right) \bar{R}_{nz}\left(r_z\right) r_z dr_z \quad . \qquad \text{(III-2)}$$

The amplitude transmission coefficient is symmetric about the resonator, but in general it can vary radially. However, the first case considered is that where τ_z is a constant function of mirror radius. For uniform illumination of the zoned mirror the illuminating function, $\bar{R}_{nz}\left(r_z\right)$, is constant; therefore, by setting the illuminating function equal to one, equation (III-2) becomes

$$E_f\left(0, \phi_f\right) = 2\pi j M_p \tau_z \int_0^1 \exp\left(-j\pi M_p r_z^2\right) r_z dr_z \quad . \qquad \text{(III-3)}$$

This integral can be written as the sum of the integrals across the half-period zones; that is,

$$E_f\left(0, \phi_f\right) = 2\pi j M_p \tau_z \left[\int_0^{r_{z1}} + \int_{r_{z1}}^{r_{z2}} + \ldots + \int_{r_{z\eta}}^{1} \right], \qquad \text{(III-4)}$$

where the r_{zi} are given by equation (III-1) and η is the greatest positive integer i that satisfies the relation

$$r_{zi} \leq 1 \quad .$$

The change in variable from r_z to x will now be made, where r_z and x are related by

$$x = M_p r_z^2 \qquad \text{(III-5)}$$

and

$$M_p = \frac{a_p^2}{\lambda F} \quad . \tag{III-6}$$

The x_i corresponding to the r_{zi} given by equation (III-1) are therefore given by

$$x_i = i \quad . \tag{III-7}$$

Thus, equation (III-4) can be written as

$$E_f\left(0, \phi_f\right) = \pi j \tau_z \left[\int_0^1 e^{-j\pi x} dx + \int_1^2 e^{-j\pi x} dx + \ldots + \int_\eta^{M_p} e^{-j\pi x} dx \right] . \tag{III-8}$$

Performing the indicated integrations results in

$$E_f\left(0, \phi_f\right) = \left(-\tau_z\right) \left[\left(e^{-j\pi} - 1\right) + \left(e^{-j2\pi} - e^{-j\pi}\right) + \ldots + \left(e^{-j\eta\pi} - e^{-j(\eta-1)\pi}\right) + \left(e^{-jM_p\pi} - e^{-j\eta\pi}\right) \right] . \tag{III-9}$$

This, of course, reduces to

$$E_f\left(0, \phi_f\right) = \tau_z \left(1 - e^{-jM_p\pi}\right) . \tag{III-10}$$

If the output mirror consists of an integral number of zones, M_p is an integer. Thus, the field at F is zero when there are an even number of zones on the output mirror, and it is equal to twice the transmission coefficient when there are an odd number of zones on the output mirror.

An examination of equation (III-9) shows that the field at F due to contributions from adjacent zones on the mirror have opposite signs. Therefore, the intensity at F can be increased by removing alternate zones. This is the

principle on which the Fresnel zone plate is based.[1] These zones can be removed by making τ_z equal to zero for alternate zones.

Consider the case where the output mirror has an even number of zones and the odd zones are removed. It can be shown from equation (III-8) that the field at F would then be given by

$$E_f\left(0, \phi_f\right) = \pi j \tau_z \left[\int_1^2 e^{-j\pi x} dx + \int_3^4 e^{-j\pi x} dx + \ldots + \int_{M_p-1}^{M_p} e^{-j\pi x} dx \right] . \qquad \text{(III-11)}$$

This reduces to

$$E_f\left(0, \phi_f\right) = -\tau_z M_p \ . \qquad \text{(III-12)}$$

The source field, the illuminating field on the zoned mirror, has a magnitude of one. Thus, the amplitude of the field at F is $\left(\tau_z M_p\right)$ times as large as the field on the output mirror and the intensity at F is the square of $\left(\tau_z M_p\right)$ times as large as the intensity of the source. For an integral number of zones on the output mirror it can readily be shown, via equations (III-1) and (III-6), that the number of zones is given by M_p. Therefore, since the maximum value of τ_z is one, the maximum intensity at the focal point is equal to the square of the number of half period zones on the output mirror.

---

[1]Jenkins, Francis A., and Harvey E. White, Fundamentals of Optics, McGraw-Hill Book Company, Inc., p. 360 (1957).

A more physical interpretation can be obtained by relating the number of zones to the geometry. This can be accomplished by substituting equation (III-6) into equation (III-12). The result is

$$E_f\left(0, \phi_f\right) = -\left(\frac{\tau_z a_p^2}{\lambda F}\right). \qquad \text{(III-13)}$$

The field at F is proportional to the area of the source field; this is indicated by the square of the mirror radius. The field is also proportional to the amplitude of the source field; this is measured by the transmission coefficient. The decrease in amplitude with distance is expressed by the term (1/F).

Although achieved by diffraction phenomena, the increase in intensity at F is due to a focusing of the field transmitted through the output mirror. To obtain this focused field the output mirror is considered to consist of half-period zones with only the alternate zones transmitting. Since the fields transmitted through alternate zones add, the result is a maximum field at one point on the resonator axis. This is the focal point of the zoned resonator.

The development in this section assumed that the source field was uniform over the surface of the output mirror. This can be approximated in practice only by resonators having very small Fresnel numbers. A Gaussian distribution is a more realistic resonator field configuration.

C. Gaussian Illumination of the Zoned Mirror

The field at the focal point will now be determined for a source field having a Gaussian distribution. This is begun by defining the field incident on the output mirror by

$$\bar{R}_{nz}\left(r_z\right) = \exp\left(-br_z^2\right) , \qquad \text{(III-14)}$$

where b is a real nonnegative constant. By substituting this field distribution into equation (III-2), the field at the focal point can be written as

$$E_f\left(0, \phi_f\right) = 2\pi j \int_0^1 \tau_z M_p \exp\left(-j\pi M_p r_z^2\right) \exp\left(-br_z^2\right) r_z dr_z \quad . \text{(III-15)}$$

The radii of the half-period zones on the output mirror are defined by equation (III-1). It is assumed that only alternate zones are transmitting. Thus, if the even-numbered zones are chosen to be the transmission zones, τ_z is finite over the even-numbered zones and zero over the odd-numbered zones. By using the change of variable indicated by equations (III-5) and (III-6), the field at the focal point can then be written as

$$E_f\left(0, \phi_f\right) = \pi j \tau_z \left\{ \int_1^2 \exp\left[-x\left(j\pi + \frac{b}{M_p}\right)\right] dx + \int_3^4 \exp\left[-x\left(j\pi + \frac{b}{M_p}\right)\right] dx \right.$$

$$\left. + \ldots + \int_{M_p-1}^{M_p} \exp\left[-x\left(j\pi + \frac{b}{M_p}\right)\right] dx \right\} , \qquad \text{(III-16)}$$

where for convenience it has been assumed that there are an even number of zones on the output mirror. For a source field that does not change rapidly with r_z and for large M_p, it is reasonable to approximate the value of the source field by a constant value over each zone. Thus, if it is assumed that M_p is large and that $b \ll M_p$,

$$\exp\left(-xb/M_p\right) \approx \exp\left(-ib/M_p\right)$$

in the interval

$$i \leq x \leq (i + 1) \quad .$$

Therefore, equation (III-16) can be approximated by

$$E_f\left(0, \phi_f\right) = \pi j \tau_z \left[e^{-b/M_p} \int_1^2 e^{-j\pi x} dx + e^{-3b/M_p} \int_3^4 e^{-j\pi x} dx \right.$$

$$\left. + \ldots + e^{-\left(M_p - 1\right) b/M_p} \int_{M_p - 1}^{M_p} e^{-j\pi x} dx \right] . \qquad \text{(III-17)}$$

By performing the indicated integrations and factoring out the term $\exp\left(-b/M_p\right)$, this equation can be reduced to

$$E_f\left(0, \phi_f\right) = \left(-2\tau_z\right) e^{-b/M_p} \left[1 + \left(e^{-2b/M_p} \right) + \left(e^{-2b/M_p} \right)^2 \right.$$

$$\left. + \ldots + \left(e^{-2b/M_p} \right)^{\frac{M_p - 2}{2}} \right] . \qquad \text{(III-18)}$$

The term in the brackets is a geometric series; therefore, when this series is summed, equation (III-18) becomes

$$E_f\left(0, \phi_f\right) = \left(-2\tau_z\right) e^{-b/M_p} \left[\frac{1 - e^{-b}}{1 - e^{-2b/M_p}} \right] . \qquad \text{(III-19)}$$

By assumption, M_p is much larger than b; therefore,

$$\exp\left(-b/M_p\right) \approx 1 - \left(b/M_p\right)$$

and

$$\exp\left(-2b/M_p\right) \approx 1 - \left(2b/M_p\right) .$$

When these approximations are used in equation (III-19) and the results are rearranged, it can be shown that equation (III-19) can be approximated by

$$E_f\left(0, \phi_f\right) = \left(-\tau_z\right) \left(M_p - b\right) e^{-b/2} \left(\frac{\sinh b/2}{b/2} \right) . \qquad \text{(III-20)}$$

It is desirable to examine the focused field as function of both the number of zones on the output mirror and the taper of the source field. This will be done by considering a normalized form of the field at the focal point. This normalized field is defined as the ratio of $E_f\left(0, \phi_f\right)$ given by equation (III-20) to the field obtained with a uniform source field. This reference field is given by equation (III-12), but it also can be obtained from equation (III-20) by taking the limit as b approaches zero. In either case, the resulting normalized field is given by

$$\bar{E}_f\left(0, \phi_f\right) = \left(\frac{M_p - b}{M_p}\right) e^{-b/2} \left(\frac{\sinh b/2}{b/2}\right) . \qquad \text{(III-21)}$$

In Figure 4 this normalized field is shown as a function of source field taper b for different values of half-period zones M_p. The field falls off fairly rapidly with increasing b and it falls off slowly with decreasing M_p.

D. Optimization of the Transmission Zone Area

The usual configuration for the zoned mirror is such that all the half-period zones occupy equal area. For Gaussian illumination of the zoned mirror this configuration results in a maximum intensity at the focal point. However, it may be more desirable to maximize the intensity at the focal point per unit power out of the resonator; this would be a reasonable basis for optimizing the power transmitted out of the resonator. If this basis is used for optimization, it is shown that the area of the transmission zones should be decreased. This decrease in transmission area is used to increase the reflection area on the zoned mirror.

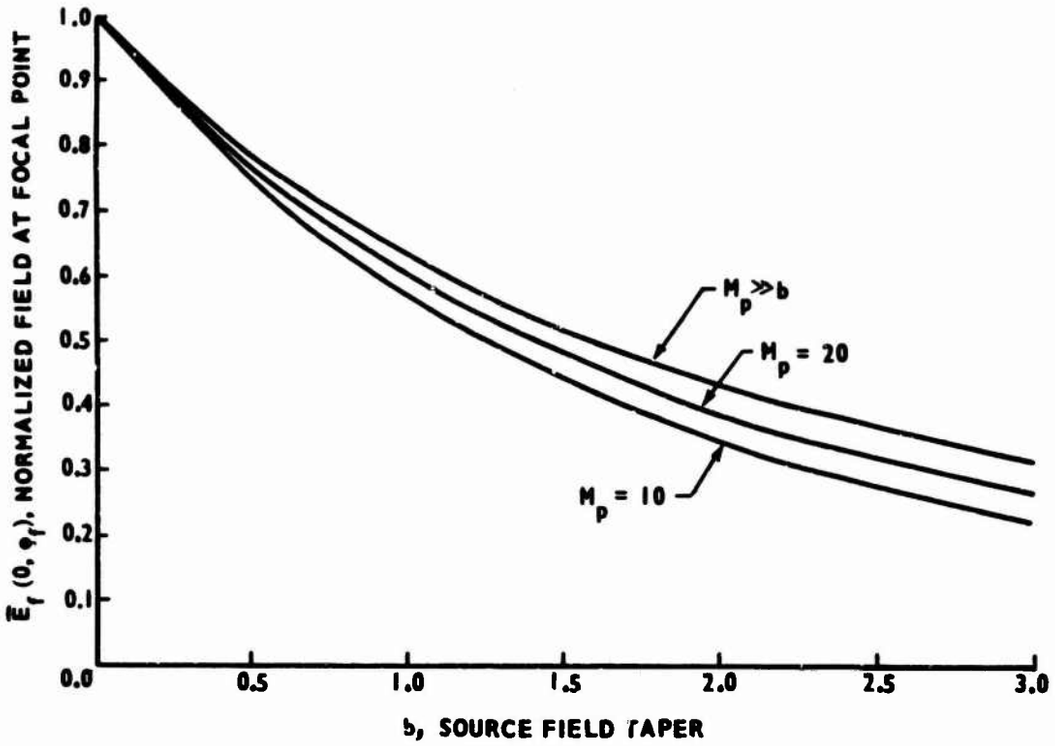

Figure 4. Normalized Field at Focal Point as a Function of Source Field Taper

It is assumed that the field on the output mirror has a Gaussian distribution of the form given by equation (III-14). The inner radius of each transmission zone is held fixed, and the area of each transmission zone is varied by changing the outer radius of the zone. It is assumed that the mirror has M_p half-period zones, that M_p is even, and that the transmission zones begin at the beginning of the even-numbered half-period zones; these latter assumptions are for mathematical convenience. They do not restrict the generality of the results.

The width of the transmission zones is established by the following criteria. If $(i\lambda/2)$ represents the path difference at the inner radius of a

transmission zone, then the path difference at the outer radius is given by $[(i+\delta)\lambda/2]$, where δ is a real parameter satisfying the relation

$$0 \leq \delta \leq 2 \ ,$$

and where $i = 1, 3, 5, \ldots, \left(M_p - 1\right)$. The remaining portions of the zoned mirror are reflecting zones.

The radius of the inner edge of the $(i + 1)^{th}$ transmission zone corresponds to the inner radius of the $(i + 1)^{th}$ half-period zone. Therefore, from equation (III-1), the inner radius of the $(i + 1)^{th}$ transmission zone is given by

$$r_{zi} = \left(\frac{i\lambda F}{a_p^2}\right)^{1/2} \ , \qquad \text{(III-22)}$$

and the radius to the outer edge is given by

$$r_{z(i+\delta)} = \left[\frac{(i + \delta)\lambda F}{a_p^2}\right]^{1/2} \ . \qquad \text{(III-23)}$$

By defining A_t to be the area of this transmission zone,

$$A_t = \pi\left(r^2_{z(i+\delta)} - r^2_{zi}\right) \ .$$

Using equations (III-22) and (III-23) in this equation, the area can be expressed as

$$A_t = \left(\frac{\pi\delta\lambda F}{a_p^2}\right) \ . \qquad \text{(III-24)}$$

It is interesting to note that the area of this transmission zone is independent of the zone number; hence, the areas of all transmission zones are equal.

By referring to equation (III-16), and by noting the differences on the limits of integration, it can easily be shown that the field at the focal point is given by

$$E_f\left(0, \phi_f\right) = \pi j \tau_z \left\{ \int_1^{1+\delta} \exp\left[-x\left(j\pi + \frac{b}{M_p}\right)\right] dx + \int_3^{3+\delta} \exp\left[-x\left(j\pi + \frac{b}{M_p}\right)\right] dx \right.$$

$$\left. + \ldots + \int_{M_p-1}^{M_p-1+\delta} \exp\left[-x\left(j\pi + \frac{b}{M_p}\right)\right] dx \right\} . \qquad \text{(III-25)}$$

It is assumed that M_p is large and that b is much less than M_p; therefore,

$$\exp\left(-xb/M_p\right) \approx \exp\left(-ib/M_p\right)$$

in the interval

$$i \leq x \leq i$$

Thus, equation (III-25) can be evaluated in [39] .r to that used to evaluate equation (III-16). The result is that the i. d field can be approximated by

$$E_f\left(0, \phi_f\right) = \left(-\tau_z\right)\left(\frac{1 - e^{-j\pi\delta}}{2}\right)\left(M_p - b\right)e^{-b/2}\left(\frac{\sinh b/2}{b/2}\right) . \qquad \text{(III-23)}$$

Before proceeding, the assumption made previously that $b \ll M_p$ will be invoked and the term $\left(M_p - b\right)$ in equation (III-26) will be replaced by M_p. The field at the focal point is then given by

$$E_f\left(0, \phi_f\right) = \left(-\tau_z\right)\left(\frac{1 - e^{-j\pi\delta}}{2}\right)\left(M_p\right)e^{-b/2}\left(\frac{\sinh b/2}{b/2}\right) . \qquad \text{(III-27)}$$

The intensity at the focal point is proportional to the square of the absolute value of the field at the focal point. Thus, by using equation (III-27) the intensity at the focal point is given by

$$I_f = 2C_T\left[\tau_z\left(\frac{M_p}{2}\right)e^{-b/2}\left(\frac{\sinh b/2}{b/2}\right)\right]^2 (1 - \cos \pi\delta) , \qquad \text{(III-28)}$$

where C_T is the constant of proportionality. To emphasize the relation between

focused intensity and the area of the transmitting zones, a normalized form of the intensity is defined by

$$\bar{I}_f = 1 - \cos \pi\delta \ . \qquad \text{(III-29)}$$

In order to maximize the focused intensity per unit output power, an expression for output power must now be obtained. From Chapter II, equation (II-17), this transmitted power is given as

$$P_T = 2\pi C_T \int_0^1 |\tau_z \bar{R}_{nz}(r_z)|^2 r_z dr_z \ . \qquad \text{(III-30)}$$

By using the source field as given by equation (III-14) and the radii of the transmission zones as defined by equations (III-22) and (III-23), the output power can be written as

$$P_T = 2\pi C_T \tau_z^2 \left[\int_{r_{z1}}^{r_{z(1+\delta)}} \exp\left(-2br_z^2\right) r_z dr_z + \int_{r_{z3}}^{r_{z(3+\delta)}} \exp\left(-2br_z^2\right) r_z dr_z \right.$$

$$\left. + \ \ldots \ + \int_{r_{z(M_p-1)}}^{r_{z(M_p-1+\delta)}} \exp\left(-2br_z^2\right) r_z dr_z \right] . \qquad \text{(III-31)}$$

By using the change of variable as indicated in equations (III-5) and (III-6), this equation can be expressed as

$$P_T = \left(\frac{\pi C_T \tau_z^2}{M_p}\right) \left[\int_1^{1+\delta} \exp\left(-2bx/M_p\right) dx + \int_3^{3+\delta} \exp\left(-2bx/M_p\right) dx \right.$$

$$\left. + \ \ldots \ + \int_{M_p-1}^{M_p-1+\delta} \exp\left(-2bx/M_p\right) dx \right] . \qquad \text{(III-32)}$$

Since $b \ll M_p$, P_T is given approximately by

$$P_T = \left(\frac{\pi C_T \tau z^2}{M_p}\right)(\delta) e^{-2b/M_p} \left[1 + \left(e^{-4b/M_p}\right) + \left(e^{-4b/M_p}\right)^2 + \ldots + \left(e^{-4b/M_p}\right)^{\frac{M_p - 2}{2}}\right] . \qquad \text{(III-33)}$$

This, of course, reduces to

$$P_T = \left(\frac{\pi C_T \tau z^2}{M_p}\right)(\delta) \left(e^{-2b/M_p}\right) \left(\frac{1 - e^{-2b}}{1 - e^{-4b/M_p}}\right) . \qquad \text{(III-34)}$$

Finally, by using

$$\exp\left(-2b/M_p\right) \approx 1$$

and

$$1 - \exp\left(-4b/M_p\right) \approx 4b/M_p ,$$

equation (III-34) can be approximated by

$$P_T = \frac{1}{2} \pi C_T \tau z^2 \delta e^{-b} \left(\frac{\sinh b}{b}\right) . \qquad \text{(III-35)}$$

The intensity at the focal point per unit output power is obtainable from equations (III-28) and (III-35). The result is

$$\left(\frac{I_f}{P_T}\right) = \left(\frac{M_p^2}{\pi}\right) \left[\frac{\left(\frac{\sinh b/2}{b/2}\right)^2}{\left(\frac{\sinh b}{b}\right)}\right] \left(\frac{1 - \cos \pi\delta}{\delta}\right) . \qquad \text{(III-36)}$$

The dependence of this ratio on the transmission zone parameter can be determined from a normalized ratio defined by

$$\left(\frac{\overline{I_f}}{\overline{P_T}}\right) = \left(\frac{1 - \cos \pi\delta}{\delta}\right) . \qquad \text{(III-37)}$$

Both this equation and equation (III-29) are shown in Figure 5 as a function of the transmission zone parameter δ. As was mentioned previously, the focused intensity is a maximum when the transmission zones correspond to alternate half-period zones; this condition occurs when δ is equal to one. On the other hand, to maximize the focused intensity per unit output power, each transmission zone area should be decreased to about 74 percent of the area of a half-period zones.

One of the assumptions used in this development was that the dimensions of the output mirror be much greater than a wavelength. This limitation was imposed so as to assure the dominance of aperture effects over edge effects. This constraint can be better specified by requiring a minimum zone width of at least ten wavelengths. Since the minimum zone width and the maximum number of zones are related, this minimum zone width can be used to determine the maximum number of zones that can be placed on a given mirror.

To determine this relationship let M_{pm} be the maximum number of zones on the output mirror and assume that δ is equal to one. Thus, for an integral number of half-period zones on the output mirror, the width of the minimum zone is obtainable from equations (III-22) and (III-23) as

$$\Delta r = \left[\frac{M_{pm}\lambda F}{a_p^2}\right]^{1/2} - \left[\frac{\left(M_{pm} - 1\right)\lambda F}{a_p^2}\right]^{1/2} .$$

The term $\left(a_p^2/\lambda F\right)$ is equal to the number of half-period zones on the output mirror [equation (III-6)]. Therefore,

$$\Delta r = 1 - \left[1 - \left(\frac{1}{M_{pm}}\right)\right]^{1/2} .$$

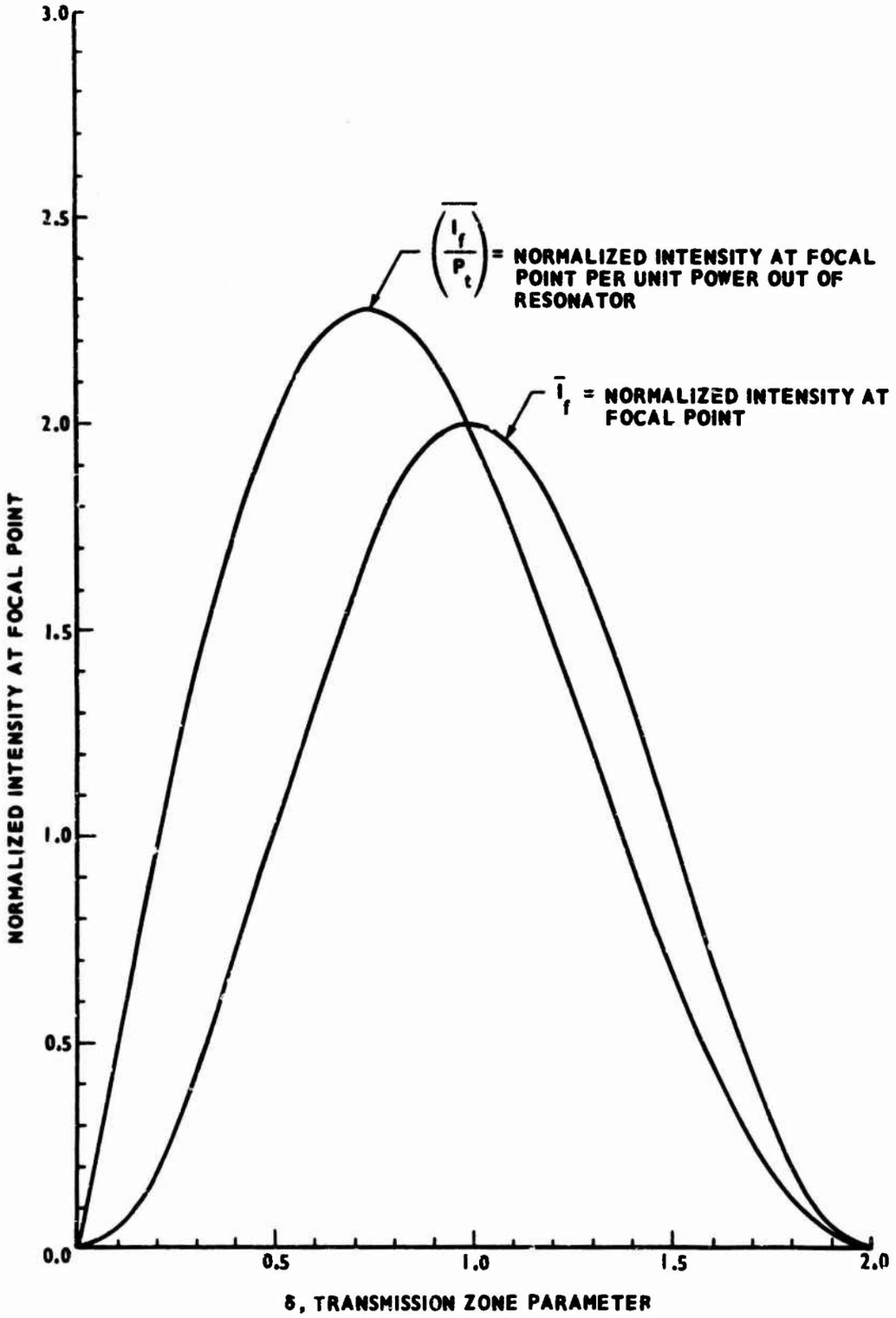

Figure 5. Normalized Intensity at Focal Point as a Function of Transmission Zone Parameter

For M_{pm} large,

$$\Delta r \approx \left(\frac{1}{2M_{pm}}\right) . \qquad \text{(III-38)}$$

The minimum zone width was fixed at ten wavelengths; however, in equations (III-22) and (III-23), radii normalized to the radius of the mirror are used. Therefore, if this is taken into account,

$$M_{pm} \approx \frac{a_p}{20\lambda} ; \qquad \text{(III-39)}$$

that is, the maximum number of zones that can be placed on the output mirror is approximately equal to the radius of the output mirror divided by twenty times the wavelength.

The magnitude of the field at the focal point is proportional to the reciprocal of the focal distance; thus, focusing cannot be achieved at arbitrarily large distances. The maximum focal distance is hereby defined to be the maximum distance such that the focal point intensity is ten times as large as the maximum intensity of the source field. In all cases, the source field has a maximum magnitude of one. Consider the case where the source field is uniform and the area of the transmission zones are equal to the area of the half-period zones. The maximum focal distance F_m can be obtained from equation (III-13) by setting the focused field equal to $\sqrt{10}$. The result is

$$F_m = \frac{a_p^2 \tau_z}{\sqrt{10}\lambda} \qquad \text{(III-40)}$$

For Gaussion illumination of the output mirror the maximum focal length will be less than that given by equation (III-40). This can be seen by

referring to the expression for the field at the focal point for Gaussian illumination of the output mirror, equation (III-20).

CHAPTER IV

RESONATOR MODE ANALYSIS

The numerical techniques used to determine the mode structure of the self-focusing resonator are discussed in this chapter. In the first section the resonator equations are reduced to a matrix form. Following this, the method used to find the fundamental resonator mode is presented. In the last section the method used to determine higher-order resonator modes is presented.

A. Matrix Formulation

The resonator equations are given in Chapter II, equations (II-3) and (II-4); they are repeated below for reference. These equations relate the field at a point on one mirror to the integral of the field over the other mirror. On the output mirror the field is given by

$$R_{nz}\left(r_z\right) = \int_0^1 \rho_s NK_m\left(r_z, r_s\right) \bar{R}_{ns}\left(r_s\right) r_s dr_s \qquad \text{(IV-1)}$$

and the field on the input mirror is given by

$$R_{ns}\left(r_s\right) = \int_0^1 \rho_z NK_m\left(r_z, r_s\right) \bar{R}_{nz}\left(r_z\right) r_z dr_z \ . \qquad \text{(IV-2)}$$

The field on the output mirror at a radial distance r_{2i} is given by

$$R_{nz}\left(r_{zi}\right) = \int_0^1 \rho_s NK_m\left(r_{zi}, r_s\right)\bar{R}_{ns}\left(r_s\right) r_s dr_s \quad . \tag{IV-3}$$

The field on the output mirror can be written in a sampled form as a column vector. That is,

$$\left[R_{nz}\left(r_z\right)\right] = \begin{bmatrix} R_{nz}\left(r_{z0}\right) \\ R_{nz}\left(r_{z1}\right) \\ \vdots \\ R_{nz}\left(r_{z(p-1)}\right) \end{bmatrix} . \tag{IV-4}$$

In a similar manner, the field on the input mirror can be expressed as

$$R_{ns}\left(r_{sj}\right) = \int_0^1 \rho_z NK_m\left(r_z, r_{sj}\right)\bar{R}_{nz}\left(r_z\right) r_z dr_z \quad , \tag{IV-5}$$

and in a sampled form

$$\left[R_{ns}\left(r_s\right)\right] = \begin{bmatrix} R_{ns}\left(r_{s0}\right) \\ R_{ns}\left(r_{s1}\right) \\ \vdots \\ R_{ns}\left(r_{s(p-1)}\right) \end{bmatrix} . \tag{IV-6}$$

By utilizing a numerical integration scheme the integrals in equations (IV-3) and (IV-5) can be replaced by summations. Then, if the sampling intervals are made equivalent to the integration intervals, the resonator equations can be placed into a matrix form.

By using Simpson's rule for integration, the resonator equation relating the field on the output mirror to the normalized field on the input mirror is

given by

$$\begin{bmatrix} R_{nz}(r_{z0}) \\ R_{nz}(r_{z1}) \\ \vdots \\ R_{nz}(r_{z(p-1)}) \end{bmatrix} = \frac{hN}{3}[K][\rho_s][r_s][S] \begin{bmatrix} \bar{R}_{ns}(r_{s0}) \\ \bar{R}_{ns}(r_{s1}) \\ \vdots \\ \bar{R}_{ns}(r_{s(p-1)}) \end{bmatrix}, \quad \text{(IV-7)}$$

where

$$[K] = \begin{bmatrix} K_m(r_{z0}, r_{s0}) & K_m(r_{z0}, r_{s1}) & \cdots & K_m(r_{z0}, r_{s(p-1)}) \\ K_m(r_{z1}, r_{s0}) & K_m(r_{z1}, r_{s1}) & \cdots & K_m(r_{z1}, r_{s(p-1)}) \\ \vdots & & & \vdots \\ K_m(r_{z(p-1)}, r_{s0}) & K_m(r_{z(p-1)}, r_{s1}) & \cdots & K_m(r_{z(p-1)}, r_{s(p-1)}) \end{bmatrix},$$

$$[\rho_s] = \begin{bmatrix} \rho_s(r_{s0}) & 0 & \cdots & 0 \\ 0 & \rho_s(r_{s1}) & \cdots & 0 \\ \vdots & & & \\ 0 & 0 & \cdots & \rho_s(r_{s(p-1)}) \end{bmatrix},$$

$$[r_s] = \begin{bmatrix} r_{s0} & 0 & \cdots & 0 \\ 0 & r_{s1} & \cdots & 0 \\ \vdots & \vdots & & \vdots \\ 0 & 0 & \cdots & r_{s(p-1)} \end{bmatrix},$$

and

$$[S] = \begin{bmatrix} 1 & 0 & 0 & \cdots & 0 \\ 0 & 4 & 0 & \cdots & 0 \\ 0 & 0 & 2 & \cdots & 0 \\ \vdots & \vdots & \vdots & & \vdots \\ 0 & 0 & 0 & \cdots & 1 \end{bmatrix}.$$

Since the integration interval is the normalized radius of unit length, the incremental interval, h, is equal to $[1/(p-1)]$, where (p) is the number of sample points.

In a similar manner the field on the input mirror is related to the field on the output mirror by

$$\begin{bmatrix} R_{ns}(r_{s0}) \\ R_{ns}(r_{s1}) \\ \vdots \\ R_{ns}(r_{s(p-1)}) \end{bmatrix} = \frac{hN}{3} [K] [\rho_z] [r_z] [S] \begin{bmatrix} \bar{R}_{nz}(r_{z0}) \\ \bar{R}_{nz}(r_{z1}) \\ \vdots \\ \bar{R}_{nz}(r_{z(p-1)}) \end{bmatrix}, \qquad \text{(IV-8)}$$

where

$$[\rho_z] = \begin{bmatrix} \rho_z(r_{z0}) & 0 & \cdots & 0 \\ 0 & \rho_z(r_{z1}) & \cdots & 0 \\ \vdots & \vdots & & \vdots \\ 0 & 0 & \cdots & \rho_z(r_{z(p-1)}) \end{bmatrix}$$

and

$$[r_z] = \begin{bmatrix} r_{z0} & 0 & \cdots & 0 \\ 0 & r_{z1} & \cdots & 0 \\ \vdots & \vdots & & \vdots \\ 0 & 0 & \cdots & (r_{z(p-1)}) \end{bmatrix}.$$

In order to reduce the amount of notation,

$$[A_s] = \frac{hN}{3} [K] [\rho_s] [r_s] [S] \qquad \text{(IV-9)}$$

and

$$\left[A_z\right] = \frac{hN}{3}\left[K\right]\left[\rho_z\right]\left[r_z\right]\left[S\right] \qquad \text{(IV-10)}$$

are defined. If these equations are used in equations (IV-7) and (IV-8) and the column matrices are written in reduced forms, the resonator equations can be written

$$\left[R_{nz}(r_z)\right] = \left[A_s\right]\left[\bar{R}_{ns}(r_s)\right] \qquad \text{(IV-11)}$$

and

$$\left[R_{ns}(r_s)\right] = \left[A_z\right]\left[\bar{R}_{nz}(r_z)\right] \ . \qquad \text{(IV-12)}$$

The unnormalized fields are related to the normalized fields by the complex constants γ_{nz} and γ_{ns}; that is,

$$\left[R_{nz}(r_z)\right] = \gamma_{nz}\left[\bar{R}_{nz}(r_z)\right] \qquad \text{(IV-13)}$$

and

$$\left[R_{ns}(r_s)\right] = \gamma_{ns}\left[\bar{R}_{ns}(r_s)\right] \ . \qquad \text{(IV-14)}$$

As was mentioned in Chapter II, these complex constants represent the value of the unnormalized fields at the radii where the field amplitudes are maximum. Thus, the normalized fields have a maximum magnitude of one.

Substitution of equation (IV-13) into (IV-11) and equation (IV-14) into (IV-12) leads directly to

$$\gamma_{nz}\left[\bar{R}_{nz}(r_z)\right] = \left[A_s\right]\left[\bar{R}_{ns}(r_s)\right] \qquad \text{(IV-15)}$$

and

$$\gamma_{ns}\left[\bar{R}_{ns}(r_s)\right] = \left[A_z\right]\left[\bar{R}_{nz}(r_z)\right] \ . \qquad \text{(IV-16)}$$

These equations represent the matrix formulation of the resonator equations. To reiterate, these equations relate the field on one mirror of the resonator to the field on the other. Through $\rho_z(r_z)$ and $\rho_s(r_s)$ the reflectivity of the mirrors can be made to vary as a function of mirror radius. This feature is necessary for expressing the selective reflection characteristics of the zoned mirror. In the above development Simpson's rule was used; however, other numerical integration techniques have been considered and they lead to results which can be expressed in the form given by equations (IV-15) and (IV-16).

By combining equations (IV-15) and (IV-16) the resonator problem can be put into the form of the eigenvalue problem. To show this, equation (IV-15) is substituted first into equation (IV-16) and

$$\gamma_{ns}\gamma_{nz}\left[\bar{R}_{ns}(r_s)\right] = \left[A_z\right]\left[A_s\right]\left[\bar{R}_{ns}(r_s)\right] \qquad \text{(IV-17)}$$

is obtained. With the opposite substitution,

$$\gamma_{ns}\gamma_{nz}\left[\bar{R}_{nz}(r_z)\right] = \left[A_s\right]\left[A_z\right]\left[\bar{R}_{nz}(r_z)\right] . \qquad \text{(IV-18)}$$

By defining

$$\gamma_{ns}\gamma_{nz} = \Gamma_n ,$$

$$\left[A_z\right]\left[A_s\right] = \left[B_{zs}\right] ,$$

and

$$\left[A_s\right]\left[A_z\right] = \left[B_{sz}\right]$$

and by using them in equations (IV-17) and (IV-18), it is seen, after some rearranging,

$$\left[B_{zs} - \Gamma_n I\right]\left[\bar{R}_{ns}(r_s)\right] = 0 \qquad \text{(IV-19)}$$

and

$$\left[B_{sz} - \Gamma_n I\right]\left[\bar{R}_{nz}(r_z)\right] = 0 \ , \qquad \text{(IV-20)}$$

where I is the (p) order identity matrix.

B. Fundamental Mode Analysis

A form of the power method was used to determine the fundamental modes of the self-focusing resonator. The power method is a numerical procedure that can be used to solve eigenvalue problems whose operating matrices are well behaved. By well behaved it is meant that the matrix does not have degenerate eigenvalues or eigenvalues having the same magnitude but different phases.

Mode losses are determined by the magnitude of the eigenvalues; thus, different values of eigenvalues mean that the modes have different losses. For a given angular degeneracy, the power method extracts the mode having the least loss. This mode is called the fundamental mode.

Basically, the power method of mode analysis is an iterative technique whereby an initial estimate of the field is operated upon by the resonator matrix until the field converges to a mode of the resonator. Convergence means that in a double pass the normalized field repeats itself. That is, the normalized field after one douple pass is identical to the original field; hence, the field distribution is a solution to one of the resonator equations.

According to equations (IV-19) and (IV-20), the resonator equations can be written in a matrix format in terms of the field on the input mirror as

$$\Gamma_n\left[\bar{R}_{ns}(r_s)\right] = \left[B_{zs}\right]\left[\bar{R}_{ns}(r_s)\right] \qquad \text{(IV-22)}$$

and in terms of the field on the output mirror as

$$\Gamma_n\left[\bar{R}_{nz}(r_s)\right] = \left[B_{sz}\right]\left[\bar{R}_{nz}(r_s)\right] \ . \qquad \text{(IV-23)}$$

Solutions to these equations represent the modes of the resonator. Since the fields on the two mirrors are related by equations (IV-15) and (IV-16), it is necessary only to solve for the field on one mirror. The other field would be obtainable from equations (IV-15) or (IV-16).

The initial estimate of the field is called the zeroth iteration. Thus, by working with the fields on the input mirror and by denoting the iteration by a superscript, the initial field distribution is written as $\left[\bar{R}^0_{ns}(r_s)\right]$. On each iteration the field is operated on by the resonator matrix. This operation represent a double pass of the wave in the resonator. After each iteration the field is normalized by dividing it by the value of the field where the magnitude of the field is a maximum. This normalized field is then used as the input for the next iteration and the process is repeated.

This iteration procedure from the first to the k^{th} iteration is outlined by the following equations:

$$\left[R^1_{ns}(r_s)\right] = \left[B_{zs}\right]\left[\bar{R}^0_{ns}(r_s)\right] \qquad \text{(IV-24)}$$

$$\left[R^2_{ns}(r_s)\right] = \left[B_{zs}\right]\left[\bar{R}^1_{ns}(r_s)\right] \qquad \text{(IV-25)}$$

$$\left[R^3_{ns}(r_s)\right] = \left[B_{zs}\right]\left[\bar{R}^2_{ns}(r_s)\right] \qquad \text{(IV-26)}$$

$$\vdots$$

$$\left[R^k_{ns}(r_s)\right] = \left[B_{zs}\right]\left[\bar{R}^{k-1}_{ns}(r_s)\right] \ . \qquad \text{(IV-27)}$$

The unnormalized and normalized fields are related by

$$\left[R^i_{ns}(r_s)\right] = \Gamma^i_n\left[\bar{R}^i_{ns}(r_s)\right] , \qquad \text{(IV-28)}$$

where i = 1, 2, ..., k, and Γ^i_n is the value of $\left[R^i_{ns}(r_s)\right]$ where its magnitude is a maximum. It is essential to note that if $\left[\bar{R}^i_{ns}(r_s)\right]$ is a mode of the resonator, that is, a solution to equation (IV-22), then Γ^i_n is the corresponding eigenvalue for that mode. If $\left[\bar{R}^i_{ns}(r_s)\right]$ is not a resonator mode then Γ^i_n is not an eigenvalue, but merely a complex constant used to normalize the field.

By using the above equations, the normalized field at the k^{th} iteration can be expressed in terms of the initial field as

$$\left[\bar{R}^k_{ns}(r_s)\right] = \left(\frac{1}{\Gamma^1_n \Gamma^2_n \cdots \Gamma^k_n}\right)\left[B_{zs}\right]^k\left[\bar{R}^0_{ns}(r_s)\right] . \qquad \text{(IV-29)}$$

It has been shown that in the limit as $k \to \infty$ the k^{th} distribution is independent of the initial distribution.[1] Because of this, there is some liberty in choosing the form of the initial field.

To keep the results relatively general, suppose that the initial field is composed of all possible modes for a given angular degeneracy. The initial field can therefore be written as

$$\left[\bar{R}^0_{ns}(r_s)\right] = \sum_{j=0}^{p-1} a_j\left[\bar{R}_{js}(r_s)\right] , \qquad \text{(IV-30)}$$

where the a_j are finite, complex constants. The resonator matrix is of order (p) and therefore has (p) solutions. These solutions are represented by the

---

[1] Hildebrand, F. B., Methods of Applied Mathematics, Prentice-Hall, Inc., p. 427 (1952).

field distributions $\left[\bar{R}_{js}(r_s)\right]$. It will be assumed that these fields are ordered in relation to their eigenvalues such that

$$|\Gamma_j| > |\Gamma_{j+1}| \qquad \text{(IV-31)}$$

where $j = 0, 1, \ldots, (p-2)$.

Substituting equation (IV-30) into equation (IV-29) results in

$$\left[\bar{R}^k_{ns}(r_s)\right] = \left(\frac{1}{\Gamma^1_n \Gamma^2_n \cdots \Gamma^k_n}\right)\left[B_{zs}\right]^k \sum_{j=0}^{p-1} a_j \left[\bar{R}_{js}(r_s)\right] \quad . \qquad \text{(IV-32)}$$

Taking the operator matrix inside the summation gives

$$\left[\bar{R}^k_{ns}(r_s)\right] = \left(\frac{1}{\Gamma^1_n \Gamma^2_n \cdots \Gamma^k_n}\right) \sum_{j=0}^{p-1} aj \left[B_{zs}\right]^k \left[\bar{R}_{js}(r_s)\right] \quad . \qquad \text{(IV-33)}$$

If one uses the knowledge that the $\left[\bar{R}_{js}(r_s)\right]$ are solutions to equation (IV-22), it can be observed that operating with $\left[B_{zs}\right]$ on $\left[\bar{R}_{js}(r_s)\right]$ is equivalent to multiplying the field by its eigenvalue; therefore, (IV-33) can be written as

$$\left[\bar{R}^k_{ns}(r_s)\right] = \left(\frac{1}{\Gamma^1_n \Gamma^2_n \cdots \Gamma^k_n}\right) \sum_{j=0}^{p-1} a_j \left(\Gamma_j\right)^k \left[\bar{R}_{js}(r_s)\right] \quad . \qquad \text{(IV-}$$

From equation (IV-31) it is obvious that for large k, the j = 0 term will dominate. Therefore, the field on the k^{th} iteration, for large k, is given by

$$\left[\bar{R}^k_{ns}(r_s)\right] = \left(\frac{1}{\Gamma^1_n \Gamma^2_n \cdots \Gamma^k_n}\right) a_0 (\Gamma_0)^k \left[\bar{R}_{0s}(r_s)\right], \qquad \text{(IV-35)}$$

and since Γ^1_n, Γ^2_n, ... Γ^k_n, a_0, and Γ_0 are constants it follows that

$$\left[\bar{R}^k_{ns}(r_s)\right] = \left[\bar{R}_{0s}(r_s)\right] \quad . \qquad \text{(IV-36)}$$

This heuristic development has led to the important result that the field distribution obtained by the power method is the dominant mode of the resonator.

This mode represents the field distribution which experiences the least double pass loss.

If an initial field is chosen that has no component of $\left[\bar{R}_{0s}(r_s)\right]$ one might be tempted to assume that the final field would be $\left[\bar{R}_{1s}(r_s)\right]$. This would not be true; the final field is independent of the initial field. This can be visualized in a practical sense by noting that although the sampling process can be made accurate to any degree, it is not exact. Therefore, it is impossible to start with an initial field that is exactly a pure mode, and it can be assumed that because of this inexactness, the initial field contains at least a small portion of the dominant mode. This way of looking at the initial field distribution is analogous to a laser resonator having an initial field generated by the spontaneous emission. The probability of the spontaneous emission not having a component of the dominant field is inconceivably small.

As was noted previously, the power method results in the field converging to a configuration independent of the initial field distribution. Hence, the field at any iteration can be considered to be independent of the final field; and therefore convergence depends on the accuracy of the resonator matrix and not the initial field. On every iteration the field is operated on by the same resonator matrix. This matrix acts as a reference to which the field is continually compared. Convergence occurs when the normalized field reproduces itself from one iteration to the next.

This concept of convergence can be formalized in the following manner. By referring to equation (IV-34), the field is said to be converged if

$$|\bar{R}_{ns}^{k}(r_s) - \bar{R}_{ns}^{k-1}(r_s)| < \Delta \ll 1$$

for all values of r_s. This means that the field has converged when the maximum difference of the field from one iteration to the next is less than Δ. This converged field represents a pure mode of the resonator model to within an accuracy given by Δ. Values of Δ used in this study varied from 10^{-7} to 10^{-4}.

It is important to realize that convergence to a given degree does not imply that the resulting field has the same degree of accuracy. Convergence in itself is a measure of the stability of the numerical model.

Consider the accuracy with which a mode obtained with the numerical model represents an actual resonator mode. This is a measure of the accuracy with which the numerical model represents the integral equations. A method described by Scarborough[2] was used to determine this accuracy. To measure the accuracy of a given result a second solution is obtained by using twice the number of sample points. The error in the first solution then has a magnitude of approximately (16/15) times the difference in the two solutions. In this study it was found that the resonator modes were obtained to within an accuracy of about one percent.

The iterating procedure given above results in the field being calculated on every double pass. However, it is sometimes advantageous to calculate the field on every pass. This single pass power method makes use of the form of the resonator equations as given by equations (IV-11) and (IV-12).

---

[2]Scarborough, J. B., Numerical Mathematical Analysis, Fourth Edition, The Johns Hopkins Press, pp. 178-179 (1958).

For the single pass method an initial field distribution is assumed, say $\left[\bar{R}^0_{ns}(r_s)\right]$. This is used in equation (IV-11) and the field on the output mirror is calculated. This field is normalized and substituted into equation (IV-12). Normalizing the field obtained with this equation gives $\left[\bar{R}^1_{ns}(r_s)\right]$. This field is substituted back into equation (IV-11). This procedure is continued until the field converges to $\left[\bar{R}^k_{ns}(r_s)\right]$. An examination of the pertinent equations will show that this field is identical to that obtained with the double pass method.

Although the results are identical, there are differences in the computational times. It is because of this difference that one method might be preferable over the other. For both methods, each iteration involves the multiplication of a p-term column matrix by a $(p)^{th}$ order matrix. These operations will be denoted by P_p. For the double pass method (k) iterations are required for convergence, and for the single pass method (2k) iterations are required; therefore, the single pass iterating procedure requires kP_p more operations. However, the operating matrix for the double pass method, obtained by multiplying the two $(p)^{th}$ order operating matrices $\left[A_s\right]$ and $\left[A_z\right]$ together, requires pP_p computations. Therefore, if $(k/p) < 1$ it would require fewer total operations to use the single pass power method, and if $(k/p) > 1$ the double pass power method would require fewer operations.

In the procedure used above, the basic power method was modified merely by using a different form for the resonator matrix. In doing so it was found that under certain conditions computational time could be reduced. With the goal in mind of minimizing computational time, another modification of the operating matrix will be developed.

Consider the form of the power method as expressed by equation (IV-29). This equation can be rewritten as

$$\left[\bar{R}^{k}_{ns}(r_s)\right] = \left(\frac{1}{\Gamma^{1}_{n}\Gamma^{2}_{n}\cdots\Gamma^{k}_{n}}\right)\left[\left[B_{zs}\right]^{j}\right]^{k/j}\bar{R}^{0}_{ns}(r_s) \quad , \qquad \text{(IV-37)}$$

where (k) represents the number of iterations required for convergence and (j) is an integral submultiple of (k). This immediately suggests the possibility of using $\left[\left[B_{zs}\right]^{j}\right]$ as the operating matrix and iterating (k/j) times. Each iteration would then be equivalent to (j) double passes in the resonator; hence, (k/j) iterations would be equivalent to (k) double passes. For some resonators this modified power method offers the advantage of decreased computational time.

Each iteration involves the multiplication of a p-term column matrix by a $(p)^{th}$ order matrix. As before, these operations are denoted by P_p. Therefore, there are a total of $(k/j)\,P_p$ operations involved in this iterating process.

The number of computational operations required to generate the operating matrix from $\left[B_{zs}\right]$ can also be related to P_p. If the values of (k) and (j) are limited in such a way that $j = 2^h$, where (h) is an integer, the method of multiple squaring can be used to calculate the operating matrix. In this method $\left[B_{zs}\right]$ is squared, the result is then squared, etc., until $\left[\left[B_{zs}\right]^{j}\right]$ is obtained. Each squaring operation is equivalent to multiplying a $(p)^{th}$ order matri. times a $(p)^{th}$ order matrix; therefore, each squaring requires pP_p computations; and since (h) squaring operations are required, a total of hpP_p computations are needed to generate the operating matrix.

the operating matrix.

The practical limitations resulting from the constraints placed on (k) and (j) are not as severe as one might imagine. This is because (k) cannot be accurately predetermined, and to assure a high probability of convergence (k) is usually estimated somewhat high. Therefore, since (k) is only approximately correct, little is lost by using the permissible value of (k) nearest to that estimated.

The computations required for normalizing the field, for cases where $p \gtrsim 10$, are small compared to P_p. Since these are the cases of interest, the computations required for normalizing the field will be neglected. Therefore, the total number of calculations, T, will be approximated by the sum of those required for iterating and those required for generating the resonator matrix; that is,

$$T = \left(\frac{k}{2^h} + hp\right)P_p \quad . \tag{IV-38}$$

Since it is desirable to minimize the number of calculations, (h) is temporarily assumed to be continuous and T is differentiated with respect to (h). Setting the result equal to zero and simplifying gives

$$(k/p) = \left(2^h/\ln 2\right) \quad . \tag{IV-39}$$

This ratio, (k/p), is shown as a function of (h) by the dashed curve in Figure 6. However, (h) can take only integral values, and therefore this curve is only correct for these integers. For values of (k/p) that give an (h) between the integers (h_i) and $(h_i + 1)$, equation (IV-38) must be examined to determine which of these integers results in minimum T. This can be done by equating $T(h_i)$ and $T(h_i + 1)$, where

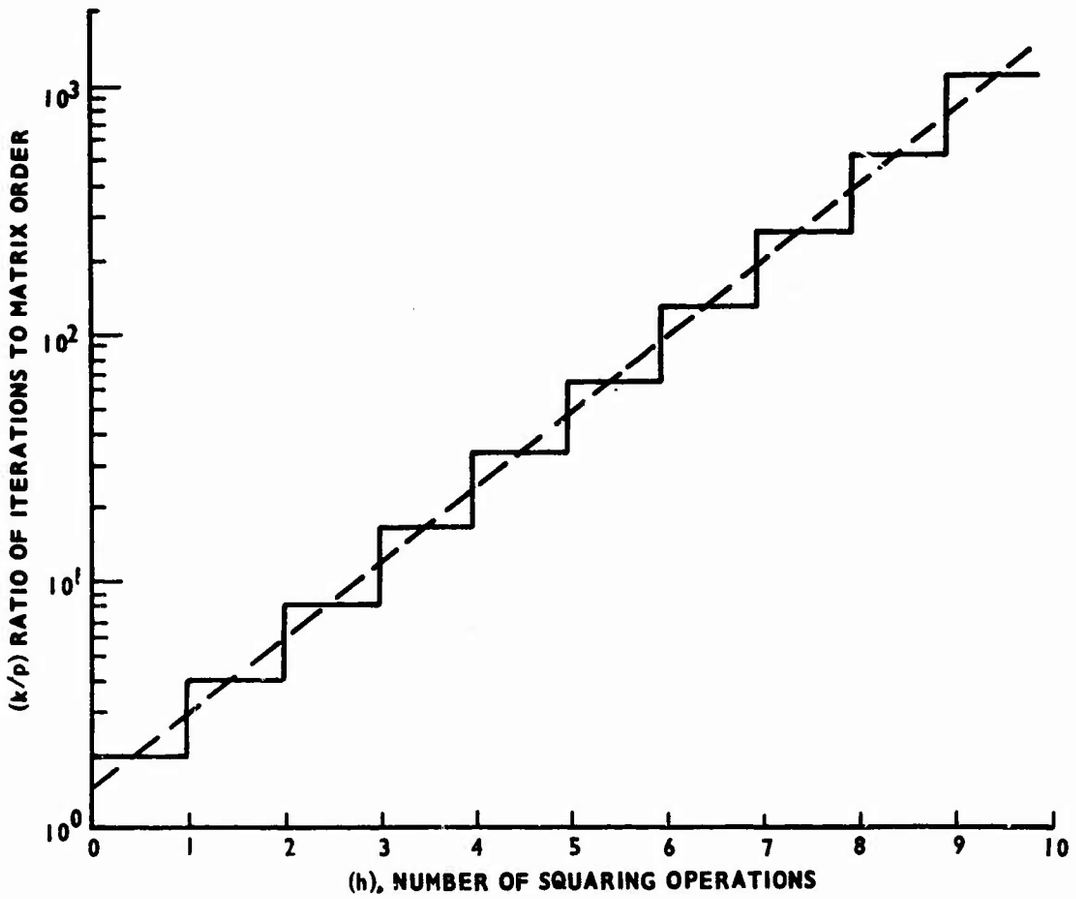

Figure 6. Ratio of Iterations to Matrix Order as a Function of the Number of Squaring Operations

$$T(h_i) = \left(\frac{k}{2^{h_i}} + h_i p \right) \qquad \text{(IV-40)}$$

and

$$T(h_i + 1) = \left(\frac{k}{2^{h_i+1}} + (h_i + 1)p \right) P_p \ , \qquad \text{(IV-41)}$$

and solving for the corresponding value of (k/p). This gives

$$(k/p) = 2^{h_i+1} \ . \qquad \text{(IV-42)}$$

The value of (k/p), as given by equation (IV-42), represents the cutoff between (h_i) and $(h_i + 1)$. That is, one would use an (h) of value (h_i) for values of (k/p) such that

$$2^{h_i} \leq (k/p) \leq 2^{h_i+1} \ .$$

This is indicated by the stairstep curve in Figure 6.

A measure of the computational time saved by using this modified power method can be obtained by comparing the number of computations required for this method to that required for the double pass power method. For the double pass power method, (j) is equal to one, and therefore (h) is zero. Using this in equation (IV-38) gives the number of computations as kP_p. The ratio of the number of computations required for the power method to that required for the modified power method is given by

$$\frac{T(h = 0)}{T(h)} = \frac{(k/p)\,2^h}{(k/p) + h2^h} \ . \qquad \text{(IV-43)}$$

The (k/p) obtained from this equation is shown as a function of T(h = 0)/T(h) in Figure 7. Thus, if an estimate of (k/p) is known, an estimate of the advantage gained by using the modified power method can be obtained. For instance, if (k/p) is ten, approximately twice as many calculations are needed for the power method as are needed for the modified power method. To summarize, for $(k/p) \leq 1$ the single pass power method requires the fewest computations, for $1 \leq (k/p) \leq 2$ the double pass power method requires the fewest computations, and for $(k/p) \geq 2$ the modified power method requires the fewest computations.

C. Higher-Order Mode Analysis

The method used to obtain higher-order modes is based on a technique suggested by Wells.[3] It is a mathematical operation whereby the normally dominant mode is suppressed in such a way that the next order mode becomes dominant. The process can be extended to higher-order modes.

This technique requires that the field distribution be operated on with the matrix operator $[\mathcal{A}]$, where

$$[\mathcal{A}] = \left[B_{zs}\right] - \Gamma_s [I] \quad . \tag{IV-44}$$

The term $\left[B_{zs}\right]$ is the resonator matrix, Γ_s is the eigenvalue of the mode being suppressed, and [I] is the identity matrix.

---

[3]Wells, W. H., IEEE J. Quantum Electronics, Volume QE-2, pp. 94-102 (1966).

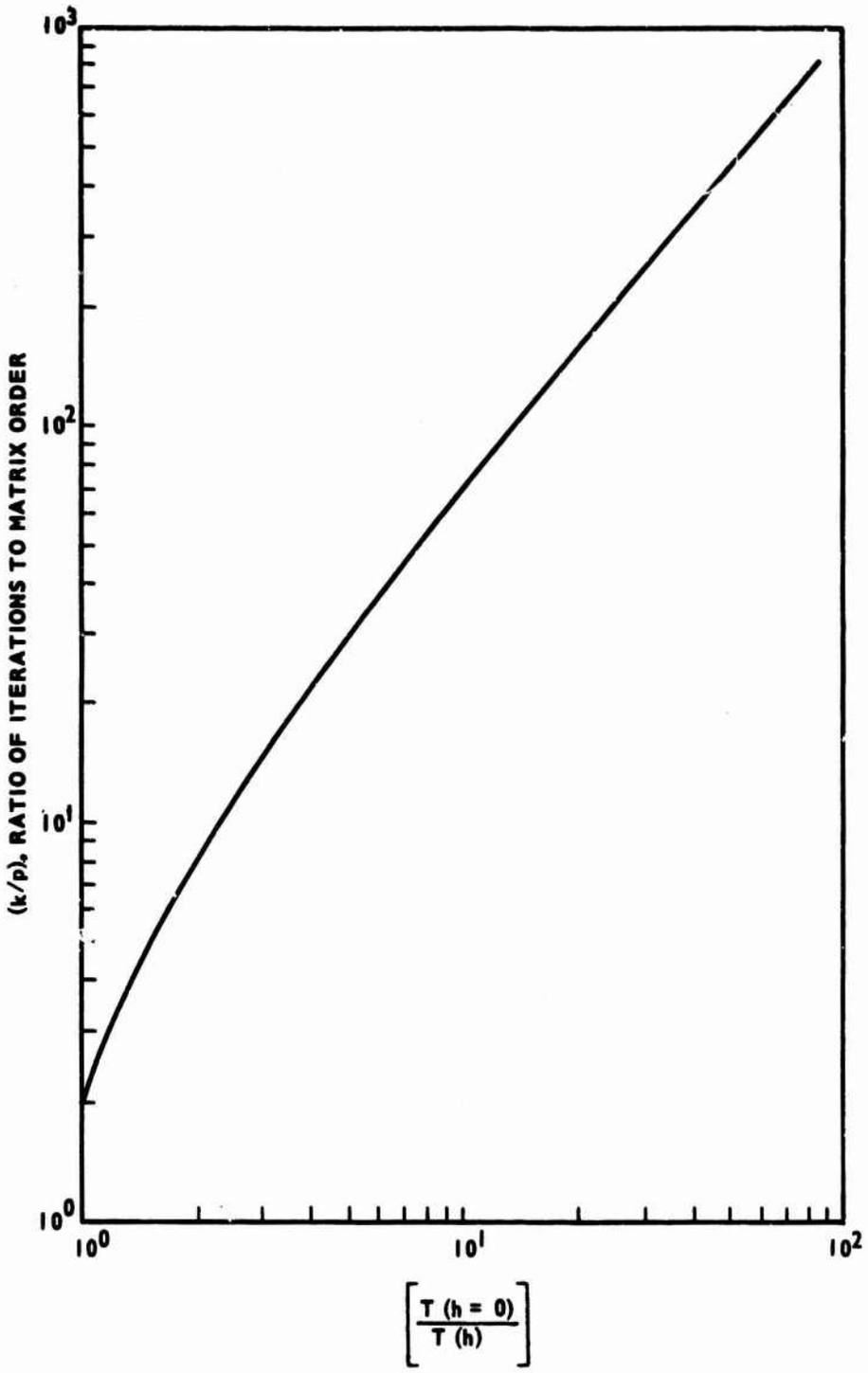

Figure 7. Ratio of Iterations to Matrix Order as a Function of the Number of Computations

To illustrate how this operation suppresses a given mode, the most general form of the initial distribution will be assumed. As before, this means that the initial distribution is represented by a sum of all possible modes. For the p^{th} order resonator matrix this is written as

$$\left[\bar{R}^0_{ns}(r_s)\right] = \sum_{j=0}^{p-1} a_j \left[\bar{R}_{js}(r_s)\right] , \qquad \text{(IV-45)}$$

where the a_j are finite. Assuming further that the mode being suppressed is the zeroth order, the initial field is then operated on by $[\mathcal{L}]$; this gives

$$[\mathcal{L}]\left[\bar{R}^0_{ns}(r_s)\right] = \left[B_{zs}\right] \sum_{j=0}^{p-1} a_j \left[\bar{R}_{js}(r_s)\right] - \Gamma_0 \sum_{j=0}^{p-1} a_j \left[\bar{R}_{js}(r_s)\right] . \qquad \text{(IV-46)}$$

Operating with the resonator matrix on a resonator mode is equivalent to multiplying that mode by its eigenvalue. Thus, equation (IV-46) can be written as

$$[\mathcal{L}]\left[\bar{R}^0_{ns}(r_s)\right] = \sum_{j=0}^{p-1} a_j \Gamma_j \left[\bar{R}_{js}(r_s)\right] - \Gamma_0 \sum_{j=0}^{p-1} a_j \left[\bar{R}_{js}(r_s)\right] . \qquad \text{(IV-47)}$$

When the summations on the right-hand side are combined, the lowest-ordered mode subtracts out. The result is

$$[\mathcal{L}]\left[\bar{R}^0_{ns}(r_s)\right] = \sum_{j=1}^{p-1} a_j \left(\Gamma_j - \Gamma_0\right) \left[\bar{R}_{js}(r_s)\right] . \qquad \text{(IV-48)}$$

This field is normalized to a peak magnitude of one and then used in place of $\left[\bar{R}^0_{ns}(r_s)\right]$ as the input field for the iteration. The resulting normalized field can be expressed by

$$(b)\,[\mathcal{L}]\left[\bar{R}^{0}_{ns}(r_s)\right] = \sum_{j=1}^{p-1} ba_j\left(\Gamma_j - \Gamma_0\right)\left[\bar{R}_{js}(r_s)\right] \ . \qquad \text{(IV-49)}$$

where (b) represents the normalization constant. Therefore, by defining

$$C_j = ba_j\left(\Gamma_j - \Gamma_0\right) \ ,$$

$$(b)\,[\mathcal{L}]\left[\bar{R}^{0}_{ns}(r_s)\right] = \sum_{j=1}^{p-1} C_j\left[\bar{R}_{js}(r_s)\right] \ . \qquad \text{(IV-50)}$$

Comparing the right-hand sides of equations (IV-50) and (IV-45) shows that they are similar except that in (IV-50) the lowest-order mode has been completely suppressed. Thus, applying the power method to the field given by equation (IV-50) will result, at least conceptually, of $\left[\bar{R}_{1s}(r_s)\right]$ dominating. That is, after k iterations, the $\left[\bar{R}_{1s}(r_s)\right]$ field will dominate over the higher-ordered modes. The field after k iterations is given by

$$\left[\bar{R}^{k}_{ns}(r_s)\right] = \left(\frac{1}{\Gamma^1_n \Gamma^2_n \cdots \Gamma^k_n}\right)\sum_{j=1}^{p-1} C_j\left(\Gamma_j\right)^k\left[\bar{R}_{js}(r_s)\right] \ , \qquad \text{(IV-51)}$$

where Γ^i_n is the normalization constant after the i^{th} iteration and $\left(\Gamma_j\right)^k$ is the eigenvalue of the j^{th} mode raised to the k^{th} power. Thus, for sufficiently large k and finite C_1,

$$\left|C_1(\Gamma_1)^k\right| \gg \left|C_j\left(\Gamma_j\right)^k\right| \ , \qquad \text{(IV-52)}$$

for j = 2, 3, ..., (p - 1), and equation (IV-51) becomes

$$\left[\bar{R}^{k}_{ns}(r_s)\right] = \left(\frac{C_1(\Gamma_1)^k}{\Gamma^1_n \Gamma^2_n \cdots \Gamma^k_n}\right)\left[\bar{R}_{1s}(r_s)\right] \ . \qquad \text{(IV-53)}$$

Since C_1, Γ_1, and $\Gamma^1_n, \Gamma^2_n, \ldots, \Gamma^k_n$ are constants,

$$\left[\bar{R}^{k}_{ns}(r_s)\right] = \left[\bar{R}_{1s}(r_s)\right] . \qquad \text{(IV-54)}$$

The implementation of this mode suppression technique is not as straightforward as the above example indicates. This is because the lowest-order mode cannot be exactly suppressed. Inexactness in the value of Γ_s results in the field containing a portion of the mode being suppressed. Therefore, even though it is small, the magnitude of this mode increases with every iteration with respect to the higher-ordered modes. If the field is iterated sufficiently the lowest-order mode will dominate.

The immediate conclusion is that the mode suppression operation should be applied more than once. However, if it is applied too often the resulting field distribution may not be that of the desired mode. This is because application of the suppression operation may result in higher-order modes increasing in magnitude relative to the mode being extracted.

The lack of accuracy in the eigenvalue of the mode being suppressed can be denoted by substituting $\left(\Gamma_s + \Delta\right)$ for Γ_s, where Δ represents a measure of this inaccuracy. In making this substitution it can be shown that every application of the suppression operation is equivalent to multiplying the j^{th} mode by $\left(\Gamma_j - \Gamma_s - \Delta\right)$. As was mentioned previously, each iteration is equivalent to multiplying the j^{th} mode by its eigenvalue. Therefore, if the zeroth order mode is being suppressed, and the initial field is that given by equation (IV-45), the field after (u) suppressions and (k) iterations will be proportional to

$$\sum_{j=0}^{p-1}{}' a_j\left(\Gamma_j - \Gamma_0 - \Delta\right)^u\left(\Gamma_j\right)^k\left[\bar{R}_{js}\left(r_s\right)\right] \quad . \tag{IV-55}$$

Thus, for the j = 1 mode to dominate the following condition must hold:

$$\left(\frac{|\Gamma_1 - \Gamma_0 - \Delta|}{|\Gamma_j - \Gamma_0 - \Delta|}\right)^u\left(\frac{|\Gamma_1|}{|\Gamma_j|}\right)^k \gg \frac{|a_j|}{|a_1|} \quad , \tag{IV-56}$$

where j = 0, 2, 3, ..., (p - 1).

From (IV-56) it is seen that the relative magnitude of the 1^{st} mode to the j^{th} mode changes by a factor of $\left|\frac{\Gamma_1 - \Gamma_0 - \Delta}{\Gamma_j - \Gamma_0 - \Delta}\right|$ for each application of the suppression operation. As has been stated previously, the eigenvalues are assumed to be ordered such that

$$|\Gamma_0| > |\Gamma_1| > |\Gamma_2| > \ldots > |\Gamma_{p-1}| \quad . \tag{IV-57}$$

Thus, it is reasonable to expect that for some cases $|\Gamma_0| \gg |\Gamma_j|$. If the condition also exists that $|\Delta| \ll |\Gamma_1 - \Gamma_0|$, then

$$\left(\frac{|\Gamma_1 - \Gamma_0 - \Delta|}{|\Gamma_j - \Gamma_0 - \Delta|}\right) \approx \left|\frac{\Gamma_1}{\Gamma_0} - 1\right| \quad . \tag{IV-58}$$

This means that whenever

$$\left|\frac{\Gamma_1}{\Gamma_0} - 1\right| < 1 \quad ,$$

it is possible that the suppression of the zeroth mode results in the $j \geq 2$ mode increasing relative to the j = 1 mode.

Consider now equation (IV-56) for the case j = 0. For each application of the suppression operation, the ratio of the j = 1 mode to the j = 0 mode is multiplied by $\left|\frac{\Gamma_1 - \Gamma_0 - \Delta}{\Delta}\right|$; therefore, for the ratio of these modes to increase, it must be that

$$|\Delta| < |\Gamma_1 - \Gamma_0 - \Delta| \ . \qquad \text{(IV-59)}$$

Simpler but more stringent requirements can be placed on $|\Delta|$ by noting that

$$|\Gamma_1 - \Gamma_0 - \Delta| \geq |\Gamma_1 - \Gamma_0| - |\Delta|$$

and that if

$$|\Delta| < |\Gamma_1 - \Gamma_0| - |\Delta|,$$

the inequality in (IV-59) is satisfied. Therefore, reducing this last inequality gives

$$|\Delta| < \frac{1}{2} |\Gamma_1 - \Gamma_0| \ . \qquad \text{(IV-60)}$$

This inequality expresses a sufficient condition on Δ such that each application of the suppression operation will result in the $j = 1$ mode increasing relative to the $j = 0$ mode.

It is apparent that both mode suppression and iteration operations are necessary for the $j = 1$ mode to dominate. Consider the inequality expressed in (IV-56); in particular consider the $j = 0$ mode, $j = 1$ mode, and $j \geq 2$ mode. Obviously, for the $j = 1$ mode to dominate over the $j = 0$ mode one must have

$$\left|\frac{\Gamma_1 - \Gamma_0 - \Delta}{\Delta}\right|^u \left|\frac{\Gamma_1}{\Gamma_0}\right|^k \gg \left|\frac{a_0}{a_1}\right| \ , \qquad \text{(IV-61)}$$

and for it to dominate over the $j \geq 2$ mode one must have

$$\left|\frac{\Gamma_1 - \Gamma_0 - \Delta}{\Gamma_j - \Gamma_0 - \Delta}\right|^u \left|\frac{\Gamma_1}{\Gamma_j}\right|^k \gg \left|\frac{a_j}{a_1}\right| \ . \qquad \text{(IV-62)}$$

More strict requirements are

$$\left(\frac{|\Gamma_1 - \Gamma_0| - |\Delta|}{|\Delta|}\right)^u \left|\frac{\Gamma_1}{\Gamma_0}\right|^k \gg \left|\frac{a_0}{a_1}\right| \qquad \text{(IV-63)}$$

and

$$\left(\frac{|\Gamma_1 - \Gamma_0| - |\Delta|}{|\Gamma_j - \Gamma_0| + |\Delta|}\right)^u \left|\frac{\Gamma_1}{\Gamma_j}\right|^k \gg \left|\frac{a_j}{a_1}\right| . \qquad \text{(IV-64)}$$

These requirements are somewhat more amenable to evaluation than (IV-61) and (IV-62).

It is assumed that Δ is given by

$$|\Delta| \approx \frac{1}{100} |\Gamma_1 - \Gamma_0| . \qquad \text{(IV-65)}$$

For most cases of interest this should be an easily obtainable accuracy.

From equation (IV-57) one can obtain

$$1 > \left|\frac{\Gamma_1}{\Gamma_0}\right| > \left|\frac{\Gamma_j}{\Gamma_0}\right|$$

and

$$1 > \left|\frac{\Gamma_j}{\Gamma_1}\right| > \left|\frac{\Gamma_j}{\Gamma_0}\right| .$$

Therefore, it is assumed that

$$\left|\frac{\Gamma_j}{\Gamma_1}\right| \approx \left|\frac{\Gamma_1}{\Gamma_0}\right| . \qquad \text{(IV-66)}$$

As it is expected that*

$$\left|\frac{\Gamma_j}{\Gamma_1}\right| < \left|\frac{\Gamma_1}{\Gamma_0}\right| ,$$

---

*For a symmetrical resonator having a Fresnel number of one and plane, circular mirrors, the eigenvalues of the various modes were examined in some detail. It was found that the magnitudes of these eigenvalues obeyed the inequality $\left|\frac{\Gamma_{n+2}}{\Gamma_{n+1}}\right| < \left|\frac{\Gamma_{n+1}}{\Gamma_n}\right|$ for $n = 0, 1, 2, 3, 4$ and for angular degeneracies of 0, 1, 2, or 3.

using (IV-66) in (IV-64) should increase the convergence requirements.

For convenience it is assumed that all the modes are present in the initial field with equal magnitudes; that is,

$$|a_0| = |a_1| = |a_2| = \ldots \quad . \tag{IV-67}$$

With experience, the initial field can usually be chosen so that the magnitude of the j = 1 mode is greater than the magnitude of any other mode.

It is also assumed that

$$|\Gamma_j - \Gamma_0| \approx |\Gamma_1 - \Gamma_0| \quad . \tag{IV-68}$$

For resonators with small Fresnel numbers this assumption should be reasonable; however, it must be granted that (IV-68) is very approximate.

By using the above in equations (IV-63) and (IV-64),

$$(99)^u \left|\frac{\Gamma_1}{\Gamma_0}\right|^k \gg 1 \tag{IV-69}$$

and

$$(0.98)^u \left|\frac{\Gamma_0}{\Gamma_1}\right|^k \gg 1 \tag{IV-70}$$

are obtained. If convergence is affected equally by the j = 0 mode and the j ≥ 2 mode, then the left-hand sides of equations (IV-69) and (IV-70) can be equated. From this one can obtain

$$(k/u) \approx (2.3)/\ln \left|\frac{\Gamma_0}{\Gamma_1}\right| \quad . \tag{IV-71}$$

This relates the number of iteration operations per number of suppression operations required for convergence to the j = 1 mode. A plot of this expression is given in Figure 8. The ratio $\left|\frac{\Gamma_0}{\Gamma_1}\right|$ varies in some inverse manner to the resonator Fresnel number; for large Fresnel numbers the ratio approaches

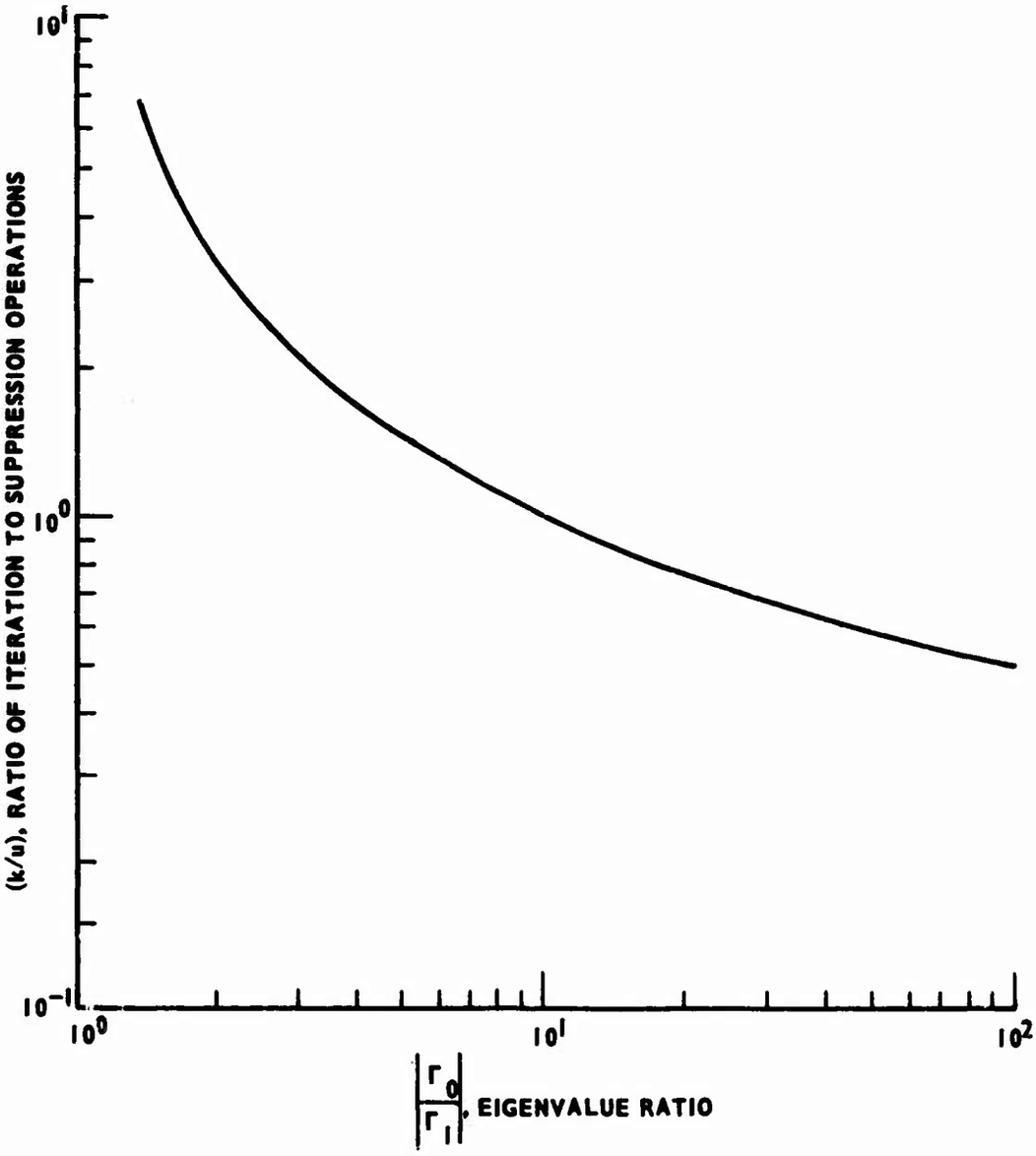

Figure 8. Ratio of Iterations to Suppression Operations as a Function of Eigenvalue Ratio

one and for small Fresnel numbers it is much larger than one. Thus, for resonators having large Fresnel numbers (k/u) should be large and vice versa.

It should be noted that the more accurate Γ_0 is known, the larger the ratio of (k/u) can be used. In practical terms this means that the total number of suppression operations can be reduced. However, a word of caution is in order: The computational time saved in reducing the number of suppression operations may be less than that required to obtain Γ_0 to a greater accuracy.

CHAPTER V

TRANSVERSE MODE CONTROL

For optimum operation of the self-focusing laser the resonator must oscillate in a single transverse mode. Although focusing can be achieved with higher-order modes, it has been found that the best results are obtained when the laser oscillates in the TEM_{00} mode. This mode has the field configuration which must closely approximate the desired uniform field. In the usual plane parallel resonator the TEM_{00} mode is the dominant mode; however, this study has shown that the selective reflection characteristics of the zoned mirror may change the order of the mode losses. In this case a higher-order mode becomes dominant, and mode control is then necessary.

The usual technique for transverse mode control is based on the fact that diffraction losses are different for different order modes. Mode control is achieved by placing apertures in the resonator in such a way that undesired modes experience losses greater than those of the desired mode. These apertures decrease the beam cross section; and since the zoned mirror of the self-focusing resonator should have a large radiating area, this method of mode control is not desirable.

In this chapter another method of transverse mode control is considered. It is based on a principle of mode enhancement: Losses of the desired mode

are reduced by introducing a field distribution, identical to the desired mode, into the laser resonator. This has the effect of reducing the net loss of the desired mode; and if its loss is reduced beyond that of all other modes, this desired mode will dominate.

This mode enhancement technique is based on the mode switching work of Johnston, et al.,[1] who experimentally demonstrated that the transverse mode structure of one laser could be switched to another mode by coupling radiation into the resonator from a second laser. Based on their results that the transverse mode structure of one laser could be controlled by another laser, a computer model was developed to simulate the coupling of radiation from one laser into another. This model was then used to evaluate the effectiveness of using mode enhancement for transverse mode control.

A block diagram of the physical arrangement for mode enhancement is shown in Figure 9. The control laser is operated in the desired transverse mode. The radiation out of the control laser is directed through an optical isolator and mode matching optics into the output laser. Both of the lasers are oscillators; hence, the isolator is necessary to assure that the control laser operates on the output laser and not vice versa. The mode matching optics transform the mode structure of the control laser to that of the output laser. It should be noted that the two oscillators must be operated within the same laser line.

---

[1]Johnston, W. D., Jr., Tingye Li, and P. W. Smith, Journal of Quantum Electronics, Volume QE-4, pp. 469-471 (1968).

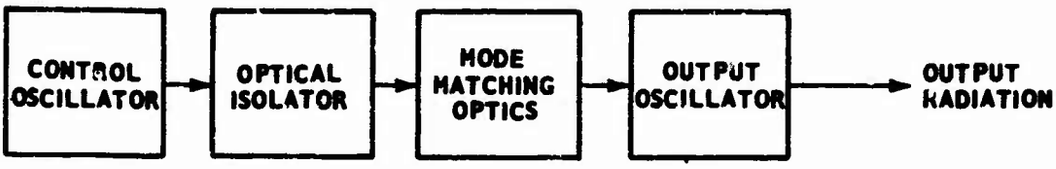

Figure 9. Block Diagram of Mode Enhancement System

The numerical model used to represent this physical system is an idealization of the actual physical processes involved. First a given resonator is described by the resonator equations; this represents the output oscillator. Two modes of this resonator are then determined, the dominant mode and a higher loss mode. The field configuration of the higher loss mode is used as the input from the control laser. The model was used to determine the system constraints required to force the output resonator to oscillate in the higher loss mode.

To understand the model, the iterating process described in the preceding chapter needs to be briefly reviewed. The iteration process represents a wave traveling back and forth in the resonator. At each mirror the wave experiences both diffraction and transmission losses. On each iteration the field is normalized to a magnitude of one; therefore, the normalization represents a constant gain. If the initial field is composed of many modes, then after many passes through the resonator the mode having the least loss dominates.

The enhancement model differs only slightly from this iteration process. The difference is that each time the field is on the input mirror an input field is added to the resonator field, and the summed field is then used as the source field in the iteration process. This input field represents the

radiation from the control oscillator and it has the field configuration of a mode of the output resonator. Thus, the input field can be viewed as a selective gain mechanism; it continually adds a pure mode to the field within the output resonator. If this increase in gain more than makes up for the greater resonator losses, the input field will become dominant.

The processes involved in the numerical model are as follows:

(1) The dominant mode of the output resonator is determined. It is designated the TEM_{mn} mode; its normalized field on the input mirror is given by $\left[\bar{R}_{ns}(r_s)\right]$.

(2) One of the higher loss modes of the output resonator is determined. It is designated the TEM_{mc} mode; its normalized field is given by $\left[\bar{R}_{nc}(r_s)\right]$. This field is used as the source field from the control resonator. To allow for changes in magnitude of the input, it is assumed that the control field transmitted into the output resonator is given by $\left[T_s \bar{R}_{nc}(r_s)\right]$, where T_s is a real nonnegative constant.

(3) An initial distribution is assumed in the output resonator; to this is added the input from the control resonator, $\left[T_s \bar{R}_{nc}(r_s)\right]$.

(4) The following iterative procedure is then used:

   (a) The field resulting from a double pass through the resonator is calculated.

   (b) This field is phase normalized and $\left[T_s \bar{R}_{nc}(r_s)\right]$ is added.

   (c) This summed field is normalized to a peak magnitude of one.

   (d) From step (c) go to step (a). This procedure is continued

until the normalized field in the output resonator converges to a fixed value.

The field on the input mirror is designated as $\left[P_{ns}(r_s)\right]$. As was done in Chapter IV, the field on the output mirror, $\left[R_{nz}(r_z)\right]$, can be related to this field by

$$\left[R_{nz}(r_z)\right] = \left[A_s\right]\left[\bar{P}_{ns}(r_s)\right] , \qquad \text{(V-1)}$$

and the field reflected back to the input mirror, in terms of the field on the output mirror, is given by

$$\left[R_{ns}(r_s)\right] = \left[A_z\right]\left[\bar{R}_{nz}(r_z)\right] . \qquad \text{(V-2)}$$

The terms $\left[A_s\right]$ and $\left[A_z\right]$ are the single pass resonator matrices defined by equations (IV-9) and (IV-10). The bars over the fields represent the usual normalizations obtained by dividing the fields by their value at maximum magnitude.

The field on the input mirror is obtained by adding the field transmitted from the control resonator to the phase normalized reflected field. This phase normalization is necessary as the resonator equations do not preserve the absolute phase of the fields. The field on the input mirror is given by

$$\left[P_{ns}(r_s)\right] = \left[T_s \bar{R}_{cs}(r_s)\right] + \left|\gamma_{ns}\gamma_{nz}\right|\left[\bar{R}_{ns}(r_s)\right] . \qquad \text{(V-3)}$$

The terms γ_{ns} and γ_{nz} are the complex constants obtained in normalizing $\left[R_{ns}(r_s)\right]$ and $\left[R_{nz}(r_z)\right]$ respectively. As shown by the resonator equations, if $\left[\bar{P}_{ns}(r_s)\right]$ represents a field on the input mirror, the field after a double pass is given by $\left[A_z\right]\left[A_s\right]$ times $\left[\bar{P}_{ns}(r_s)\right]$. From equations (V-1) and (V-2) it can be shown that

$$\left[A_z\right]\left[A_s\right]\left[\bar{P}_{ns}(r_s)\right] = \gamma_{ns}\gamma_{nz}\left[\bar{R}_{ns}(r_s)\right] \cdot$$

Therefore, comparing this to the second term on the right-hand side of equation (V-3) the effect of the phase normalization is apparent; the phase normalization allows the system to reach a steady state where the two components of the field on the input mirror have a fixed relationship.

Equations (V-1), (V-2), and (V-3) represent the characteristics of the mode enhancement system. These equations relate the fields at the mirrors of the output resonator in terms of the resonator characteristics and the input field from the control resonator. The equations were programmed for use on an IBM 7094 computer in the iterative format given above. The resulting computer model represents an oscillating resonator being injected with a constant field from another resonator. The model was set up so that the initial field, resonator characteristics, and the rate that the input signal was injected into the resonator could be varied.

Before some of the results obtained with model are presented, a simplified steady-state analysis will be given.

First, it will be assumed that a steady-state exists; by this it is meant that the normalized resonator field repeats itself after a double pass through the resonator. Since the model is linear it is reasonable to expect that the steady-state field is a linear combination of the input field and the normally dominant resonator field. Thus, the normalized, steady-state field on the input mirror can be expressed as

$$\bar{P}_{ns}(r_s) = a_n\bar{R}_{ns}(r_s) + a_c\bar{R}_{nc}(r_s) \quad , \qquad \text{(V-4)}$$

where a_n and a_c are complex constants, and where $\bar{R}_{ns}(r_s)$ is the normally dominant field of the resonator and $\bar{R}_{nc}(r_s)$ is the input field from the control resonator. Both fields are pure modes; therefore, a double pass through the resonator is equivalent to multiplying the fields by their eigenvalues. Thus, after a double pass through the resonator the field is given by

$$a_n \Gamma_n \bar{R}_{ns}(r_s) + a_c \Gamma_c \bar{R}_{nc}(r_s) \quad , \tag{V-5}$$

where Γ_n and Γ_c are the eigenvalues of $\bar{R}_{ns}(r_s)$ and $\bar{R}_{nc}(r_s)$, respectively.

To satisfy the condition of a fixed phase relation between the input field and the resonator field the phase is normalized. This is accomplished by multiplying (V-5) by $(|A|/A)$, where A is the value of (V-5) where its magnitude is maximum. The result is

$$\frac{|A|}{A}\left[a_n \Gamma_n \bar{R}_{ns}(r_s) + a_c \Gamma_c \bar{R}_{nc}(r_s)\right] \quad . \tag{V-6}$$

This represents the phase normalized form of $\bar{P}_{ns}(r_s)$ after a double pass through the resonator. To this field is added the input field, $T_s \bar{R}_{nc}(r_s)$, and

$$\left[\frac{|A| a_n \Gamma_n}{A}\right]\bar{R}_{ns}(r_s) + \left[\frac{|A| a_c \Gamma_c + T_s A}{A}\right]\bar{R}_{nc}(r_s) \tag{V-7}$$

is obtained.

Gain is expressed by normalizing (V-7) so that the peak field has a magnitude of one. This is done by dividing (V-7) by B, where B is the value of (V-7) where its magnitude is maximum. By assumption, steady conditions exist; therefore, after this last normalization the field is identical to the initial field. Thus,

$$\bar{P}_{ns}(r_s) = \left[\frac{|A|a_n\Gamma_n}{AB}\right]\bar{R}_{ns}(r_s) + \left[\frac{|A|a_c\Gamma_c + T_sA}{AB}\right]\bar{R}_{nc}(r_s) \quad . \quad \text{(V-8)}$$

Equating coefficients of the fields in equations (V-4) and (V-8) results in

$$B = \frac{|A|}{A}\Gamma_n \quad \text{(V-9)}$$

and

$$a_c = \frac{T_sA}{AB - |A|\Gamma_c} \quad . \quad \text{(V-10)}$$

Substituting (V-9) into (V-10) and taking the absolute value of the result gives

$$|a_c| = \frac{T_s}{|\Gamma_n - \Gamma_c|} \quad . \quad \text{(V-11)}$$

From this it can be seen that the magnitude of the TEM_{mc} field is proportional to the rate it is being introduced into the resonator and inversely proportional to the difference between the eigenvalues of the TEM_{mc} and the TEM_{mn} modes. Although this result is intuitively satisfying, in that one would expect the portion of the TEM_{mc} mode present to be related to the rate it is being supplied to the resonator, it is difficult to obtain usable results from this approach.

It is more instructive to determine the requirements on the system for maintaining a TEM_{mc} mode once this mode has been established. To do this one assumes that the field on the input mirror is given by

$$\bar{P}_{ns}(r_s) = \Delta\bar{\Pi}_{ns}(r_s) + \bar{R}_{nc}(r_s) \quad , \quad \text{(V-12)}$$

where

$$|\Delta| \ll |\Gamma_c| \quad .$$

In a double pass through the resonator the field becomes

$$\Delta\Gamma_n \bar{R}_{ns}(r_s) + \Gamma_c \bar{R}_{nc}(r_s) \quad . \tag{V-13}$$

By normalizing the phase one obtains, approximately,

$$\left[\frac{|\Gamma_c|\Delta\Gamma_n}{\Gamma_c}\right]\bar{R}_{ns}(r_s) + |\Gamma_c|\bar{R}_{nc}(r_s) \quad . \tag{V-14}$$

To this is added the input field, $T_s \bar{R}_{nc}(r_s)$, and

$$\left[\frac{|\Gamma_c|\Delta\Gamma_n}{\Gamma_c}\right]\bar{R}_{ns}(r_s) + \left[|\Gamma_c| + T_s\right]\bar{R}_{nc}(r_s) \tag{V-15}$$

is obtained.

Normalizing the field to a peak magnitude of one gives, approximately,

$$\left(\frac{\left[\frac{|\Gamma_c|\Delta\Gamma_n}{\Gamma_c}\right]}{\left[|\Gamma_c| + T_s\right]}\right)\bar{R}_{ns}(r_s) + \bar{R}_{nc}(r_s) \quad . \tag{V-16}$$

This term represents the field given by (V-12) after one complete iteration of the model.

A sufficient condition for the continued dominance of the TEM_{mc} mode is that with each iteration the TEM_{mn} mode decreases in magnitude. This means that the coefficient of $\bar{R}_{ns}(r_s)$ decreases in magnitude with each iteration; therefore, by comparing the coefficients of $\bar{R}_{ns}(r_s)$ as given by (V-12) and (V-16) one obtains the resulting requirement on T_s that

$$T_s > |\Gamma_n| - |\Gamma_c| \quad . \tag{V-17}$$

Thus, if the TEM_{mc} mode dominates, then its dominance will be maintained if the condition in (V-17) holds. It should be noted that the normally dominant

mode of the resonator is the TEM_{mn} mode; therefore,

$$|\Gamma_n| - |\Gamma_c| > 0 \ .$$

Further insight into the operation of this mode control laser system can be had by considering mode losses. As has been pointed out previously, for a given mode to dominate it must experience the least loss in the system. The TEM_{mn} mode is the dominant mode of the output resonator when there is no input from the control resonator. In a round trip through the resonator this mode has a power loss given by $\left[1 - |\Gamma_n|^2\right]$. The TEM_{mc} mode in the output resonator, under the same condition of no input from the control resonator, has a power loss given by $\left[1 - |\Gamma_c|^2\right]$.

Suppose now that the field structure in the output resonator is composed of the TEM_{mn} and TEM_{mc} modes and that a TEM_{mc} mode from the control laser is introduced into the resonator. The round trip power loss of the TEM_{mn} mode remains the same; however, because of the input field the round trip power loss of the TEM_{mc} mode decreases. Therefore, if one assumes that the input signal directly decreases the power loss of the TEM_{mc} mode, the TEM_{mc} mode will dominate if the condition exists that

$$\left[1 - |\Gamma_c|^2 - T_s^2\right] < \left[1 - |\Gamma_n|^2\right] . \qquad \text{(V-18)}$$

This inequality simply states that for the TEM_{mc} mode to dominate, the power loss of this mode must be less than the power loss of the TEM_{mn} mode. Solving (V-18) for T_s one obtains

$$T_s > \left[|\Gamma_n|^2 - |\Gamma_c|^2\right]^{1/2} . \qquad \text{(V-19)}$$

By comparing (V-17) and (V-19) one can show that the T_s given here is greater than that required for mode maintenance. This follows directly from the fact that since

$$|\Gamma_n| > |\Gamma_c| ,$$

$$|\Gamma_n| - |\Gamma_c| < \left[|\Gamma_n|^2 - |\Gamma_c|^2\right]^{1/2} . \qquad \text{(V-20)}$$

There are now two basic results pertaining to the mode control system. In (V-17) there is a requirement on T_s for mode maintenance, and in (V-19) there is a requirement on T_s for mode switching. Several tests were made on the numerical model of the mode control system to check these results; in all cases the computational results agreed with those specified in (V-17) and (V-19).

One of the first tests was to check the requirement for mode maintenance. Utilizing the techniques described in Chapter IV the normally dominant mode and a higher loss mode of a self-focusing resonator were determined. The higher loss mode was used as the control field, $\bar{R}_{nc}(r_c)$, and a slightly perturbed $\bar{R}_{nc}(r_c)$ was used as the initial field within the resonator. With a T_s slightly greater than the minimum, $\left[|\Gamma_n| - |\Gamma_c|\right]$, it was found that the field within the resonator remained $\bar{R}_{nc}(r_s)$. For cases where T_s was less than the minimum, the final field converged to configurations other than $\bar{R}_{nc}(r_s)$.

In the next test of the model, the same resonator and the same input field were used, but the initial field was chosen so that it contained a large component of the normally dominant field, $\bar{R}_{ns}(r_s)$. It was found that the

condition on T_s for mode maintenance was not sufficient to cause the field to converge to the TEM_{mc} mode. That is, with a T_s slightly greater than $\left[|\Gamma_n| - |\Gamma_c|\right]$, the field would not converge to the TEM_{mc} mode.

In general it was found that if the initial field had a large component of $\bar{R}_{ns}(r_s)$, then T_s had to be considerably larger than $\left[|\Gamma_n| - |\Gamma_c|\right]$ before the field would converge to the TEM_{mc} mode. In fact, for all these cases it was found that only if T_s were greater than that dictated by the power loss requirements $\left(\text{that is, } T_s > \left[\Gamma_n|^2 - |\Gamma_c|^2\right]^{1/2}\right)$ would the field converge to the TEM_{mc} mode.

For an example, some of the results obtained for a particular case are presented below. The output resonator had a Fresnel number of one. It was formed by plane circular mirrors. The input mirror had a constant reflectivity. The output mirror was a zoned mirror having thirteen half period zones. Seven of the zones were completely transmitting, and the remaining six zones were completely reflecting. The eigenvalue of the TEM_{mn} mode had a magnitude of (0.351), and the eigenvalue of the TEM_{mc} mode had a magnitude of (0.126). The initial field distribution had a strong $\bar{R}_{ns}(r_s)$ component. The final fields obtained for different values of T_s are shown in Figures 10 and 11 as a function of the normalized mirror radius; the field magnitudes are shown in Figure 10 and the corresponding phases are shown in Figure 11. When T_s was zero, the condition of no input signal existed and the field converged to its normally dominant mode. When T_s had the value (0.4), the condition

$$T_s > \left[|\Gamma_n|^2 - |\Gamma_c|^2\right]^{1/2},$$

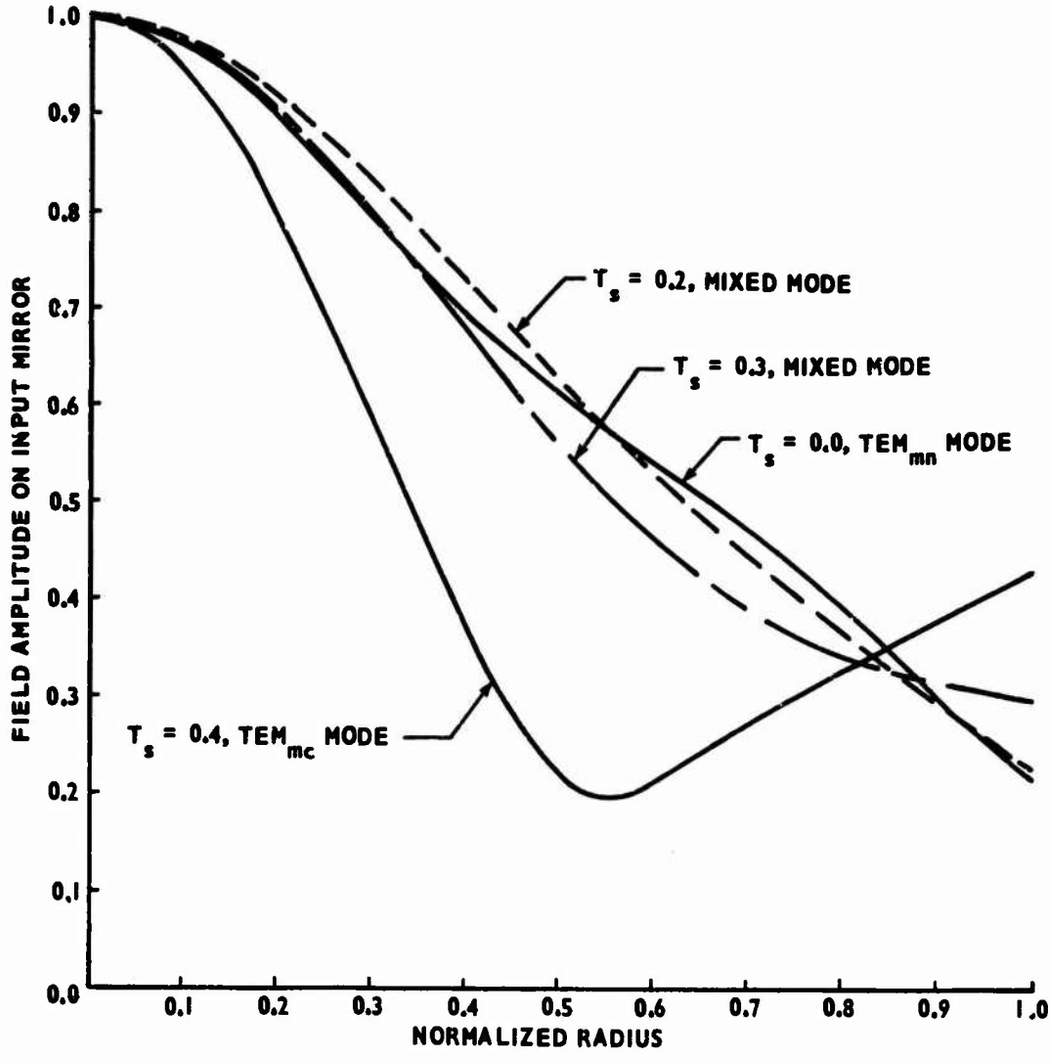

Figure 10. Field Amplitude on Input Mirror for Various Values of T_s

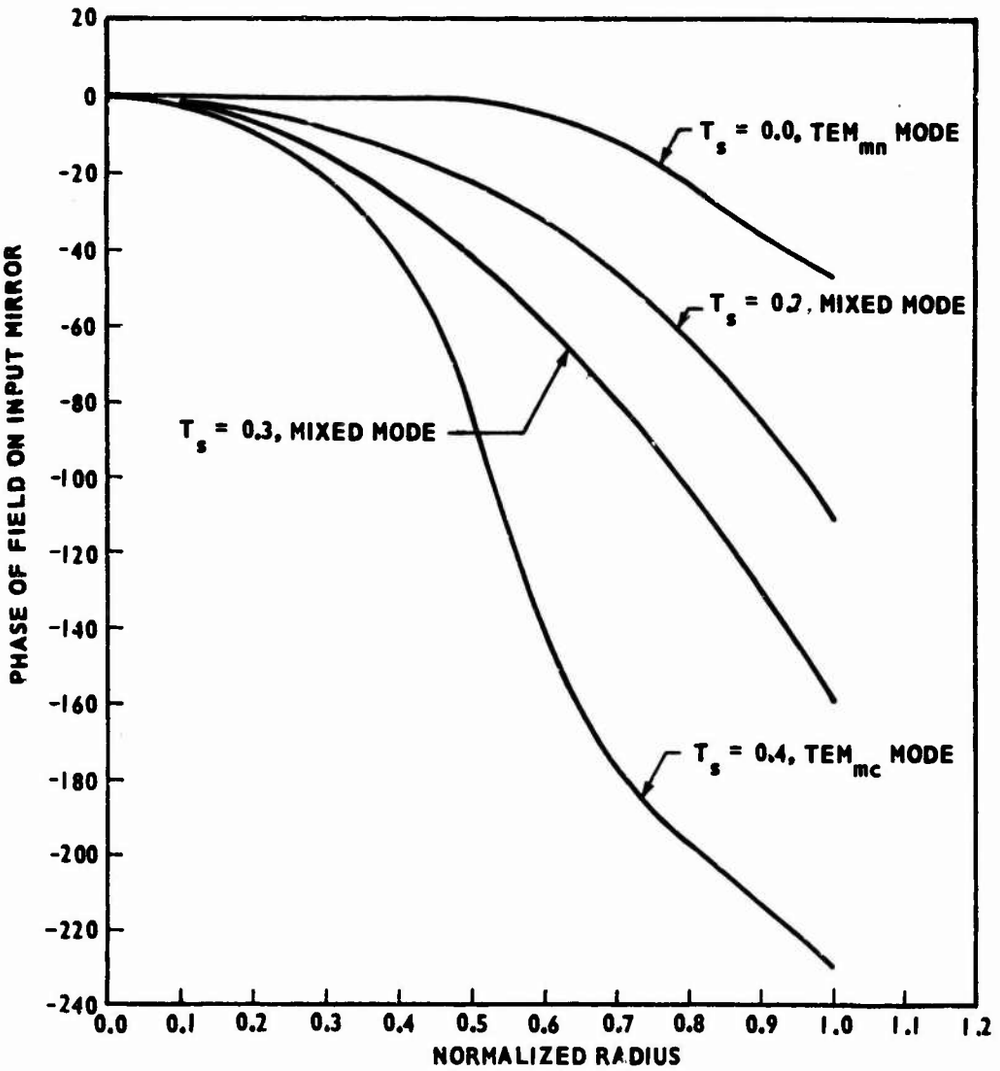

Figure 11. Phase of Field on Input Mirror for Various Values of T_s

existed, and as expected the field converged to the TEM_{mc} mode. This means that there was enough input to switch the resonator field from the TEM_{mn} mode. For T_s equal to (0.2) or (0.3) there was not sufficient input to cause the modes to switch, and the fields converged to mixed modes.

This same resonator was examined for the condition of the initial field being almost a pure TEM_{mc} mode. It was found that the field would remain TEM_{mc} if T_s obeyed the inequality expressed in (V-17).

The results of the analysis of the mode enhancement model indicate that the mode enhancement technique could be used for transverse mode control. In using this technique one should make use of the finding that less input signal is required for mode maintenance than is required to switch modes. In a practical sense, this means that the control oscillator should be activated before the output oscillator; this would assure that the initial field had the desired configuration.

CHAPTER VI

ANALYSIS OF THE SELF-FOCUSING RESONATOR

The basic self-focusing resonator is formed by flat, circular mirrors having equal radii. One of the mirrors has a uniform reflectivity of unity, it is designated as the input mirror. The other mirror is a zoned mirror, it is designated as the output mirror. The characteristics of this zoned resonator are established by the Fresnel number of the resonator and the configuration of the zoned mirror.

The zoned mirror is usually composed of alternately reflecting and transmitting zones of equal area. The reflecting zones have a reflectivity of unity. The transmission zones are assumed to have no absorption losses, but they may be partially reflecting. For some cases considered, the total number of zones and the number of transmission zones relative to the number of reflection zones have been varied. The areas of both the reflecting and transmitting zones are usually fixed so that they correspond to half-period zones; however, some cases have been considered in which the area of the zones was different from this.

The method used in analyzing a given resonator was first to calculate the resonator mode structure. This was accomplished by using the numerical techniques discussed in Chapter IV. This gives the fields on both mirrors in

terms of relative amplitudes and phases, as well as the eigenvalue of the mode obtained. From this eigenvalue the double pass power loss and double pass phase shift are directly obtainable. The next step was to utilize the transmission characteristics of the zoned mirror and the resonator field on the output mirror to specify the transmitted field. This transmitted field was used as a source field and the exterior fields were then calculated. These exterior fields included the power transmitted through the zoned mirror, the field along the resonator axis, and the field in the focal plane. The equations describing these fields are given in Chapter II. They were evaluated by using straightforward numerical integration techniques. A numerical sampling density of 100 points across the resonator mirrors was generally used; however, for some of the resonator configurations analyzed, higher sampling densities were required. As was mentioned in Chapter IV, the sampling densities were such that the resonator modes were obtained to within an accuracy of about 1 percent. The same sampling densities as those used to determine the resonator modes were used in calculating the exterior fields.

In the following sections of this chapter the results of the analysis of the self-focusing resonator are presented.

A. A Zoned Resonator

As a means of illustrating some of the basic characteristics of the self-focusing resonator, the analysis of a specific zoned resonator is presented in this section. The Fresnel number of this resonator was eighteen, and the output mirror was composed of thirteen half-period zones. Six of the zones

were completely reflecting, and the remaining seven were 50 percent reflecting and 50 percent transmitting. The partially transmitting zones provided the output coupling from the resonator, and this output field established the focused field. The transmissivity of the input mirror was uniform and had a value of one.

In order to provide a base reference for this zoned resonator, a resonator having the same Fresnel number but unzoned mirrors was also analyzed. This unzoned resonator represents the usual resonator configuration where both mirrors have uniform reflectivities.

The TEM_{00} mode structure of the unzoned resonator is shown in Figures 12 and 13. The amplitude of the field is given in Figure 12 and the phase is given in Figure 13. The amplitude of the field is given on a relative basis such that the maximum magnitude is unity, and the phase is normalized so that the phase at the center of the mirror is zero. The radius is also given in a normalized form; it is obtained by dividing the actual radius by the maximum radius of the mirror. The TEM_{00} mode is symmetrical about the resonator axis; therefore, the field is completely specified by describing the field on a single radius. Since the mirrors are identical, the normalized fields on the two mirrors of the resonator are also identical.

The round-trip power loss for this TEM_{00} mode was found to be 0.7 percent. This, of course, is for mirrors having reflectivities of unity. Thus, this loss represents the diffraction loss of the resonator; it is a measure of the radiation lost over the edges of the mirrors by a wave making a double pass through the resonator.

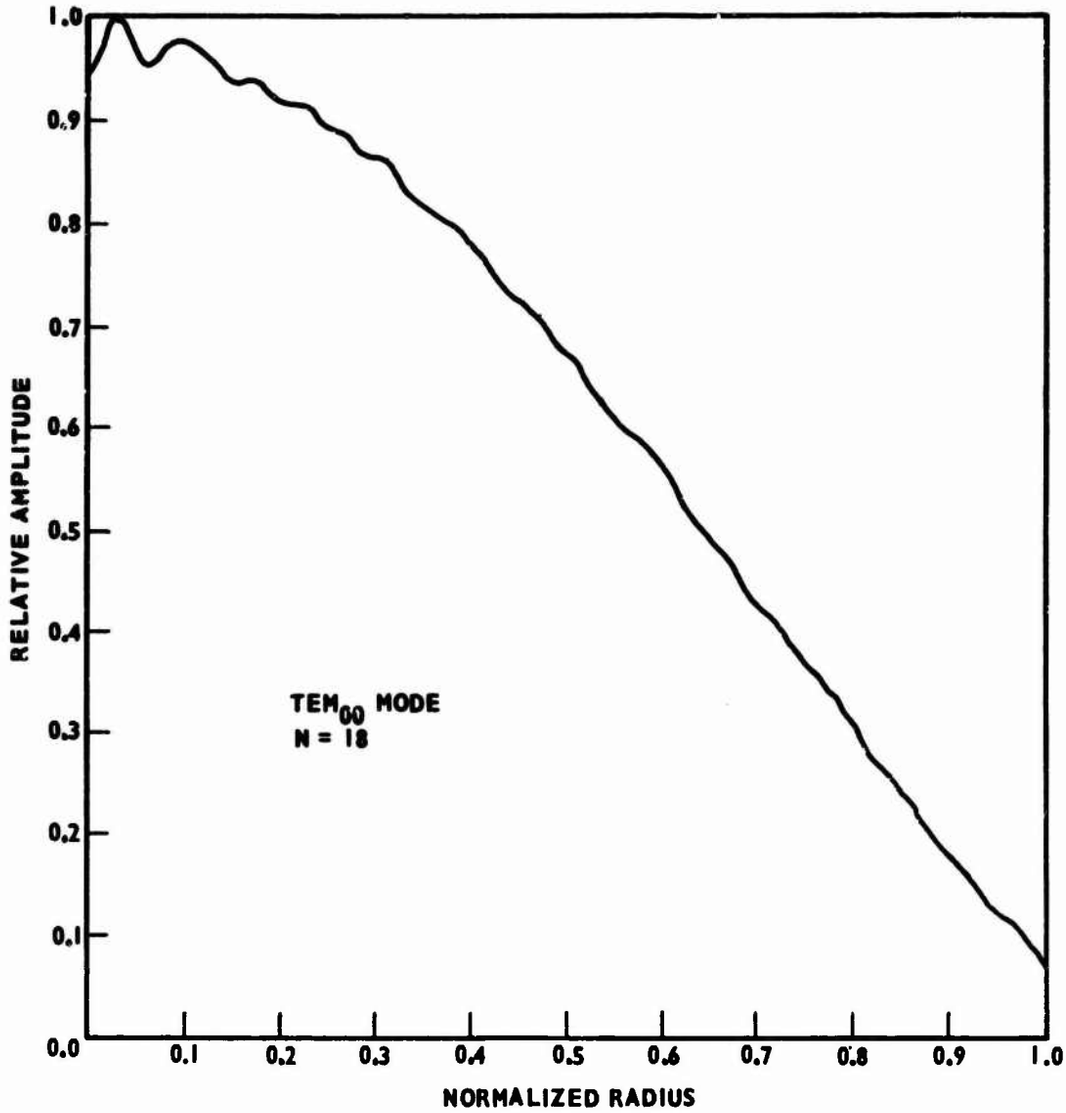

Figure 12. Relative Amplitude of the TEM_{00} Mode; Resonator Fresnel Number = 18, Unzoned Resonator

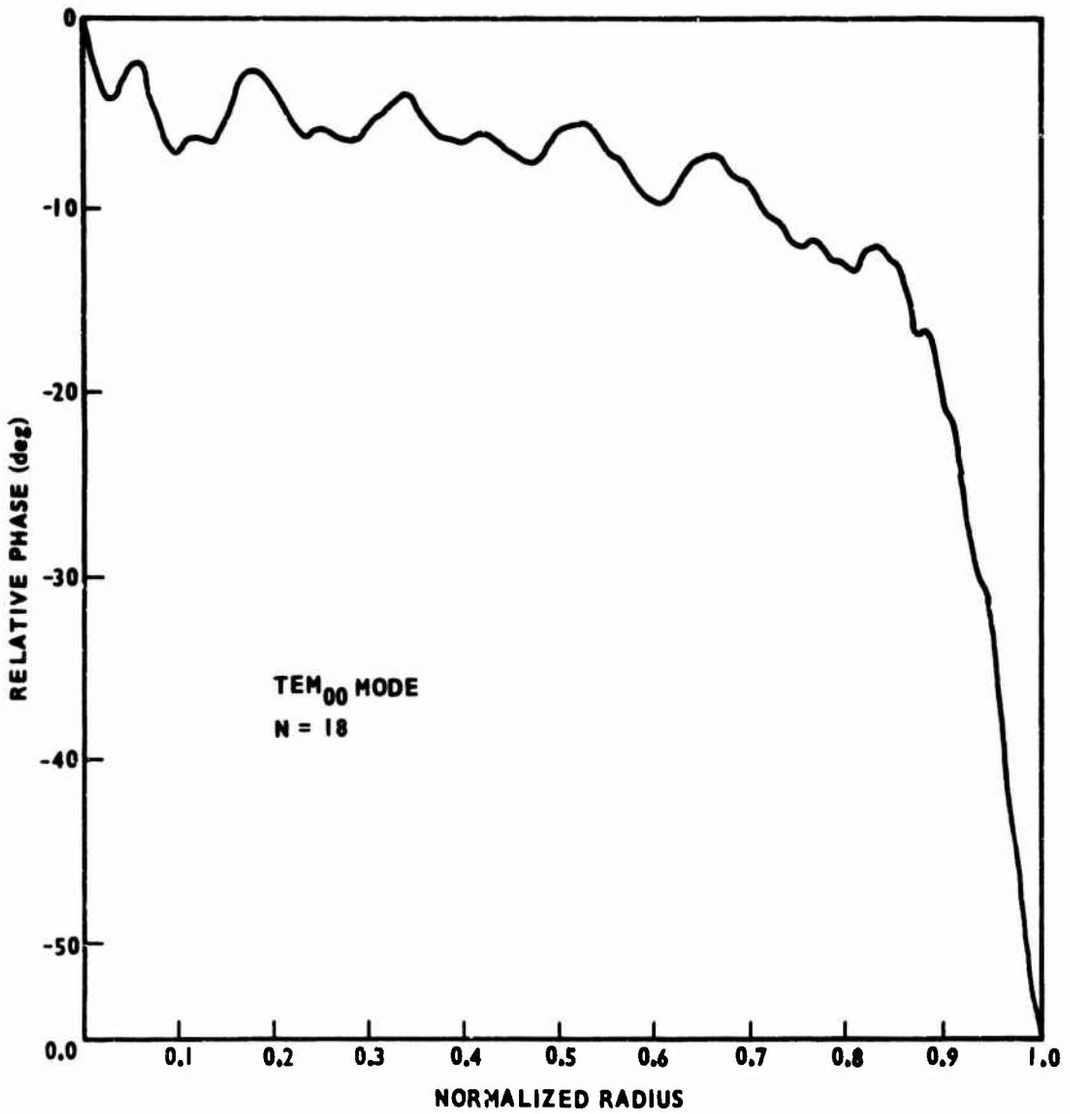

Figure 13. Relative Phase of the TEM_{00} Mode; Resonator Fresnel Number = 18, Unzoned Resonator

Although the amplitude of the field has a distribution that is quite far from uniform, the phase variation is small, changing only by about 55 degrees from the center to the edge of the mirror. Most of this phase variation occurs at the edge of the mirrors. Thus, since the amplitude is small at the outer edge of the mirrors, the phase variation should have little effect on a transmitted field. That is, if one of the mirrors were made partially transmitting, the transmitted field would be almost the same as that obtained by a field having the same amplitude distribution but a constant phase. Therefore, if one of the resonator mirrors could be replaced by a zoned mirror, without distributing the resonator field structure, one would expect some focusing of the output radiation. The problem is, of course, that when the mirror is changed, the resonator mode configuration is also changed. This new field structure may or may not be capable of producing a focused output.

All the resonators examined in this study exhibited the characteristic that the field of the unzoned resonator was more regular than the corresponding field of the zoned resonator. This leads one to the point of view of considering the field structure of the unzoned resonator as a standard and the fields of the zoned resonators as perturbations of this standard.

The field configuration of the TEM_{00} mode for the zoned resonator is shown in Figures 14 through 17. The field representing this mode on the output mirror is given as an amplitude and phase in Figures 14 and 15 respectively. The corresponding field on the input mirror is shown in Figures 16 and 17. Because the resonator mirrors are not identical the

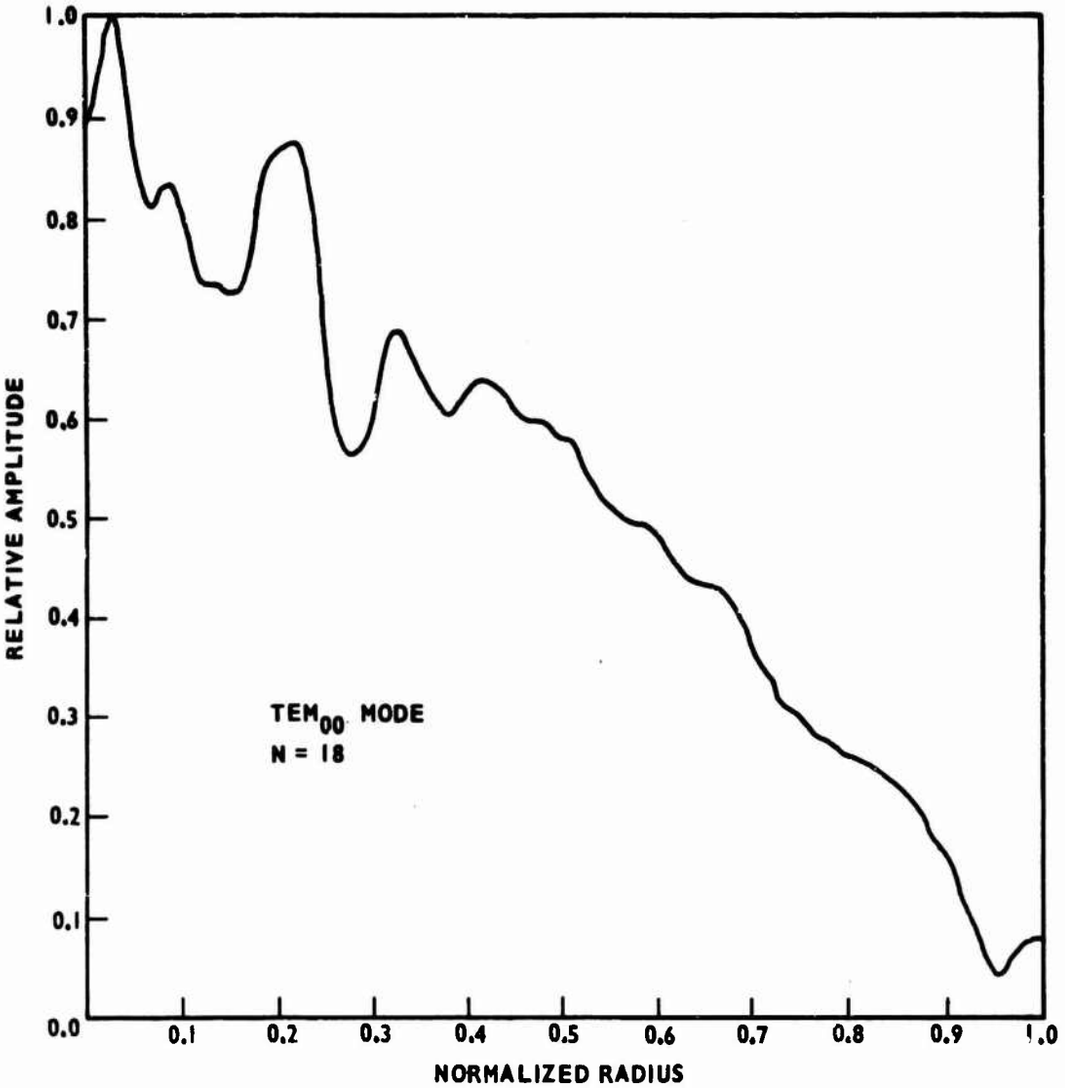

Figure 14. Relative Amplitude of the TEM_{00} Mode on the Output Mirror; Resonator Fresnel Number = 18, Output Mirror Zoned, Reflectivity of Transmission Zones = 0.500 (13 half-period zones, 7 transmission)

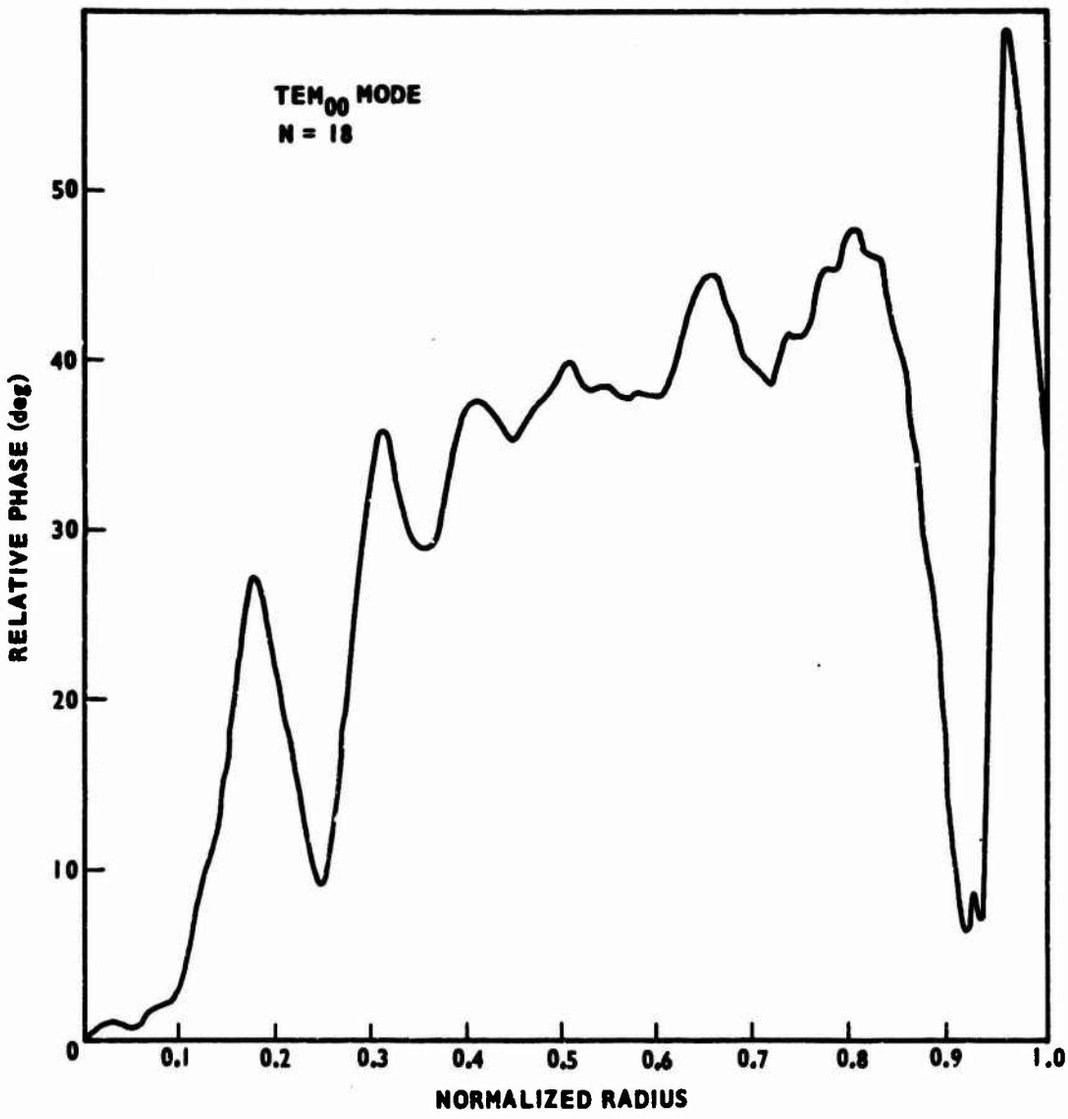

Figure 15. Relative Phase of the TEM_{00} Mode on the Output Mirror; Resonator Fresnel Number = 18, Output Mirror Zoned, Reflectivity of Transmission Zones = 0.500 (13 half-period zones, 7 transmission)

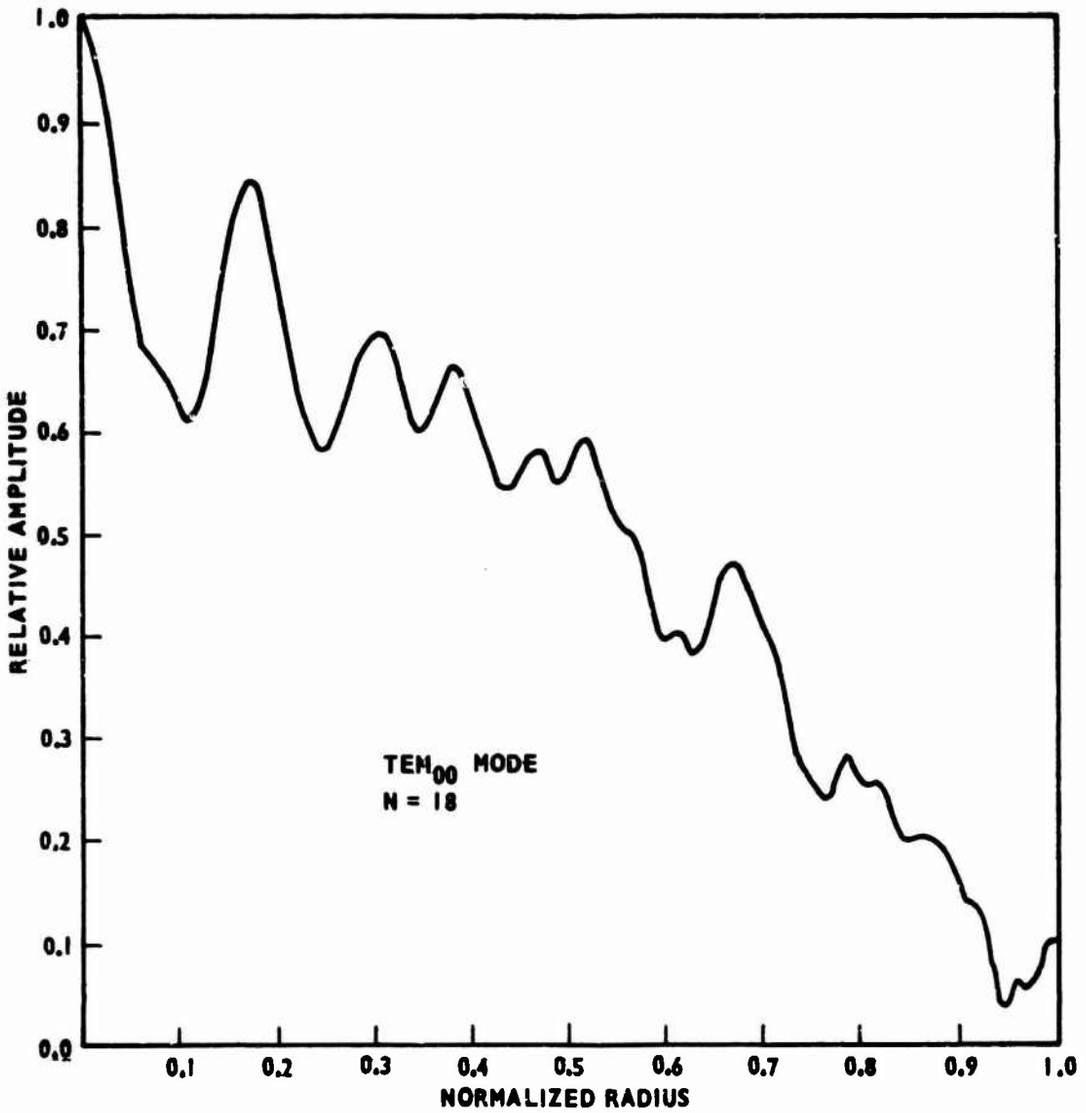

Figure 16. Relative Amplitude of the TEM_{00} Mode on the Input Mirror; Resonator Fresnel Number = 18, Output Mirror Zoned, Reflectivity of Transmission Zones = 0.500 (13 half-period zones, 7 transmission)

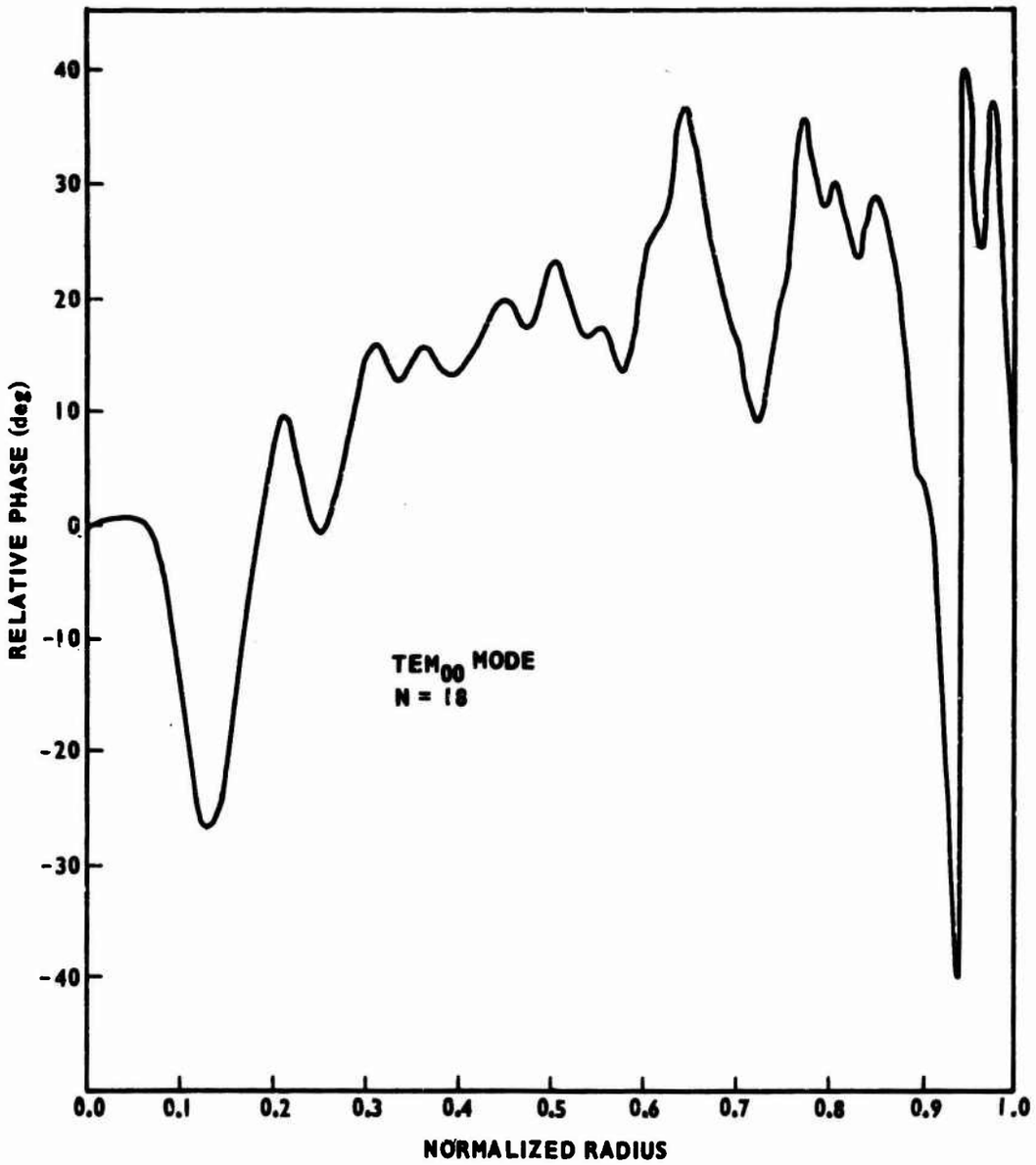

Figure 17. Relative Phase of the TEM_{00} Mode on the Input Mirror; Resonator Fresnel Number = 18, Output Mirror Zoned, Reflectivity of Transmission Zones = 0.500 (13 half-period zones, 7 transmission)

resonator is unsymmetrical. This accounts for the different field configurations on the two mirrors. It is of interest to note that the field on the output mirror is more regular than the field on the input mirror; this is a general characteristic of the mode patterns in zoned resonators. An examination of the resonator equations makes this readily apparent. The source for the field on one mirror is the field on the other mirror multiplied by the amplitude reflectivity of that mirror. Thus, because of the zones on the zoned mirror, the source for the field on the output mirror is smoother than the source for the field on the input mirror.

The gross character of the amplitude distribution on the output mirror of the zoned resonator is similar to that of the unzoned resonator. This can be seen by comparing Figures 12 and 14. In details, however, the fields differ. As can be seen by comparing Figures 13 and 15, the phase of the field on the output mirror of the zoned resonator varies much more rapidly with mirror radius than does the phase of the field of the unzoned resonator. The differences in the two fields resulted entirely from the change in characteristics of the output mirror. Changing the output mirror from a solid mirror to a zoned mirror resulted in a redistribution of the resonator field.

The double pass power loss for the TEM_{00} mode in the zoned resonator is 31.5 percent; this is considerably more than the 0.7 percent obtained for the unzoned resonator. However, the loss from the zoned resonator includes both diffraction and transmission losses. There are seven transmission zones out of a total of thirteen half-period zones on the output mirror, and each transmission zone has a power transmission of 50 percent. Therefore, from

a purely geometrical point of view, the transmission losses would be about 27 percent.

A portion of the output from the zoned resonator is focused. To obtain a measure of this focusing, the amplitude of the field along the resonator axis was calculated by using the field transmitted through the output mirror, normalized to a maximum magnitude of unity, as the source field. The results are given in Figure 18. The ordinate represents the amplitude of the field on the resonator axis relative to the source field. The abscissa is given in terms of M, the Fresnel number of the output mirror as viewed f distance from the output mirror along the resonator axis. This Fresnel number is given by

$$M = \frac{a_p^2}{\lambda f} ,$$

where a_p is the radius of the output mirror, λ is the wavelength, and f is the distance from the output mirror to the point on the axis where the resonator field was evaluated. Thus, M is a measure of reciprocal distance from the resonator.

The axial field has a definite peak, or focus, at a value of M slightly less than thirteen. From the analysis of the zoned mirror given in Chapter III, it can be seen that the focal point of the mirror is located at a value of M equal to the number of zones on the output mirror; in this case that would be thirteen. The analysis in Chapter III assumed a constant phase source; therefore, it is seen that the phase variations of the field on the output mirror did not greatly change the focal distance. This has been the case for all of the zoned resonators studied; that is, if a focused output was obtained, then the focal distance

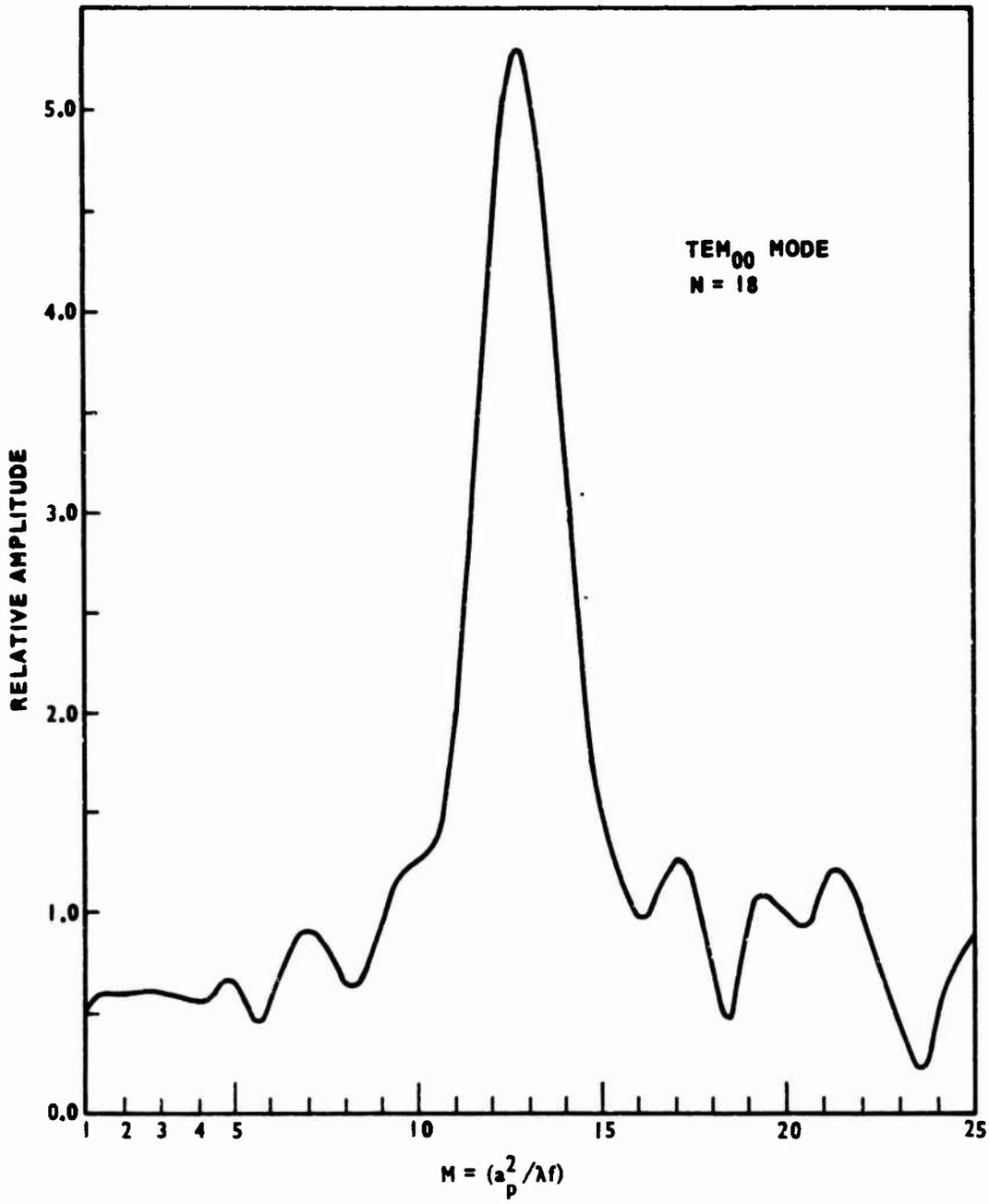

Figure 18. Relative Amplitude of Field Along Resonator Axis; Resonator Fresnel Number = 18, Output Mirror Zoned, Reflectivity of Transmission Zones = 0.500 (13 half-period zones, 7 transmission), Resonator Mode TEM_{00}

was primarily a function of the zoned mirror, and only a secondary function of the resonator field.

It might be illuminating to determine the actual focal distance for a typical laser. A convenient laboratory-sized carbon dioxide laser would be a few centimeters in diameter; for this example (5.08) centimeters will be used. The wavelength of this type of laser is 10.6 microns. Therefore, the focal distance is given approximately by

$$F \approx \frac{(2.54)^2}{(10.6 \times 10^{-4})(13)} ,$$

$$F \approx 467 \text{ cm.}$$

From Figure 18 it can be seen that the field at the focal point has an amplitude of (5.3). Since this field is referenced to the source field, the focal field has an amplitude (5.3) times as large as the maximum amplitude of the field immediately outside the zoned mirror. Thus, the intensity at the focal point is about (28) times as large as the maximum intensity immediately outside the zoned mirror. This increase in intensity is one measure of the focusing characteristics of the self-focusing resonator. Although this increase is not extraordinarily large, it was achieved without the utilization of lenses or secondary mirrors.

The focal plane is defined as the plane orthogonal to the resonator axis and passing through the focal point. The field in this focal plane was calculated as a function of distance from the resonator axis. The amplitude of this field is given in Figure 19 as a function of distance from the resonator axis. As before, the relative amplitude represents the amplitude of the field relative to

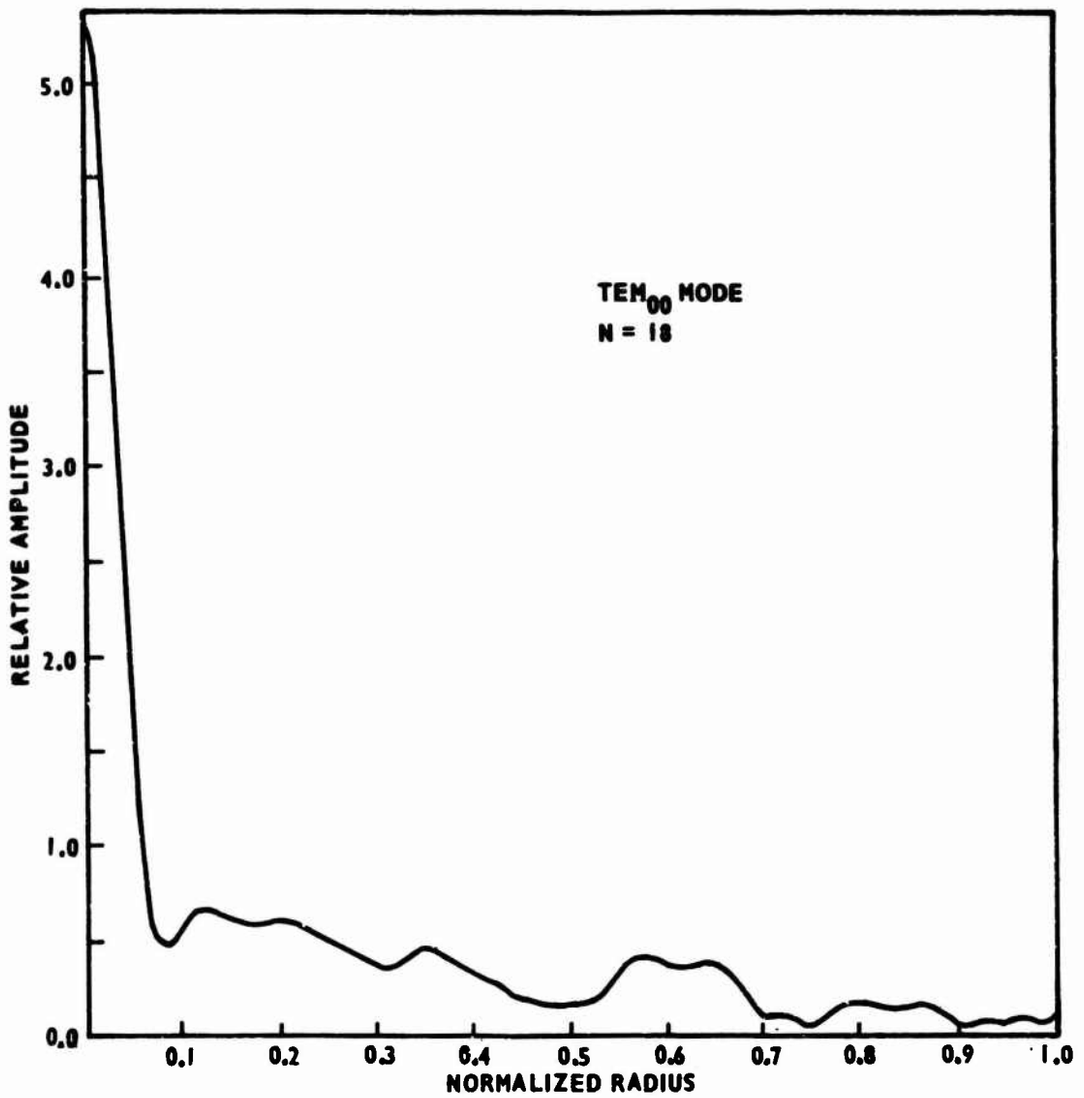

Figure 19. Relative Amplitude of Field in Focal Plane; Resonator Fresnel Number = 18, Output Mirror Zoned, Reflectivity of Transmission Zones = 0.500 (13 half-period zones, 7 transmission), Resonator Mode TEM_{00}

the source field normalized to a maximum amplitude of one. The abscissa, representing the distance from the resonator axis, has been normalized in terms of the radius of the output mirror; hence, a normalized radius of one represents a distance from the resonator axis equivalent to the radius of the output mirror.

The power passing through the main lobe in the focal plane was determined in terms of the total power transmitted out of the zoned resonator. It was found that approximately 24 percent of the output power was concentrated in the main lobe. This is a fairly typical value; for the majority of cases the percent of the output power passing through the main lobe varied from about 18 to 25 percent. However, the peak intensity of the focused field and the width of the main lobe were functions of both the characteristics of the source field and the characteristics of the zoned mirror.

In the unzoned resonator, where both mirrors have uniform reflectivities, the TEM_{00} mode is dominant. However, in the zoned resonator this is not always the case. For this particular zoned resonator the TEM_{00} mode had the least loss for zero-order angular degeneracy. However, it was found that the TEM_{10} mode had less loss. This mode has a first-order angular degeneracy and a zero-order radial degeneracy. The double pass power loss of this mode was found to be 30.6 percent, slightly less than the 31.5 percent loss for the TEM_{00} mode.

The field configuration for the TEM_{10} mode is given in Figures 20 through 23. The amplitude of the field on the output mirror is shown in Figure 20 and the corresponding phase is shown in Figure 21. The amplitude

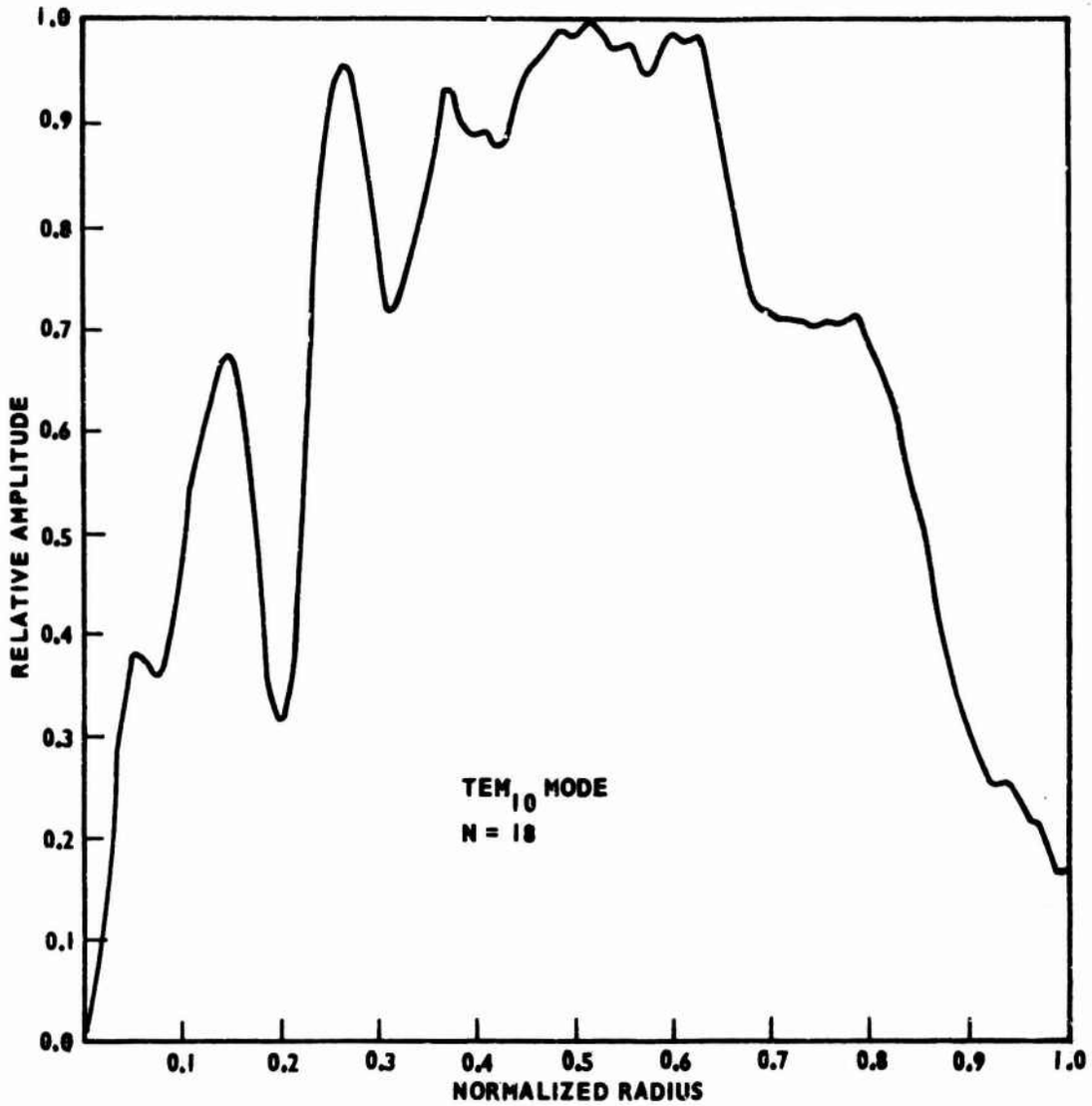

Figure 20. Relative Amplitude of the TEM_{10} Mode on the Output Mirror; Resonator Fresnel Number = 18, Output Mirror Zoned, Reflectivity of Transmission Zones = 0.500 (13 half-period zones, 7 transmission)

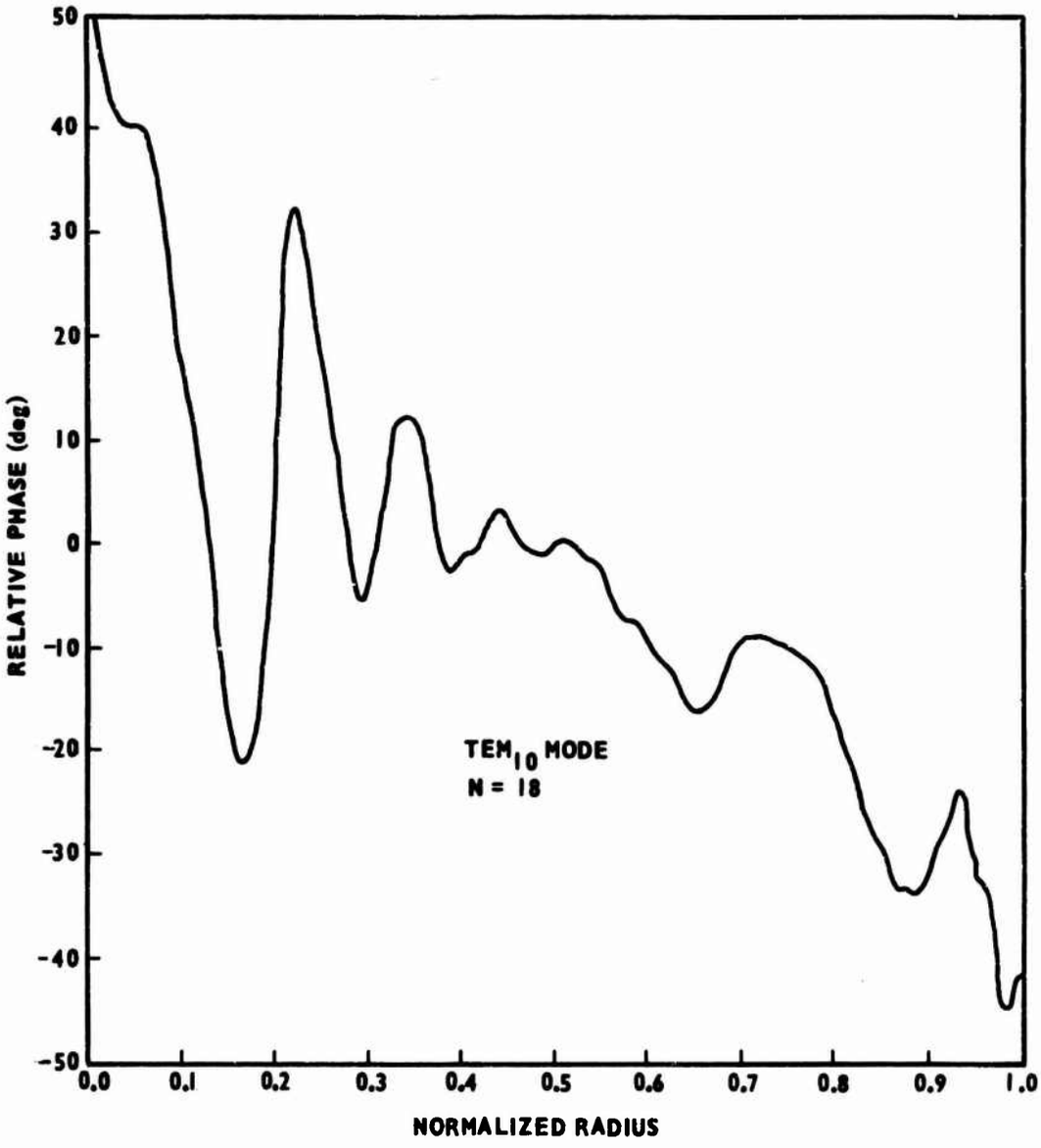

Figure 21. Relative Phase of the TEM_{10} Mode on the Output Mirror; Resonator Fresnel Number = 18, Output Mirror Zoned, Reflectivity of Transmission Zones = 0.500 (13 half-period zones, 7 transmission)

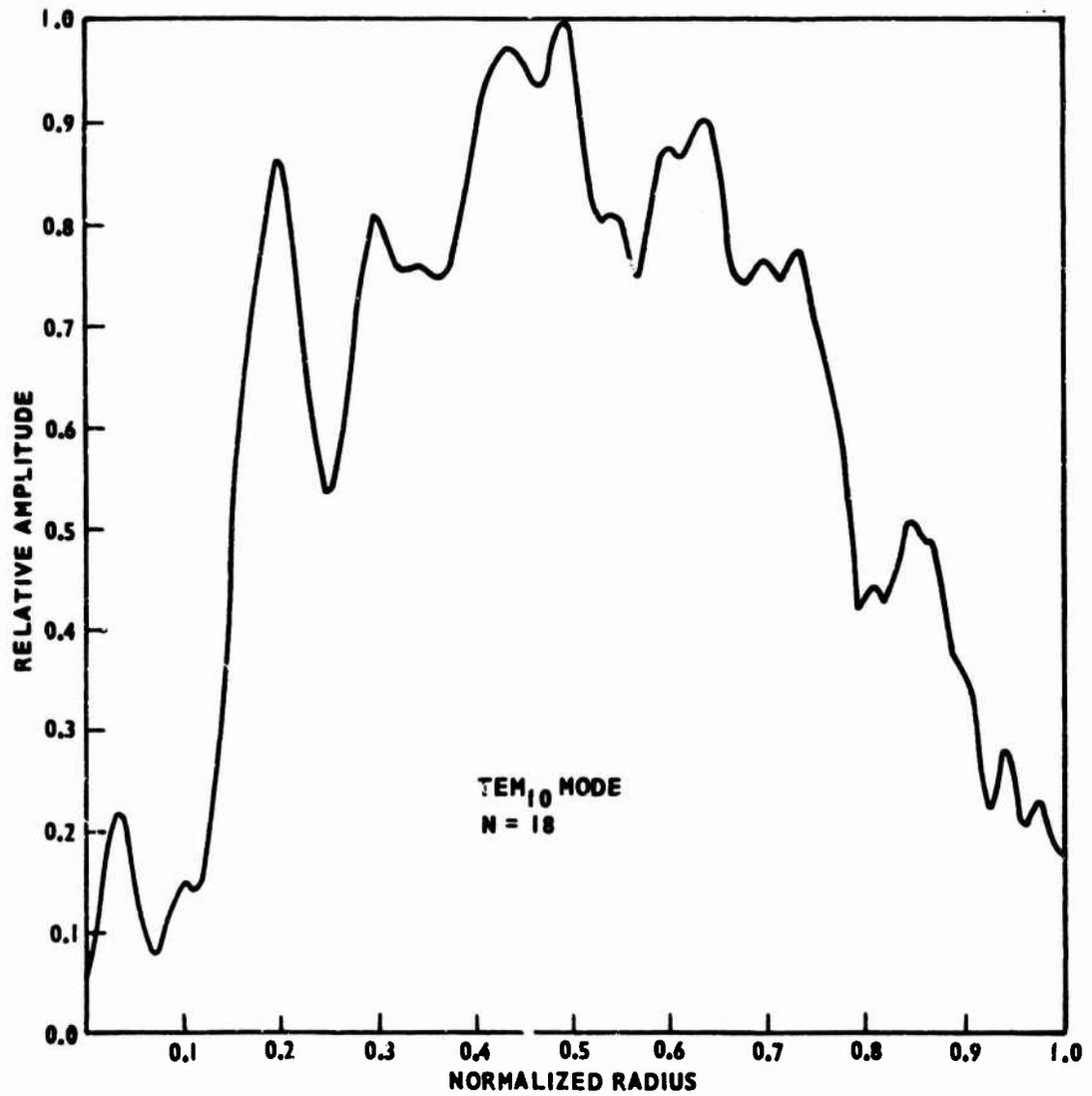

Figure 22. Relative Amplitude of the TEM_{10} Mode on the Input Mirror; Resonator Fresnel Number = 18, Output Mirror Zoned, Reflectivity of Transmission Zones = 0.500 (13 half-period zones, 7 transmission)

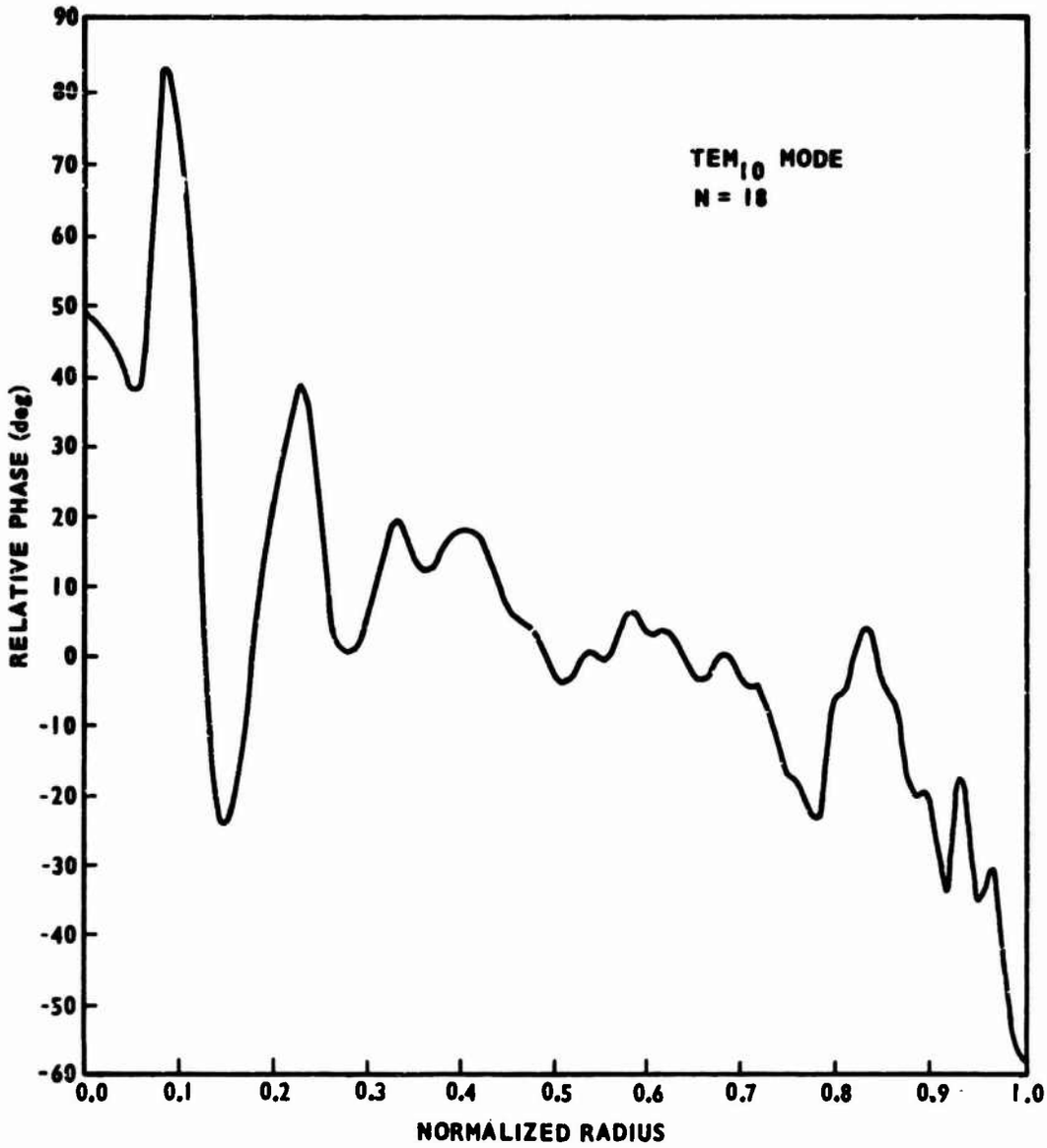

Figure 23. Relative Phase of the TEM_{10} Mode on the Input Mirror;
Resonator Fresnel Number = 18, Output Mirror Zoned,
Reflectivity of Transmission Zones = 0.500
(13 half-period zones, 7 transmission)

and phase on the input mirror are presented in Figures 22 and 23 respectively. These fields represent the radial variation only; the azmuthal variation is sinusoidal. Thus, the actual field would be represented by the radial variation given in the figures multiplied by sin ϕ, where ϕ represents the angular position on the mirrors. For the fields given, ϕ was $(\pi/2)$ radians.

The fields on the mirrors are similar to the general configuration for the TEM_{10} mode obtained in unzoned resonators: The fields at the center of the mirrors are zero, and each field has a single main peak. As was the case for the TEM_{00} mode of this zoned resonator, the field on the output mirror is more regular than the field on the input mirror.

It was pointed out in Chapter II that the axial field is zero when the angular degeneracy of the resonator mode is not zero. However, this does not mean that there is not a focused output for these higher modes. A focused output may exist, but it will be located off axis. The focused field for this resonator operating in the TEM_{10} mode was calculated. The amplitude of this field is shown in Figure 24 as a function of normalized radial distance from the resonator axis. The amplitude has been normalized to a peak source field of unity. It was also shown in Chapter II that the angular degeneracy of the source field was preserved in the focal field. Thus, there are two peaks in the focal plane, and they are located asymmetrically about the resonator axis. As can be seen by comparing Figures 24 and 19, these peaks have amplitudes of about 80 percent of the amplitude of the single peak resulting from the TEM_{00} mode.

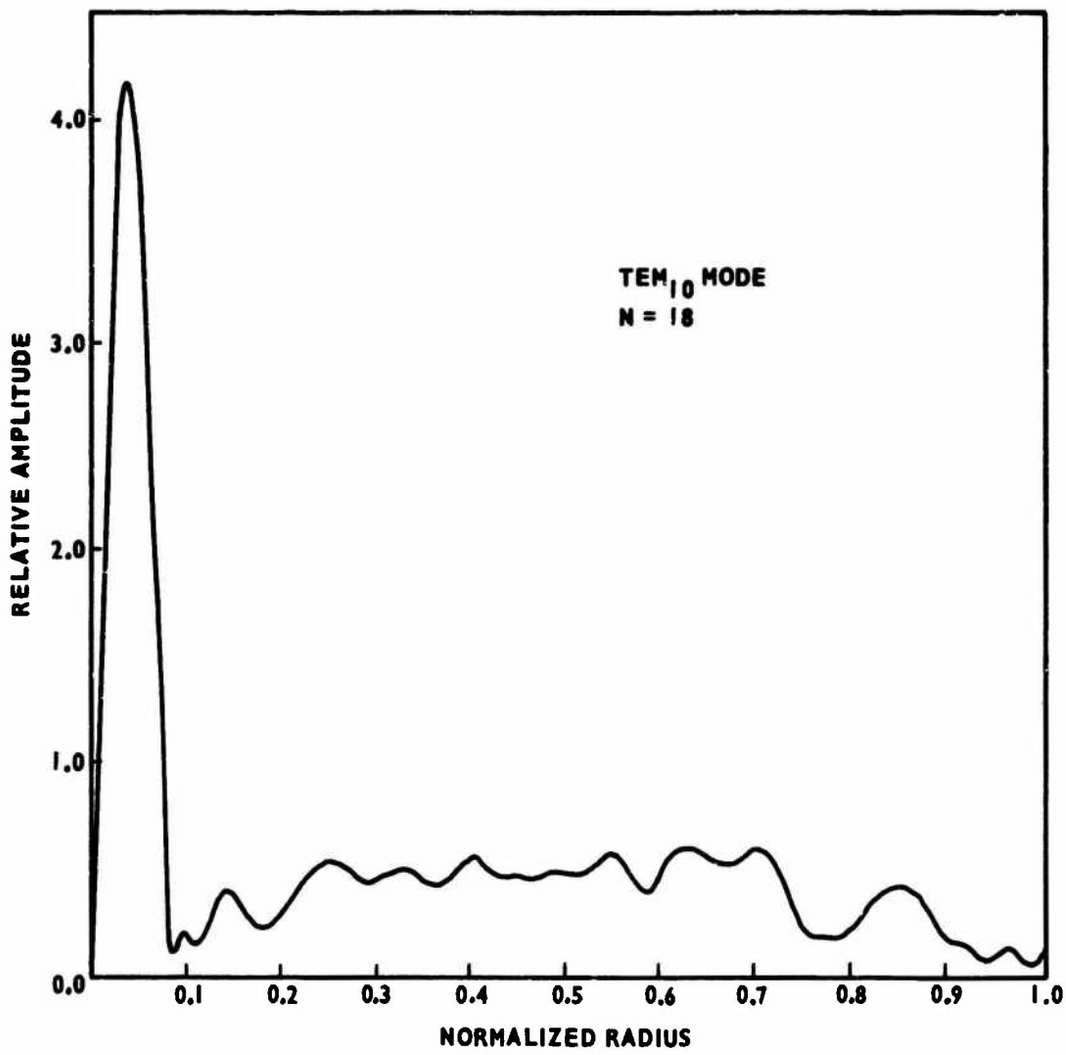

Figure 24. Relative Amplitude of Field in Focal Plane; Resonator Fresnel Number = 18, Output Mirror Zoned, Reflectivity of Transmission Zones = 0.500 (13 half-period zones, 7 transmission), Resonator Mode TEM_{10}

B. Resonator Fresnel Number

For the unzoned resonator, the field structure of a given mode is determined solely by the resonator Fresnel number, and mode dominance is determined by the diffraction losses about the edges of the mirrors. The situation is considerably more complicated for the self-focusing resonator. For this resonator the mode structure is a function of both the resonator Fresnel number and the characteristics of the zoned mirror. The zoned mirror also affects mode dominance; this is because it presents a selective transmission loss to the incident field and distorts the reflected field.

From the resonator equations given in Chapter II it can be seen that for fixed mirror parameters, the self-focusing resonator is a function only of the resonator Fresnel number. However, since the effect of the zoned mirror is related to the field structure, changes in the resonator Fresnel number sometimes result in unexpected changes in the resonator characteristics. By using its Fresnel number as a variable, the self-focusing resonator was examined in some detail. The results are presented in this section.

Consider the zoned resonator formed by flat, circular mirrors having equal radii. The input mirror has a uniform reflectivity of unity. The output mirror is composed of M_p half-period zones. These zones are alternately completely reflecting and completely transmitting. As was shown in Chapter III, the number of zones on the output mirror is related to the focal length of the mirror by

$$M_p = \frac{a_p^2}{\lambda F} ,$$

where a_p is the radius of the mirror, λ is the wavelength, and F is focal length. Although it has not been mentioned, it should be apparent that if the transmitted wave is focused F distance in front of the mirror, the reflected wave will tend to focus F distance behind the mirror. The Fresnel number of this resonator is given by

$$N = \frac{a_p^2}{\lambda d} ,$$

where (d) is the distance between mirrors. The Fresnel number gives the approximate number of half-period zones on one mirror as viewed from the center of the other mirror. For a fixed wavelength, the Fresnel number can be viewed as a measure of the relative size of the resonator; thus, for small Fresnel numbers the resonator is "thin" and for large Fresnel numbers it is "thick."

This study has revealed that there are three regions of resonator sizes which exhibit distinct characteristics. These regions are determined by the value of the resonator Fresnel number relative to the number of zones on the output mirror, and they are designated as follows: region one refers to resonators with Fresnel numbers greater than the number of zones on the output mirror, region two refers to resonators with Fresnel numbers approximately equal to the number of zones on the output mirror, and region three refers to resonators with Fresnel numbers less than the number of zones on the output mirror. These regions may also be described by relating the distance between mirrors to the focal length of the zoned mirror. In region one the focal length is greater than the distance between the mirrors, in region two the focal length

is approximately equal to the distance between the mirrors, and in region three the focal length is less than the distance between the mirrors.

For all cases studied in region one, and this included resonators having Fresnel numbers only a few percent greater than M_p, fixed resonator modes did exist. However, for every case, the dominant mode structure was highly irregular, and sharp focusing of the output could not be achieved. It should be pointed out, however, that the resonator field perturbations caused by the zoned mirror can be reduced by making the transmission zones partially reflecting and/or reducing the area of the transmission zones. By careful control of these parameters a focused output can then be achieved. For example, in the previous section a focused output was obtained from a resonator having a Fresnel number of eighteen and thirteen zones on the output mirror. For that resonator the transmission zones were partially reflecting.

Region two was unique in that no stable modes were found. Applying the power method to resonators having Fresnel numbers approximately equal to the number of zones on the output mirror did not result in the field converging to a fixed mode. The fields were allowed to iterate beyond what is usually required to obtain a resonator mode and yet no regularity of the field was observed. This condition would result if several of the resonator modes had losses of comparable magnitude. Possibly, if the system were allowed to iterate long enough, a pure mode could be obtained. However, one would expect it to be highly distorted; and therefore no focused output could be achieved. In an attempt to control the field structure of this resonator an aperture was placed immediately in front of the input mirror. This effort was

largely unsuccessful. Although this modified resonator had stable fields, the resulting field configurations were extremely distorted.

In region three it was found that fixed modes do exist, and that a focused output could be achieved. The behavior of resonators in this region will now be considered for the case where the zoned mirror has thirteen half-period zones. As was mentioned above, the transmission zones have a transmissivity of unity, and the refelecting zones have a reflectivity of unity. Most of the resonators considered had seven transmission zones, but in a few cases the transmission and reflection zones were reversed. To keep this clear, the number of transmission zones is specified on each figure given herein.

The amplitudes of the TEM_{00} fields on the input mirror for resonators having Fresnel numbers of (0.4), (1.0), (2.0), and (4.0) are shown in Figure 25. The corresponding fields on the output mirror are shown in Figure 26. The amplitude distributions for the TEM_{10} fields are shown in Figures 27 and 28; these fields have an angular degeneracy of one and a radial degeneracy of zero. The amplitude distributions for the TEM_{01} fields are shown in Figures 29 and 30; these fields have an angular degeneracy of zero and a radial degeneracy of one. All of these distributions exhibit the characteristic of decreasing regularity for increasing Fresnel number. Further, the fields on the output mirror are invariably more regular than the corresponding fields on the input mirror.

The double pass power loss for the three lowest-order modes are shown in Figure 31 as a function of resonator Fresnel number. All of the modes are quite lossy; however, since the geometrical transmission loss of the

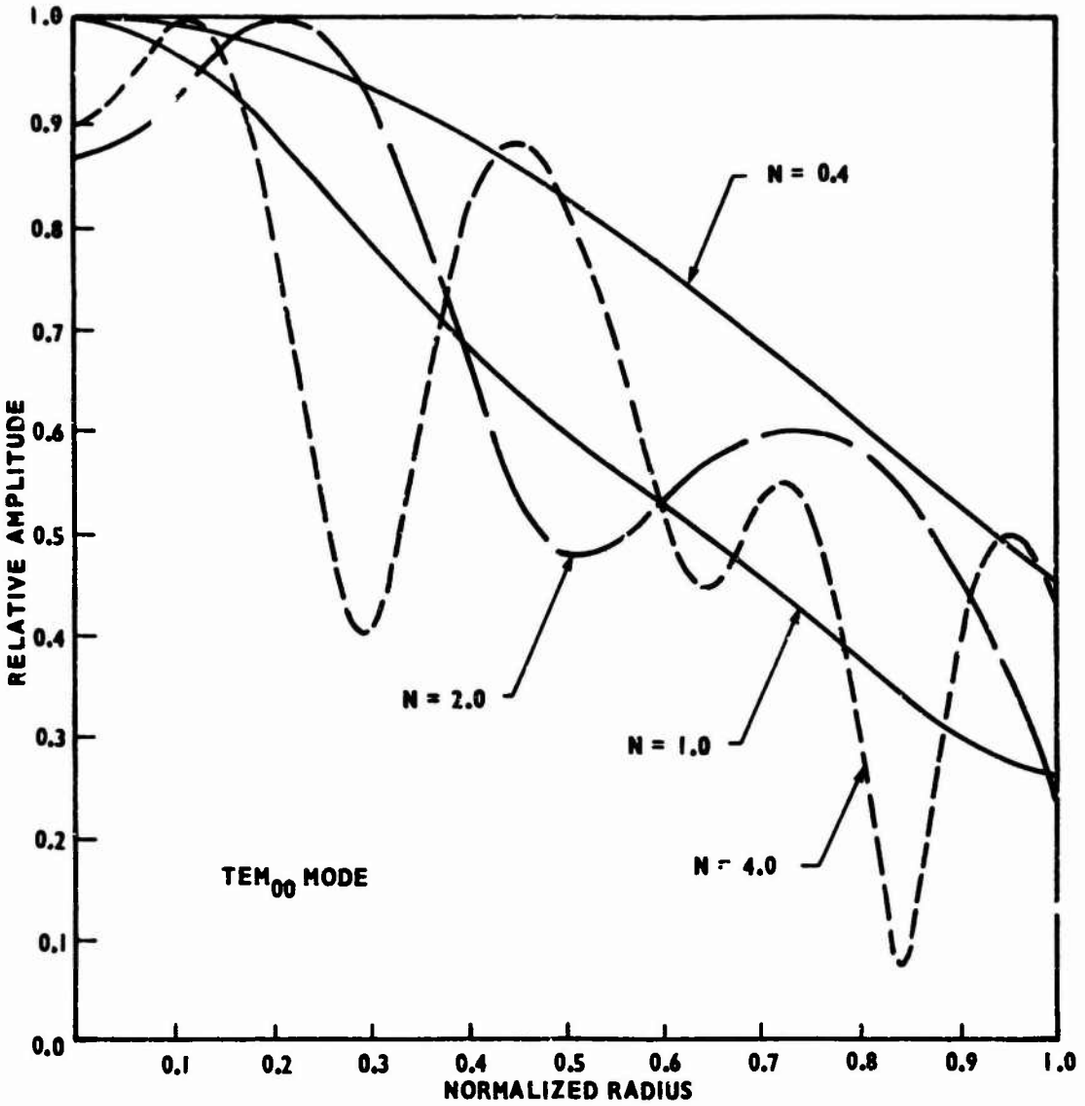

Figure 25. Relative Amplitude of the TEM_{00} Mode on the Input Mirror for Various Values of Resonator Fresnel Number; Output Mirror Divided into 13 Half-Period Zones, 7 Transmission

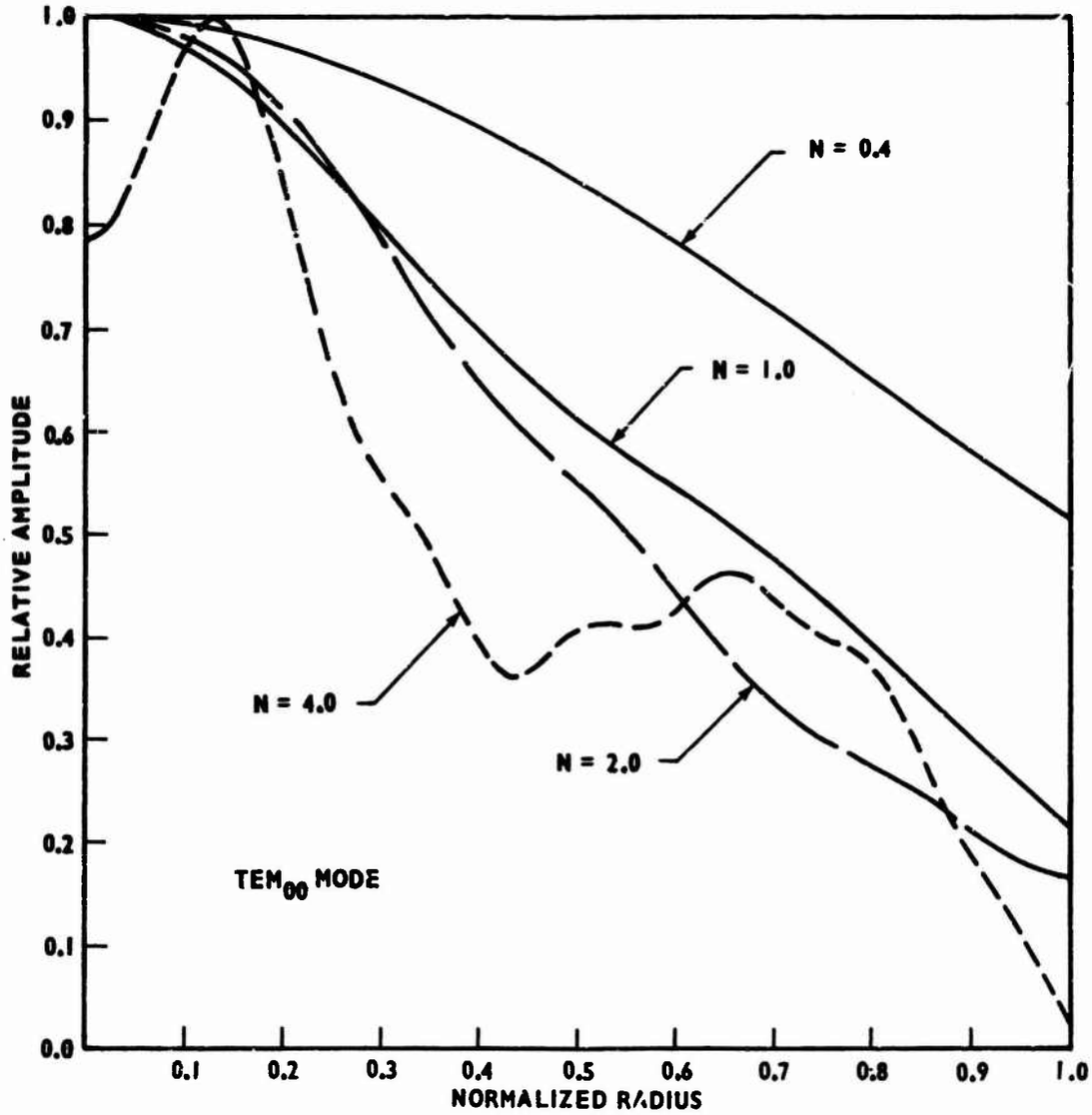

Figure 26. Relative Amplitude of the TEM_{00} Mode on the Output Mirror for Various Values of Resonator Fresnel Number; Output Mirror Divided into 13 Half-Period Zones, 7 Transmission

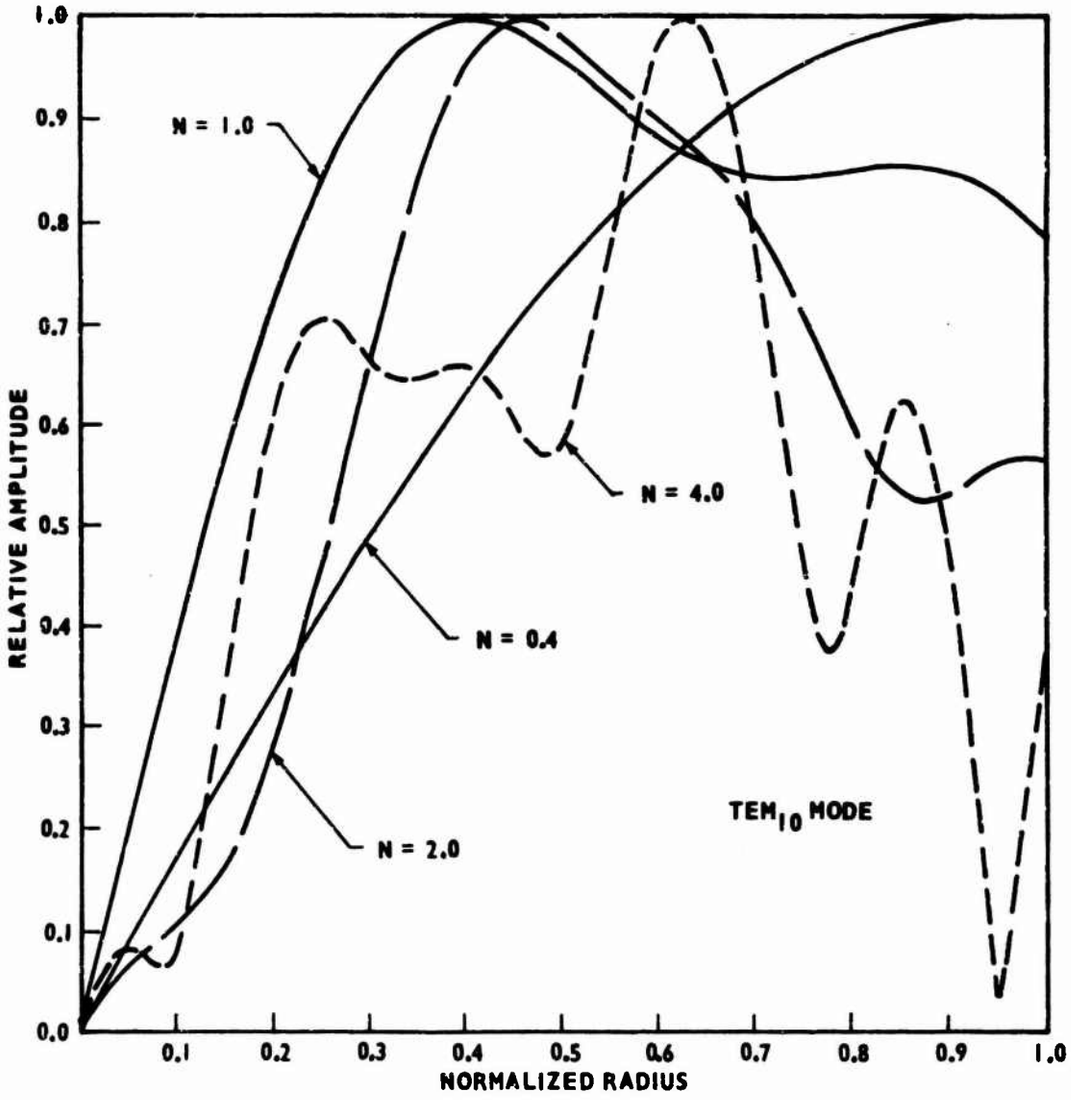

Figure 27. Relative Amplitude of the TEM_{10} Mode on the Input Mirror for Various Values of Resonator Fresnel Number; Output Mirror Divided into 13 Half-Period Zones, 7 Transmission

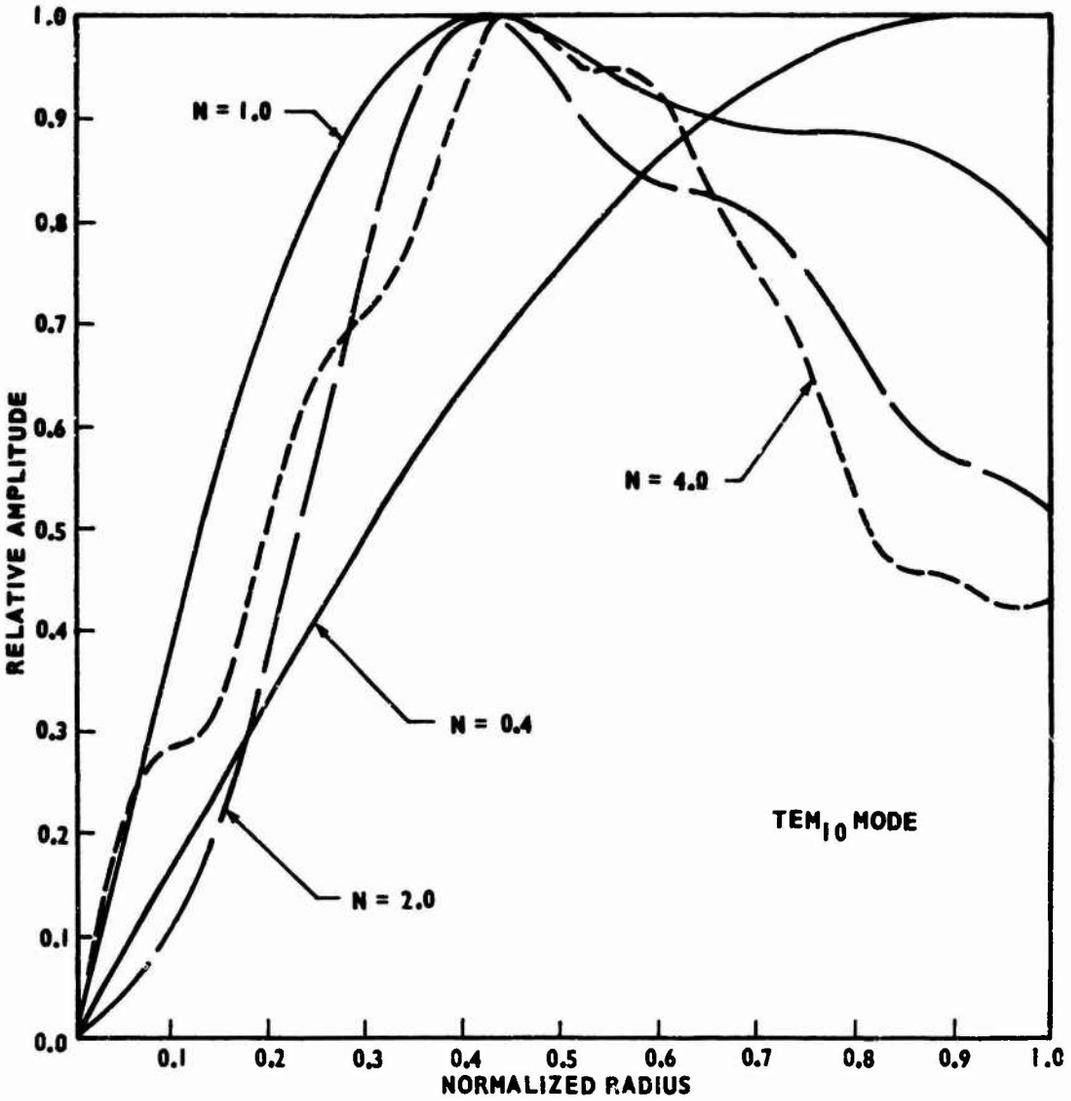

Figure 28. Relative Amplitude of the TEM_{10} Mode on the Output Mirror for Various Values of Resonator Fresnel Number; Output Mirror Divided into 13 Half-Period Zones, 7 Transmission

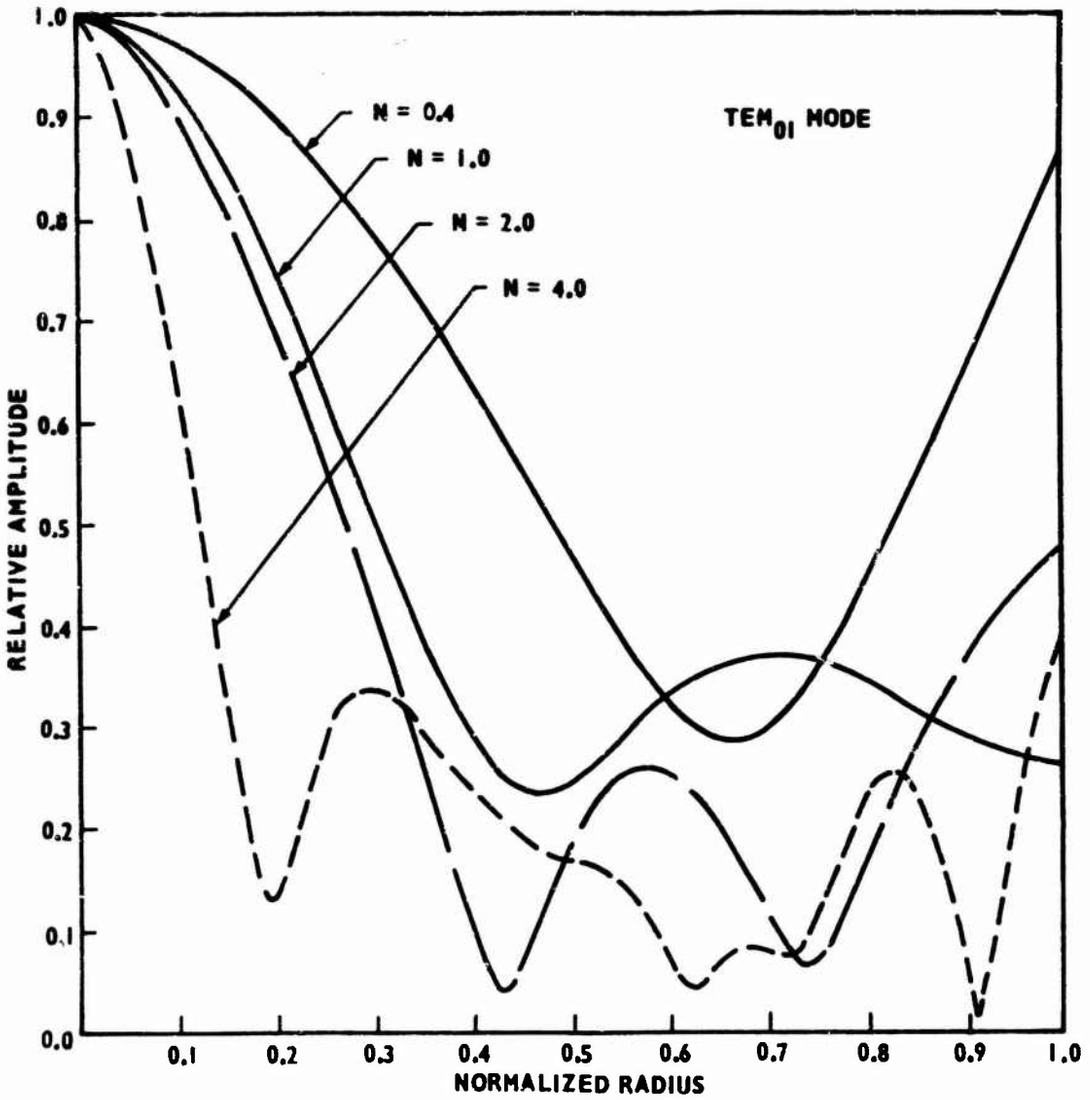

Figure 29. Relative Amplitude of the TEM_{01} Mode on the Input Mirror for Various Values of Resonator Fresnel Number; Output Mirror Divided into 13 Half-Period Zones, 7 Transmission

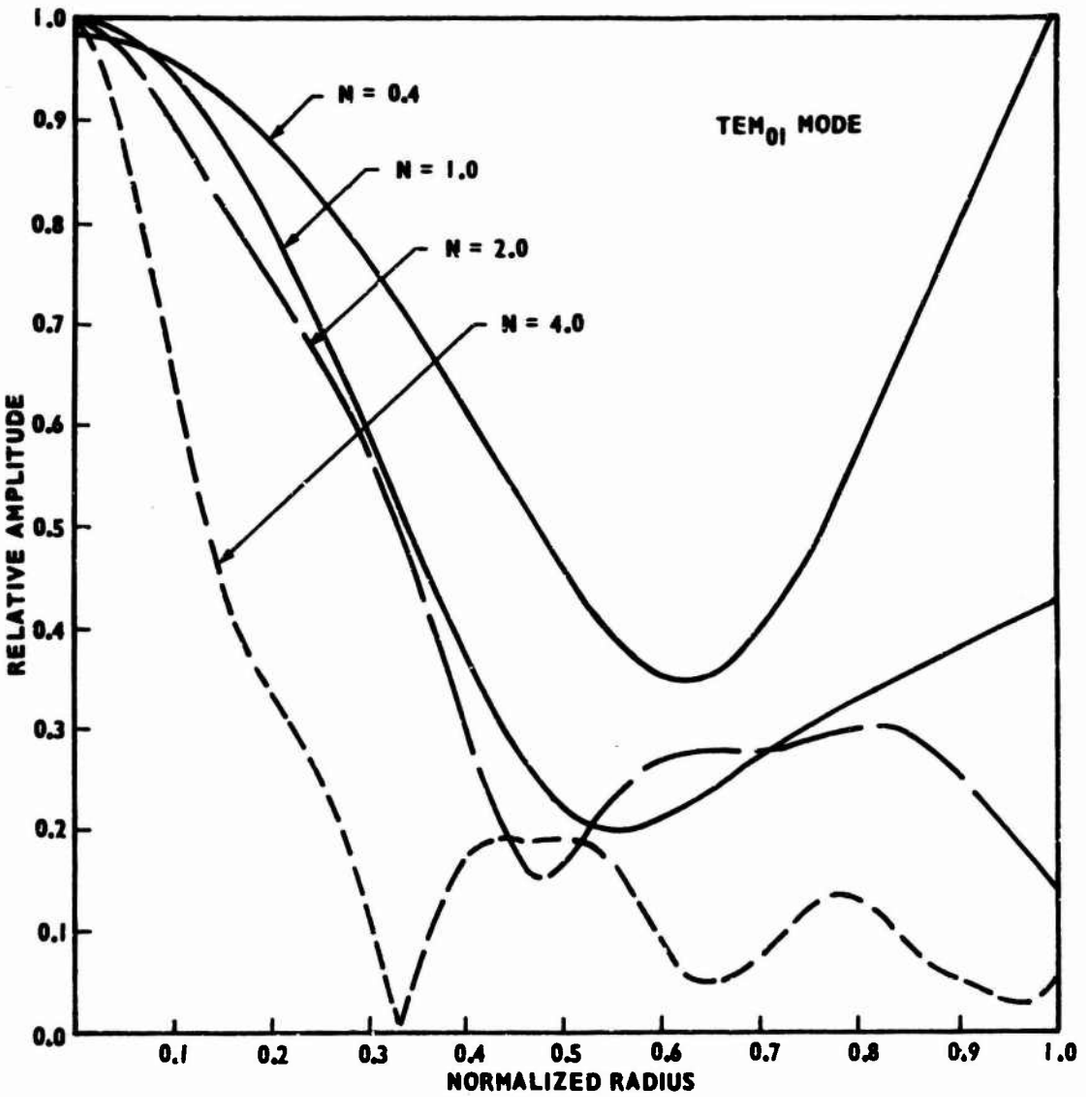

Figure 30. Relative Amplitude of the TEM_{01} Mode on the Output Mirror for Various Values of Resonator Fresnel Number; Output Mirror Divided into 13 Half-Period Zones, 7 Transmission

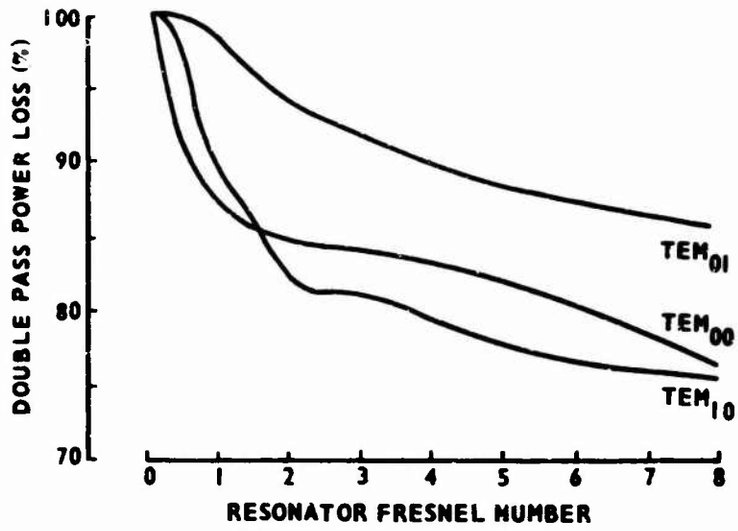

Figure 31. Double Pass Power Loss as a Function of Resonator Fresnel Number; Output Mirror Divided into 13 Half-Period Zones, 7 Transmission

output mirror is over 50 percent, large losses are to be expected. What is perhaps unexpected is the crossover of the loss curves for the TEM_{00} and TEM_{10} modes. For Fresnel numbers between about 1.5 and 8.0 the TEM_{10} mode has the least loss; hence, in this region it is the dominant mode. From the point of view of obtaining a focused output, this dominance of the TEM_{10} mode is undesirable. As was pointed out previously, the transmitted field for this mode is zero on axis and it produces a double peak in the focal plane. Thus, in order to produce the desired focused field, mode control would be needed so as to force the resonator to oscillate in the TEM_{00} mode.

This change in the usual order of mode losses has been found to be a characteristic common to many zoned resonators. It is caused by the inner reaction of the zoned mirror with the resonator field. The zoned mirror presents a selective transmission loss to the incident field; modes tending to

have large fields coincident with the transmission zones have greater transmission losses than modes which peak in regions coincident with reflection zones. The zoned mirror also diffracts the reflected field; this may change the resonator diffraction losses. The situation is further complicated in that diffraction losses are also dependent on the resonator Fresnel number.

In the limiting case of very low Fresnel numbers, diffraction losses should dominate the loss mechanism and the order of the mode losses should be established by this loss. Hence, one would expect the TEM_{00} mode to have the least loss for resonators having very small Fresnel numbers. This has been found to be true for all zoned resonators examined in this study. For the resonators presently being considered the TEM_{00} mode has the least loss for all Fresnel numbers less than about (1.5).

On the other end of region three, that is where the resonator Fresnel number approaches the number of zones on the output mirror, stable resonator modes could not be obtained. For this particular system, eight was the largest Fresnel number for which stable modes were obtained.

The double pass phase shifts of the TEM_{00}, and TEM_{10}, and TEM_{01} modes are shown as a function of Fresnel number in Figure 32. The positive phase shift indicates that the phase velocity is greater than the speed of light. As is usual, the actual phase shift is that specified in the figure plus the geometrical phase shift of (2kd) radians, where (k) is the wave number and (d) is the distance between mirrors. Although the field structures and losses of these zoned resonators are quite different from those of resonators formed by solid mirrors, it was found that the phase shifts are remarkably similar.

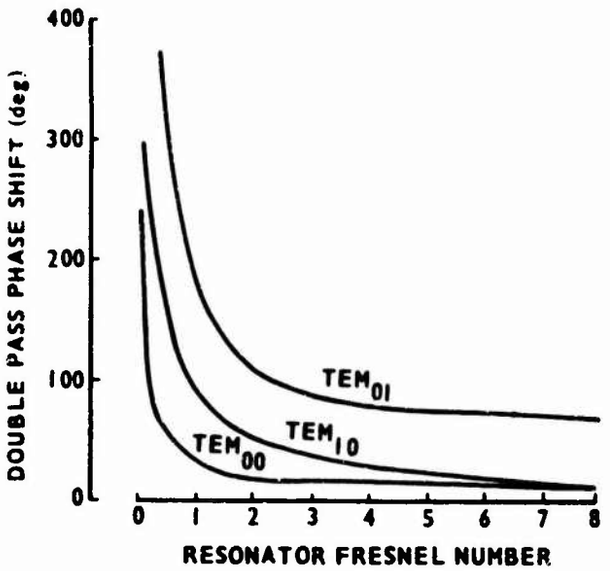

Figure 32. Double Pass Phase Shift as a Function of Resonator Fresnel Number; Output Mirror Divided into 13 Half-Period Zones, 7 Transmission

To within the accuracy of reading the curves, the phase shift of the TEM_{10} mode given in Figure 32 is the same as that given by Li[1] for the solid mirror case. For low Fresnel numbers the phase shifts for the TEM_{00} modes also agree quite closely; even for the larger Fresnel numbers they agree to within a factor of two.

The focused output field was determined for various values of resonator Fresnel number; some of the results are presented in Figure 33. In this figure the axial fields about the focal point are given for resonators having Fresnel numbers of (0.4), (1.0), (2.0), and (4.0); the distribution shown in the

---

[1]Li, Tingye, "Diffraction Loss and Selection of Modes in Maser Resonators with Circular Mirrors" The Bell System Technical Journal, Volume 44, pp. 917-932 (1965). (It should be noted that Li gives the single pass phase shift; therefore, his results must be doubled before comparing to those given herein.)

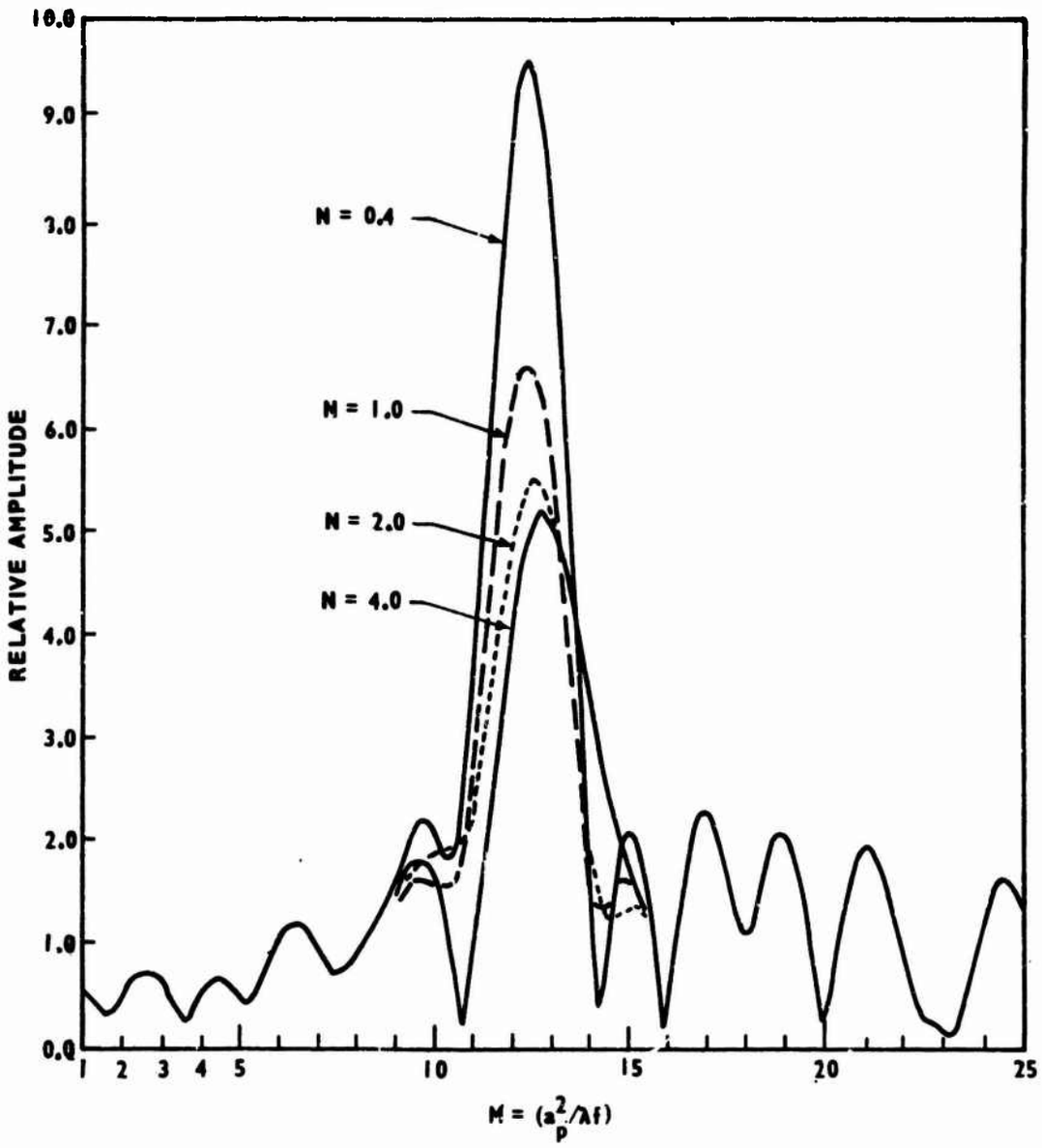

Figure 33. Relative Amplitude of Field Along Resonator Axis for Various Values of Resonator Fresnel Number; Resonator Mode TEM_{00}; Output Mirror Divided into 13 Half-Period Zones, 7 Transmission

remainder of the curve is for the Fresnel number of (0.4) The amplitudes of these axial fields are given relative to the source field normalized to a peak amplitude of unity. These axial fields were obtained for the condition of the resonator operating in the TEM_{00} mode.

For this resonator the zoned mirror was fixed. Therefore, the differences in the focused fields are due entirely to differences in the source fields. The source fields are the transmitted portions of the TEM_{00} resonator fields. The amplitude of these resonator fields was given in Figure 26, where one sees that the average amplitudes of the source fields decrease with increasing Fresnel number; a corresponding decrease in the focused field would be expected. In determining the focused fields, the phases of the source fields must also be considered; the phases are not given here, but as a general rule the phase variation across the output mirror increases with resonator Fresnel number, and it also increases as the irregularity of amplitude distribution increases.

So as to afford another view of the focusing properties of this resor the focused intensity per unit output power was determined. The results are given in Figure 34 as a function of resonator Fresnel number. The focused intensity per unit output power is a measure of the effectiveness with which the output power is utilized in achieving a focused output. It should be noted that resonators having small Fresnel numbers have large diffraction losses, and that diffraction losses are not considered as part of the output power. The most noticeable feature of the curve in Figure 34 is its relative flatness. This

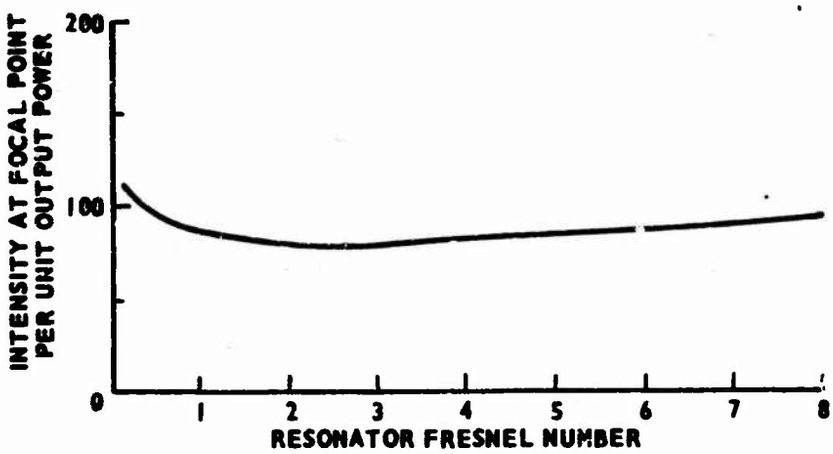

Figure 34. Intensity at Focal Point per Unit Output Power as a Function of Resonator Fresnel Number; Resonator Operating in the TEM_{00} Mode; Output Mirror Divided into 13 Half-Period Zones, 7 Transmission

indicates that fields inducive to large output powers are also inducive to good focusing.

To show that the results given in Figure 34 are reasonable, the limiting case of a uniform distribution on the output mirror can be considered. In practice, a uniform distribution is approached quite closely by resonators having very small Fresnel numbers. For instance, when the resonator Fresnel number is (0.1) the TEM_{00} field on the output mirror has a peak in the center and smoothly falls off to 95 percent of the peak at the edge of the mirror, and the phase variation across the mirror radius is only a few degrees.

Therefore, by assuming a uniform source field of unit magnitude and by using equations (II-14) and (II-17) the transmitted power can be expressed by

$$P_T = 2\pi C_T \int_0^1 (\tau_z)^2 r_z dr_z \ ,$$

where C_T is a proportionality constant and $(\tau_z)^2$ is the power transmission coefficient of the zoned mirror. This transmission coefficient has a value of one over the transmission zones and a value of zero over the reflection zones. Therefore, since there are thirteen equal area zones on the output mirror, and seven of these zones are transmission zones,

$$P_T = C_T\left(\frac{7}{13}\right)\pi \ .$$

From the results of Chapter III one can deduce that the field at the focal point is equal to twice the number of transmission zones. Thus, the intensity at the focal point is given by

$$I_f = C_T(2 \times 7)^2 = C_T(196) \ .$$

Therefore, for the case of a very small Fresnel number, the intensity per unit output power is given approximately by

$$\frac{I_f}{P_T} \approx (116) \ .$$

In Figure 34 one sees that this value corresponds quite closely to the value obtained from the curve for a Fresnel number approaching zero.

The results so far presented in this section have been limited to those obtained from a zoned mirror having a transmitting zone in the center. Since the TEM_{00} mode has a peak in the center and the TEM_{10} mode has a zero in the center, the reversing of the transmitting and reflecting zones has a large change on the relative mode losses. In Figure 35 the double pass loss for the TEM_{00} and TEM_{10} modes are shown for the case of a center reflecting zone; for comparison the double pass loss curves for the other case are repeated.

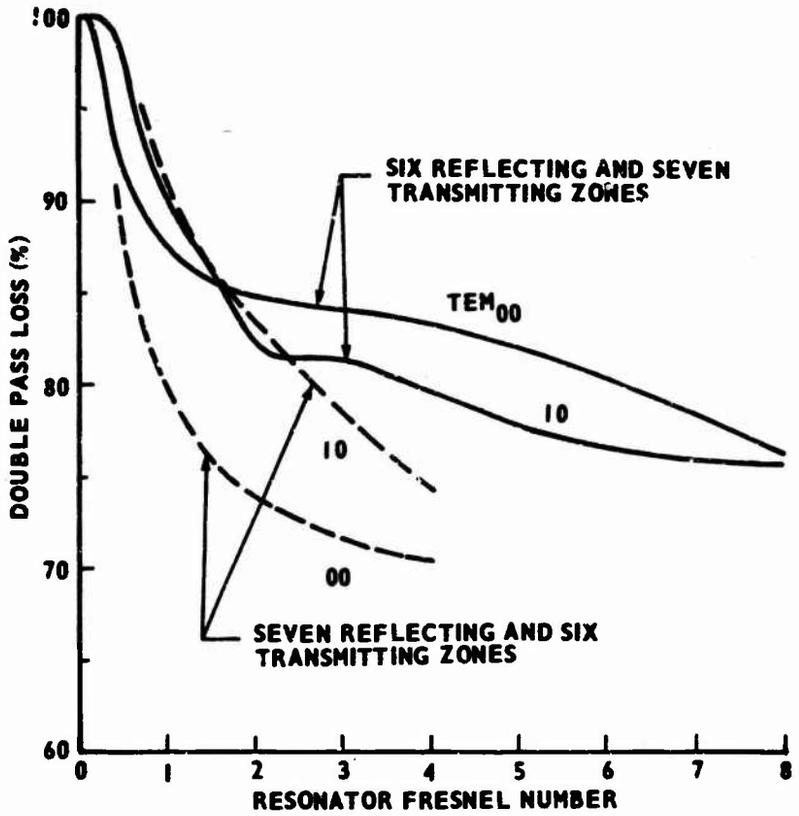

Figure 35. Double Pass Power Loss as a Function of Resonator Fresnel Number; Output Mirror Zoned

The major difference between the two types of resonators is the relative order of the losses. For resonators having seven reflecting zones no crossover for the TEM_{00} and TEM_{10} loss curves was found. The general decrease in loss for this case can be attributed partially to the decrease in transmission loss.

C. Transmission Zone Reflectivity

If the resonator mode structure were not a function of transmission zone reflectivity, the maximum intensity at the focal point would be obtained for zero reflectivity. This, of course, is because, for the lossless mirrors

considered, minimizing the reflectivity is equivalent to maximizing the transmissivity. Thus, the condition of minimum transmission zone reflectivity would result in maximum resonator output. However, the mode structure is a function of transmission zone reflectivity, and in general it has been found that a decrease in the transmission zone reflectivity results in an increase in the perturbation of resonator mode structure. Thus, since the focused field is a function of both the resonator mode structure and the zoned mirror, it might be concluded that an optimum value of transmission zone reflectivity exists. For some resonator configurations an optimum value does indeed exist.

An investigation has been made as to the characteristics of the self-focusing resonator as a function of transmission zone reflectivity. The size of the zoned mirror was fixed at thirteen half-period zones; seven of these zones were transmission zones. Two values of resonator Fresnel number were considered, one and eighteen. These values of Fresnel number were chosen as they typify the two cases of the focal length of the zoned mirror being less than the resonator length and the focal length of the zoned mirror being greater than the resonator length.

The relative amplitudes of the TEM_{00} fields on the output mirror, for various values of transmission zone power reflectivity, ρ_z^2, are presented in Figure 36 for the case where the resonator Fresnel number is one. The corresponding phase shifts are given in Figure 37. For ρ_z^2 equal to zero the resonator has the previously considered configuration of totally transmitting transmission zones. For ρ_z^2 equal to one the transmission zones on the output are nonexistent, and the resonator has the usual unzoned configuration. The

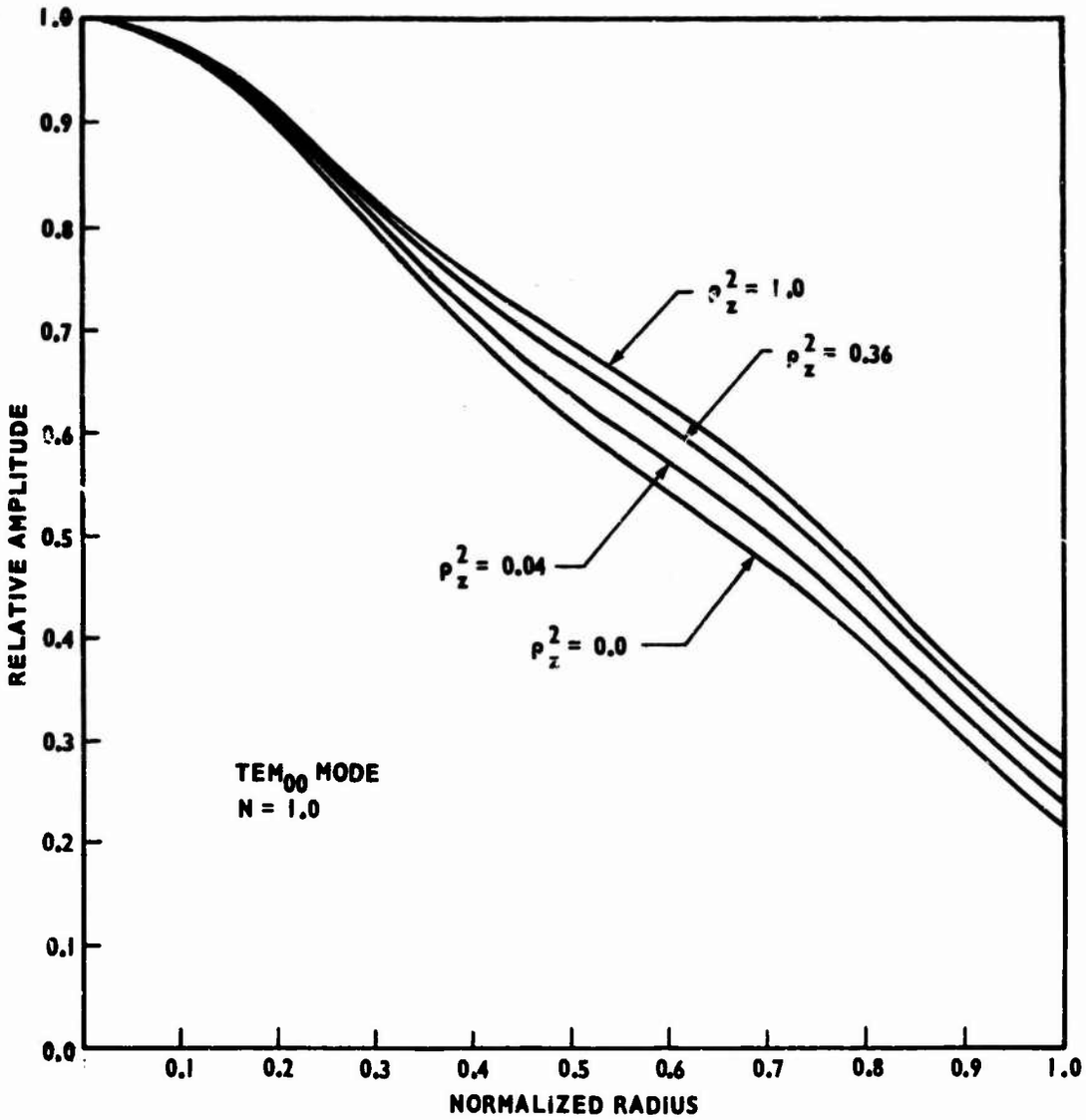

Figure 36. Relative Amplitude of the TEM_{00} Mode on the Output Mirror for Various Values of Transmission Zone Reflectivity; Fresnel Number of Resonator = 1.0; Output Mirror Divided into 13 Half-Period Zones, 7 Transmission

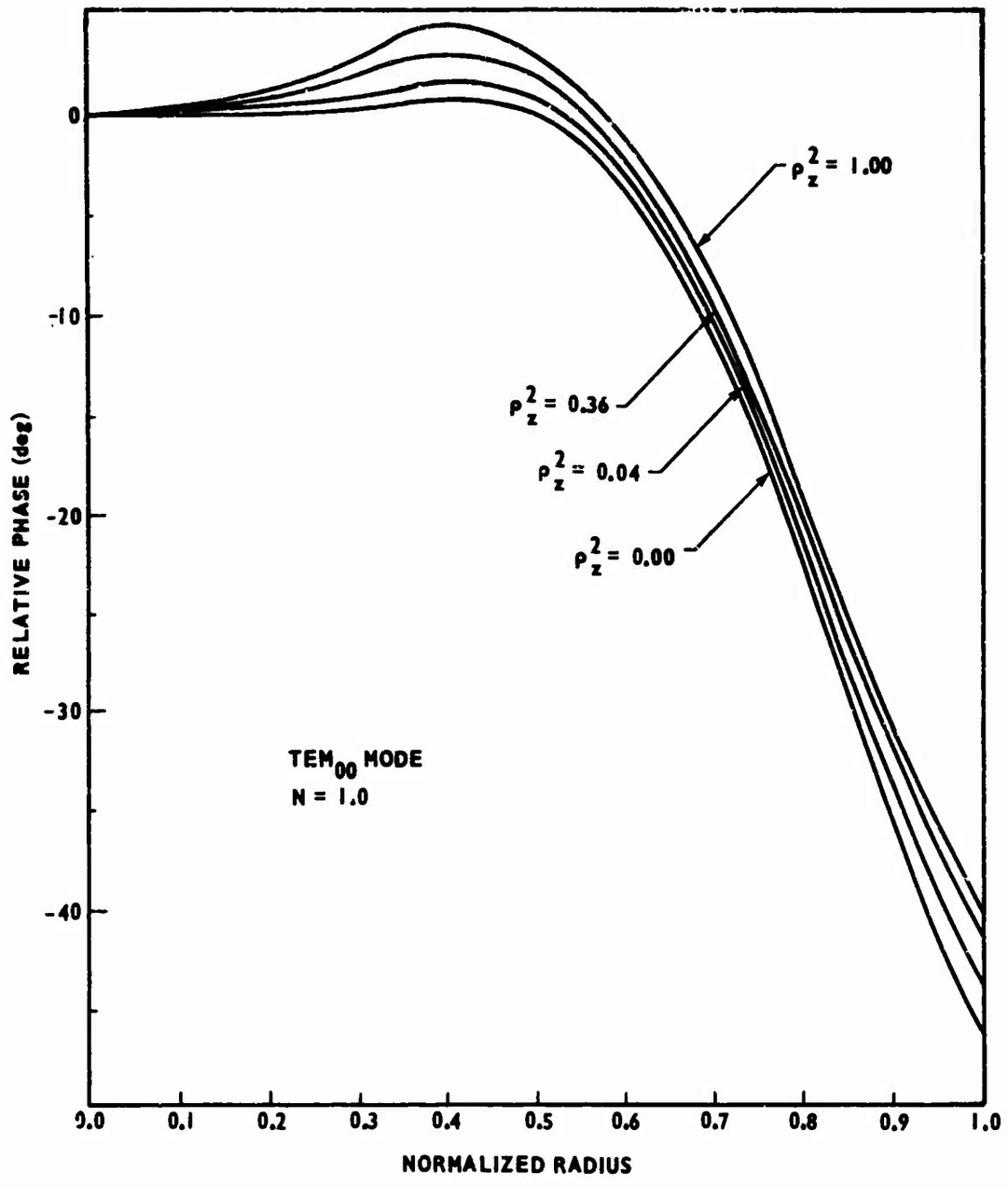

Figure 37. Relative Phase of the TEM_{00} Mode on the Output Mirror for Various Values of Transmission Zone Reflectivity; Fresnel Number of Resonator = 1.0; Output Mirror Divided into 13 Half-Period Zones, 7 Transmission

field for this condition of ρ_z^2 equal to unity was obtained from Li.[2]

As can be seen in Figures 36 and 37, changing the transmission zone reflectivity only has a small effect on the resonator fields. It should be noted, however, that although the effect is small, decreasing the transmission zone reflectivity degrades the resonator field structure; the average amplitude of the field decreases and the phase variation increases as the transmission zone reflectivity is decreased. The fact that the changes in the field are only slightly affected by the zoned mirror indicates that the resonator field configuration is being dominated by diffraction losses over the edges of the mirrors.

For the resonator having a Fresnel number of eighteen the resonator fields are strongly affected by the transmission zone reflectivity. This can readily be seen in Figures 38 and 39. In these figures the fields on the output mirror are given for various transmission zone reflectivities. These fields are those having the least loss for an angular degeneracy of zero. For the cases where ρ_z^2 is (1.000) and (0.500) the mode structure is definitely TEM_{00}. However, for ρ_z^2 equal to (0.063) it would be difficult to classify the field as TEM_{00}.

The double pass power losses for the two resonators are given in Figure 40 as a function of transmission zone power reflectivity. Also shown in this figure is a transmission loss curve; this curve represents the geometrical loss due to transmission through the transmission zones. On the output

---

[2]Li, op. cit.

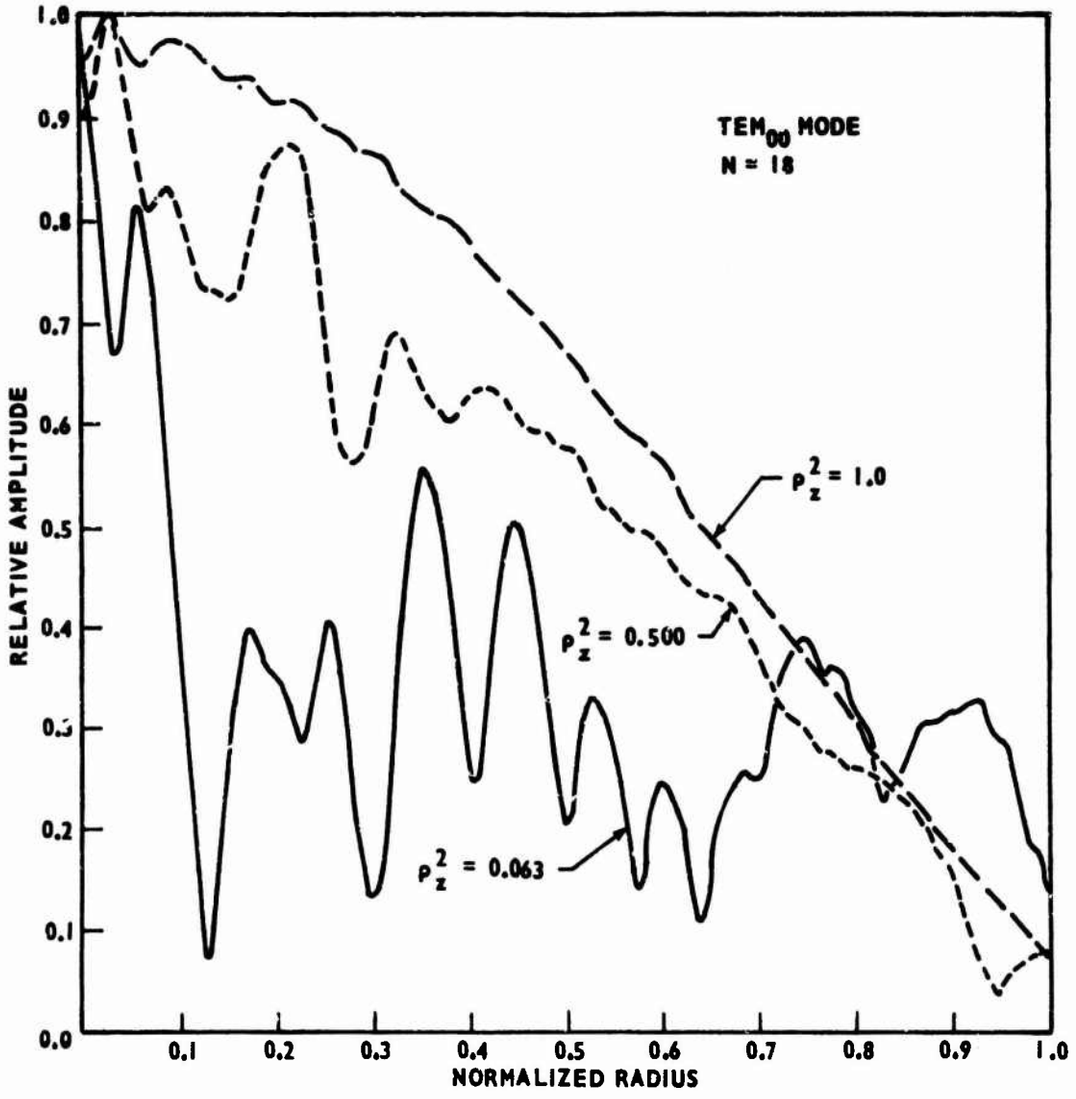

Figure 38. Relative Amplitude of the TEM_{00} Mode on the Output Mirror for Various Values of Transmission Zone Reflectivity; Fresnel Number of Resonator = 18; Output Mirror Divided into 13 Half-Period Zones, 7 Transmission

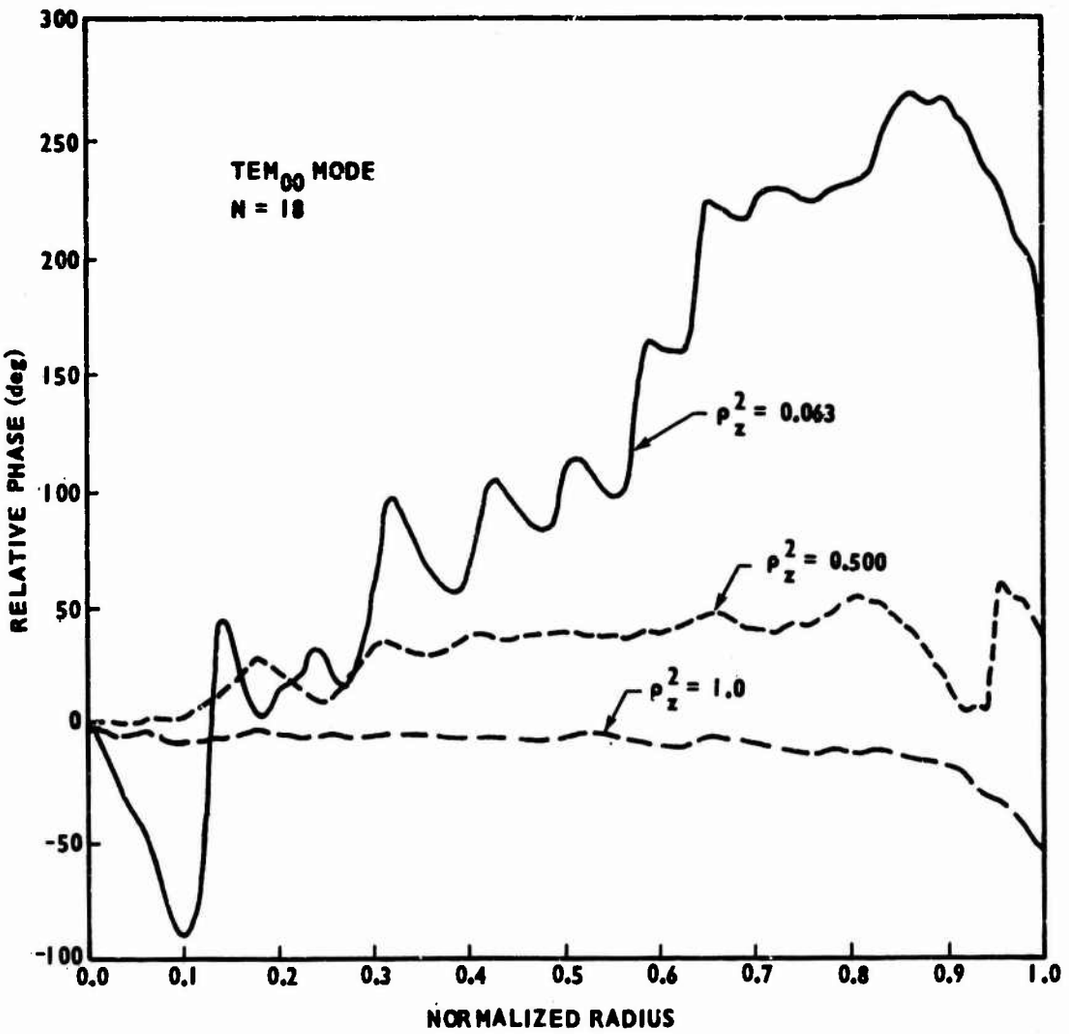

Figure 39. Relative Phase of the TEM_{00} Mode on the Output Mirror for Various Values of Transmission Zone Reflectivity; Fresnel Number of Resonator = 18; Output Mirror Divided into 13 Half-Period Zones, 7 Transmission

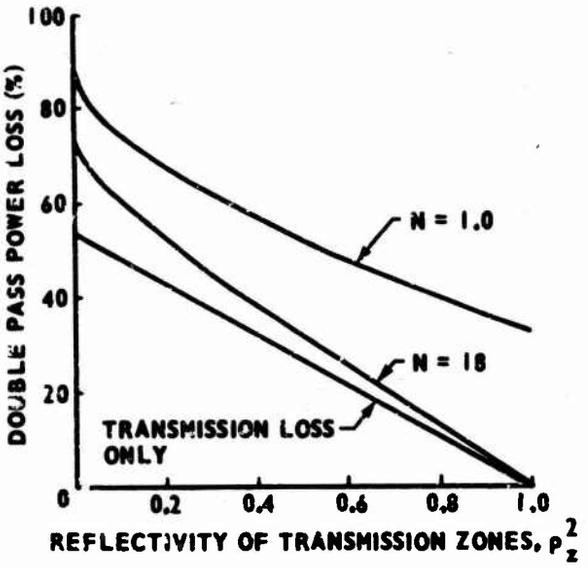

Figure 40. Double Pass Power Loss as a Function of Power Reflectivity of the Transmission Zones; Resonator Operating in TEM_{00} Mode; Output Mirror Zoned (13 half-period zones, 7 tranmission)

mirror there are seven transmission zones out of a total of thirteen zones; therefore, the transmission loss can be expressed as $\left[(7/13)\left(1 - \rho_z^2\right)\right]$. The difference between the total loss and transmission loss gives one a qualitative measure of the diffraction loss. The diffraction losses for the resonator having a Fresnel number of one are large everywhere, and they are everywhere greater than the diffraction losses of the other resonator. Except for values of reflectivities approaching unity, the resonator losses, for the resonator having a Fresnel number of eighteen, are dominated by the transmission losses.

The double pass phase shifts for the two resonators are given in Figure 41. These phase shifts have the greatest variation in the region of small values of transmission zone reflectivity; and as would be expected, the resonator having the larger Fresnel number has the greatest variation in phase shift.

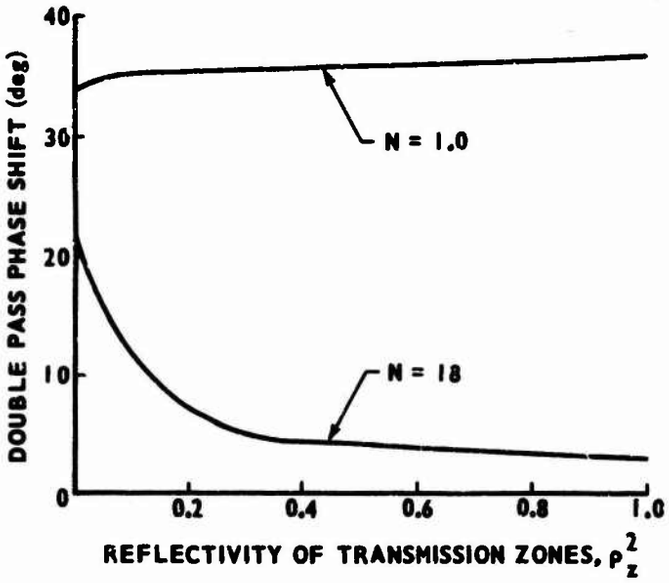

Figure 41. Double Pass Phase Shift as a Function of Power Reflectivity of the Transmission Zones; Resonator Operating in TEM_{00} Mode; Output Mirror Zoned (13 half-period zones, 7 transmission)

The intensity at the focal point, normalized to unit power out of the resonator, has been determined for both resonators. The results are given in Figure 42 as functions of the transmission zone reflectivity. As was mentioned previously, presenting the data in terms of maximum intensity per unit output power gives one a measure of the efficiency with which the output power is being utilized to create a focused output. However, as with most normalization schemes, the results must be carefully evaluated. For example, consider the upper curve in Figure 42. From this curve one might reason that, for resonators having a Fresnel number of one, the optimum value of transmission zone reflectivity is unity. However, a reflectivity of unity implies a transmissivity of zero; hence, there would be no output power. The curves do, however, give one some insight as to the focusing properties of the resonator. In particular, for the resonator having a Fresnel number of eighteen, the most efficient

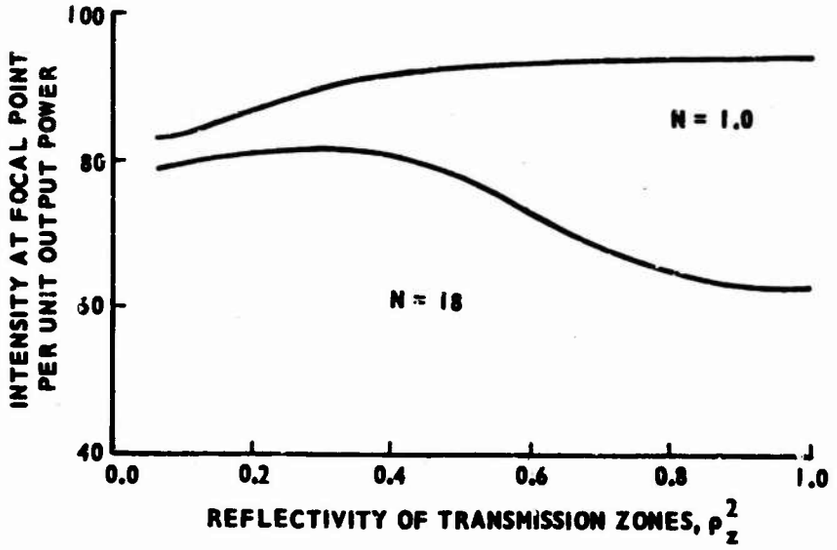

Figure 42. Intensity at Focal per Unit Output Power as a Function of Power Reflectivity of the Transmission Zones; Resonator Operating in TEM_{00} Mode; Output Mirror Zoned (13 half-period zones, 7 transmission)

use of the output power is achieved for a transmission zone reflectivity of about (0.3). It is shown below that other considerations of the focusing result in similar values for transmission zone reflectivity.

In Figure 43 the intensity at the focal point, normalized by the peak intensity immediately outside the resonator, is given as a function of the transmission zone reflectivity. Both resonator configurations have maximums for the transmission zone reflectivity approximately equal to (0.4). At this maximum, for the resonator having a Fresnel number of one, the intensity at the focal point is a factor of about 53 greater than the peak intensity immediately outside the resonator. For the other resonator, the maximum focused intensity is about 29 times greater than the peak intensity immediately outside the resonator.

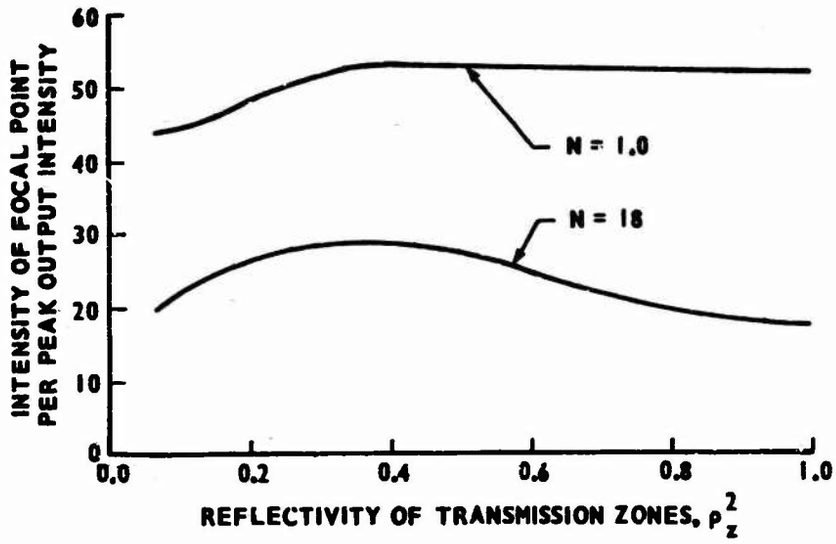

Figure 43. Intensity at Focal Point per Peak Output Intensity as a Function of Power Reflectivity of the Transmission Zones; Resonator Operating in TEM_{00} Mode; Output Mirror Zoned (13 half-period zones, 7 transmission)

Rather than compare the focused field to the transmitted field, it can be compared to the field inside the resonator. In Figure 44 the intensity at the focal point, normalized with respect to the peak intensity inside the resonator, is given as a function of transmission zone reflectivity. For the resonator having the larger Fresnel number, the maximum occurs at a transmission zone reflectivity of about (0.2); at this value of reflectivity the intensity at the focal point is about 21 times greater than the peak intensity inside the resonator.

D. Number of Transmission Zones

The zoned resonators considered thus far have had a fixed number of alternately transmitting and reflecting zones. In this section the effect on the zoned resonator caused by changing the total number of zones is

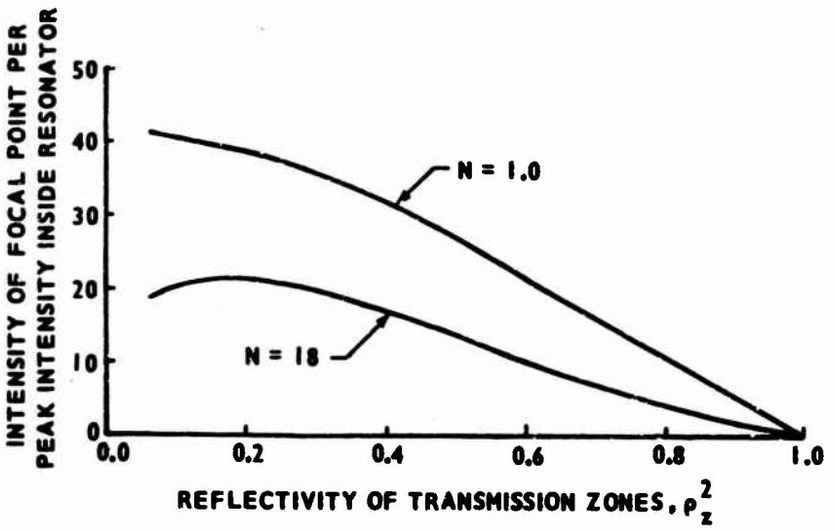

Figure 44. Intensity at Focal Point per Peak Intensity Inside Resonator as a Function of Power Reflectivity of Transmission Zones; Resonator Operating in TEM_{00} Mode; Output Mirror Zoned (13 half-period zones, 7 transmission)

considered, along with the effect caused by changing the number of transmission zones relative to the number of reflecting zones.

First the effect on the resonator caused by changing the number of zones will be considered. The resonator chosen to evaluate had a Fresnel number of one. This resonator was analyzed for the case of thirteen half-period zones on the output mirror and for the case of thirty zones on the output mirror. The zones on the output mirror were alternately completely transmitting and completely reflecting. The center zone for both output mirrors was a transmission zone. The pertinent results for the two cases are tabulated below.

The field distributions for these two resonators were similar; however, the field distribution for the thirteen-zone case was slightly more irregular than the distribution for the thirty-zone case. The differences in the losses

Table I. Characteristics of Resonators Having Different Numbers of Zones on the Output Mirror

	Thirteen Half-Period Zones	Thirty Half-Period Zones
Resonator mode	TEM_{00}	TEM_{00}
Double pass power loss	87%	85%
Double pass phase shift	34 deg	36 deg
Focal distance	M = 12.4	M = 29.7
Focused intensity per unit output power	86	490
Half power beam diameter in focal plane	$0.05\ a_p$	$0.02\ a_p$

are probably due to the fact that the thirteen-zone case has a greater transmission loss than does the thirty-zone case. The focal distances are given in terms of the parameter M; hence, the actual focal lengths are given by the relation

$$F = \left(\frac{a_p^2}{\lambda M}\right),$$

where F is the focal length, a_p is the radius of the output mirror, and λ is the wavelength. From this is obtained the expected result that if the number of zones on a mirror are increased, the focal length decreases. From the chapter on the zoned mirror, Chapter III, one would expect the ratio of the focal lengths to be inversely related to the ratio of the number of zones on the mirrors. Thus, if F_{13} represents the focal length for the thirteen-zone case and F_{30} represents the focal length for the thirty-zone case, one would expect

$$\frac{F_{13}}{F_{30}} = \left(\frac{30}{13}\right) \approx (2.3) \quad .$$

By using the data from the table, it is found that the actual value of (F_{13}/F_{30}) is about (2.4); thus, increasing the number of zones from thirteen to thirty decreased the focal distance by a factor of (2.4).

For the idealized systems considered in Chapter III, the ratio of the intensities per unit output power is equal to the square of the number of zones. Thus, if I_{13} and I_{30} are defined to be the focused intensities per unit output power for the thirteen- and thirty-zone cases respectively, one would expect that

$$\left(\frac{I_{30}}{I_{13}}\right) = \left(\frac{30}{13}\right)^2 \approx (5.3) \quad .$$

By using the data from the table, the actual value is found to be (5.7); thus, increasing the number of zones from thirteen to thirty increased the focused intensity per unit output power by a factor of (5.7).

The power passing through the main lobe in the focal plane does not change significantly when the numbers of zones is changed from thirteen to thirty. If the data tabulated above are used, the product of the intensity per unit output power and the half power area is found to be $0.054\pi a_p^2$ for the thirteen-zone case and $0.049\pi a_p^2$ for the thirty-zone case. This means that, although the peak intensity in the focal plane can be increased by increasing the number of zones, the power passing through the main lobe will not be increased. To obtain an increase of this main lobe power, the area of the output mirror must be increased.

The usual zoned resonator is constructed in such a way that all of the transmission zones have equal areas. However, since the TEM_{00} mode peaks near the center of the mirror and falls off toward the edges, the contributions

to the focused fields from the outer zones are less than the contributions from the central zones. Therefore, one or more of the outer zones could possibly be replaced with a reflection zone without the focused field being seriously degraded. This has practical significance in that the outer zones have the least width and therefore would be the most difficult to construct.

Consider now a resonator having a Fresnel number of one and an output mirror that is divided into thirteen half-period zones. The transmission zones have a power reflectivity of (0.36). This resonator has been analyzed for different numbers of transmission zones on the output mirror; the results of this analysis are presented below.

First it must be made clear what zones are present. The output mirror is divided into thirteen half-period zones, and normally seven of these zones would be transmission zones. The transmission zones are considered to be numbered from the center outward, and the higher numbered transmission zones are removed first. For example, if this resonator has three transmission zones, they are the three inner-most transmission zones. It bears repeating that when a transmission zone is removed it is assumed to be replaced with a reflection zone.

The relative amplitudes of the TEM_{00} mode distributions on the output mirror, for the cases of one and seven transmission zones, are given in Figure 45. The corresponding phase shifts are given in Figure 46. The fields, for the cases of two through six transmission zones, lie almost completely between the curves in Figures 45 and 46. Because the Fresnel number of the resonator is small and the transmission zone reflectivity is finite, the

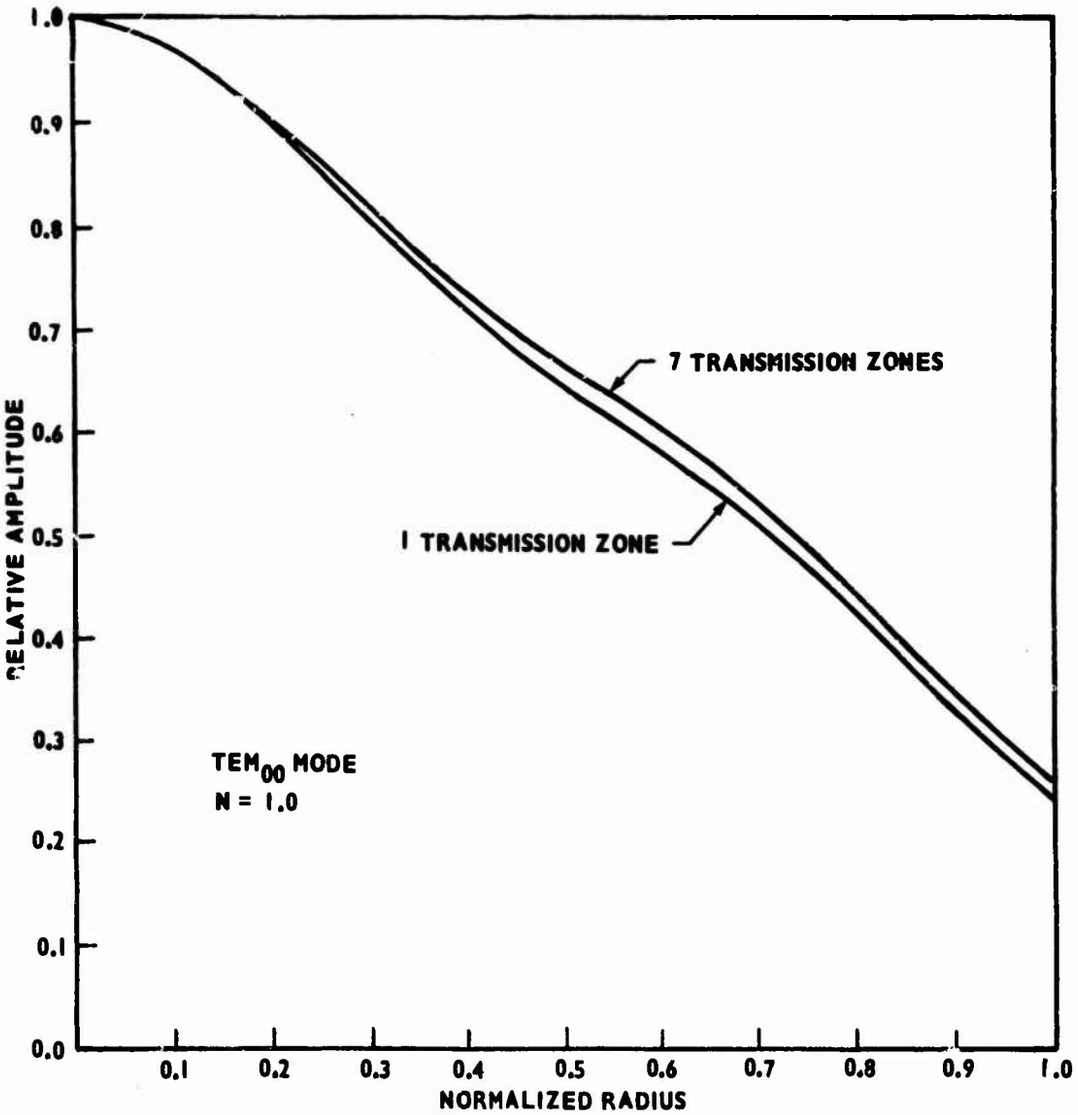

Figure 45. Relative Amplitude of the TEM_{00} Mode on the Output Mirror for Various Numbers of Transmission Zones; Resonator Fresnel Number = 1.0; Power Reflectivity of Transmission Zones = 0.36

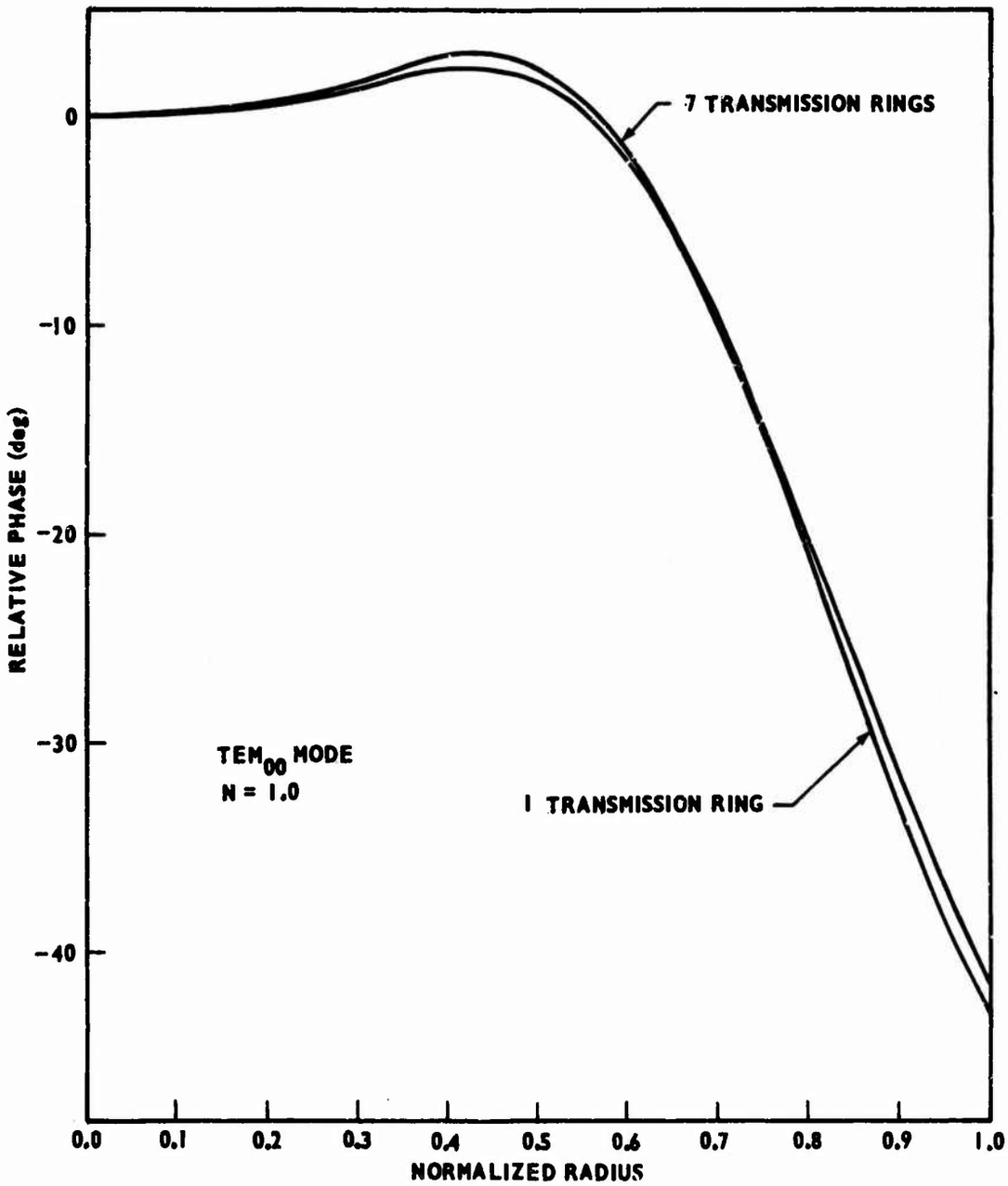

Figure 46. Relative Phase of the TEM_{00} Mode on the Output Mirror for Various Numbers of Transmission Zones; Resonator Fresnel Number = 1.0; Power Reflectivity of Transmission Zones = 0.36

presence or absence of the transmission zones have little effect on the resonator field distributions.

The double pass power loss as a function of the number of transmission zones is shown in Figure 47. Although the geometrical transmission loss increases linearly with the number of transmission zones, the double pass power loss does not. This is, of course, because less power is lost through the outer zones. The double pass phase shifts are given as a function of the number of transmission zones in Figure 48.

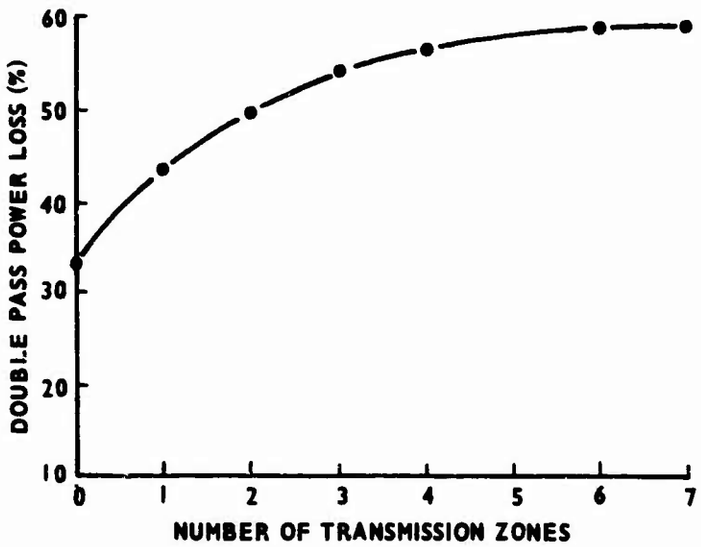

Figure 47. Double Pass Power Loss as a Function of Number of Transmission Zones; Resonator Operating in the TEM_{00} Mode; Resonator Fresnel Number = 1.0; Power Reflectivity of Transmission Zones = 0.36

The relative amplitude of the transmitted field along the resonator axis is given in Figure 49 for different numbers of transmission zones. As usual, the amplitudes of these axial fields are referenced to the source field having a maximum magnitude of unity; for example, the focused amplitude for the seven

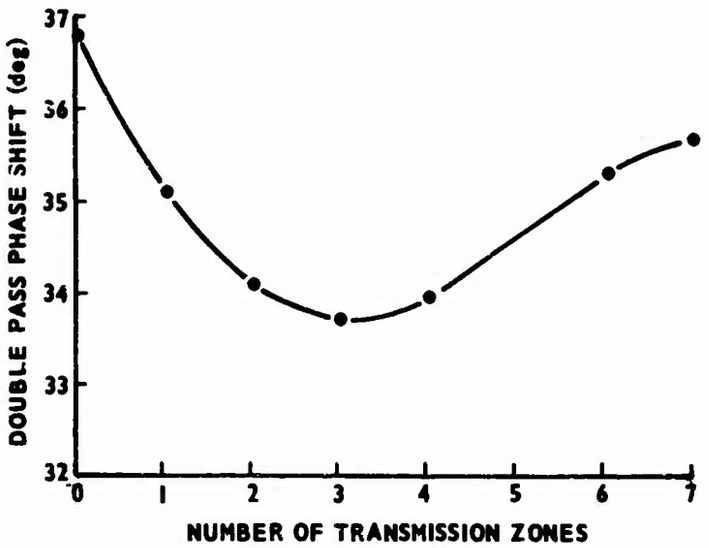

Figure 48. Double Pass Phase Shift as a Function of Number of Transmission Zones; Resonator Operating in the TEM_{00} Mode; Resonator Fresnel Number = 1.0; Power Reflectivity of Transmission Zones = 0.36

transmission zone case is about (7.3) times as large as the peak amplitude of the field immediately outside the resonator.

The case in which there is a single transmission zone on the output mirror can easily be evaluated for the limiting condition of large distances. First one notes that for a mirror having thirteen half-period zones that the central zone extends from the center of the mirror to a normalized radial distance of $(1/\sqrt{13})$. Then, by referring to Figures 45 and 46, it can be seen that the field on this center zone can be approximated by a uniform field having an amplitude of (0.9). This value represents an average value of the field across the center zone. On the resonator axis, at large distances from the output mirror, the source field will be viewed as having a uniform phase. Thus, the amplitude of the field f distance along the resonator axis, for f large, is given approximately by

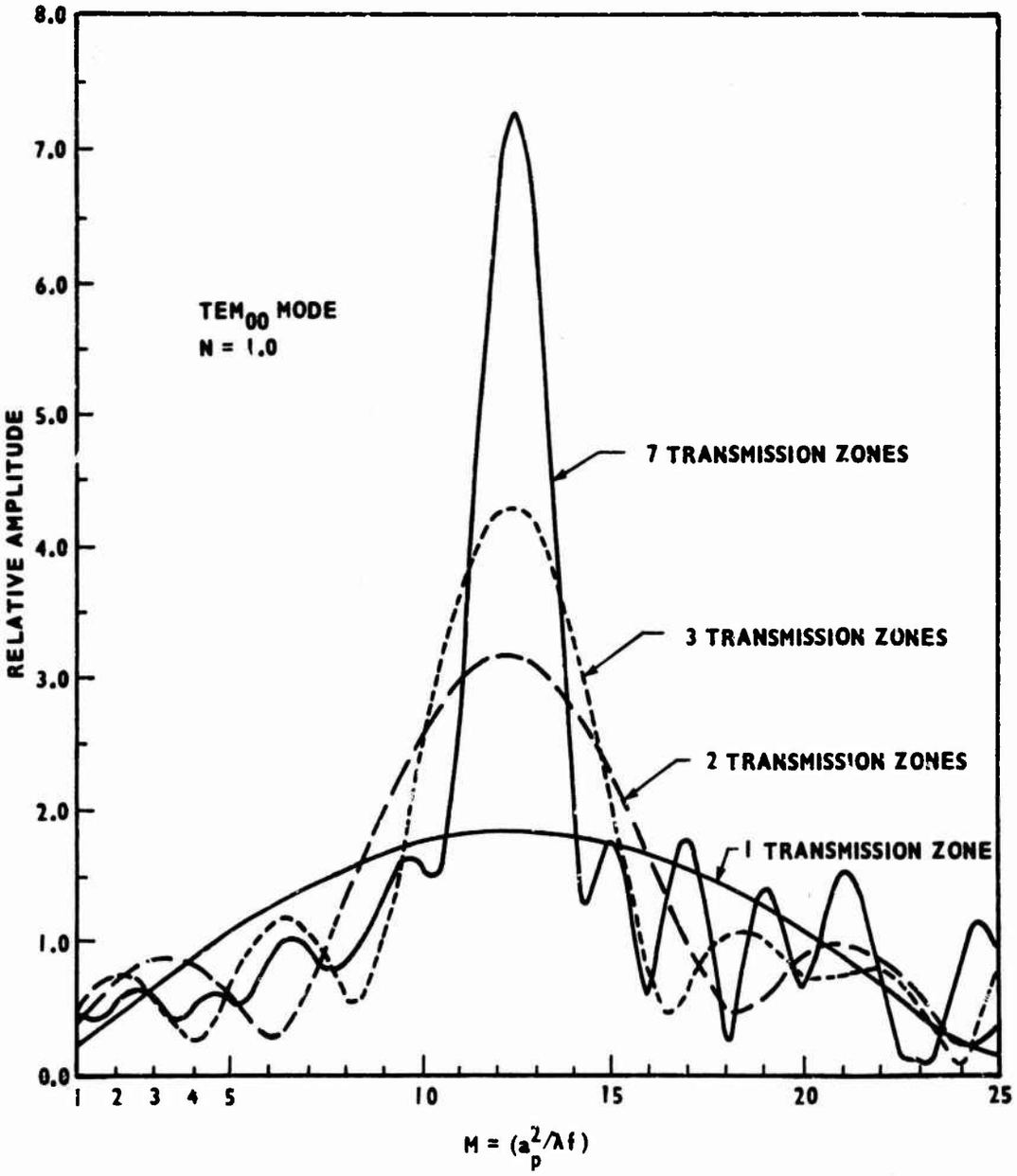

Figure 49. Relative Amplitude of Field Along Resonator Axis for Various Number of Transmission Zones; Resonator Fresnel Number = 1.0; Reflectivity of Transmission Zones = 0.36; Resonator Mode TEM_{0c}

$$E_f \approx \left[\frac{\text{(Amplitude of Source Field) (Area of Source)}}{\lambda f}\right] .$$

Since the normalized radius of the transmission zone is $(1/\sqrt{13})$, its actual radius is $\left(a_p/\sqrt{13}\right)$, where a_p is the radius of the output mirror. Therefore,

$$E_f \approx \left[\frac{(0.9)\left(\pi a_p^2/13\right)}{\lambda f}\right]$$

$$E_f \approx (0.22)\left(\frac{a_p^2}{\lambda f}\right) .$$

The term $\left(a_p^2/\lambda f\right)$ is given by M; therefore,

$$E_f \approx 0.22M .$$

For small values of M, which correspond to large values of f, this approximate value of E_f corresponds to the exact value given in Figure 49. As M increases, the axial field becomes less linear with M; this is because the source field can no longer be viewed as being uniform. In fact, viewed from the focal point, the phase of the source field varies by π radians from the center of the mirror to the edge of the first zone.

In Figure 50, the intensity at the focal point per unit output power is given as a function of the number of transmission zones. It is obvious that the focused intensity does not increase rapidly with increasing number of transmission zones. By removing the outer-most transmission zone, the intensity decreases by only a few percent.

A resonator having a larger Fresnel number was also analyzed to determine the effects caused by removing some of the outer transmission zones. This resonator had a Fresnel number of eighteen, and it was evaluated for operation in the TEM_{00} mode. The output mirror was divided into thirteen

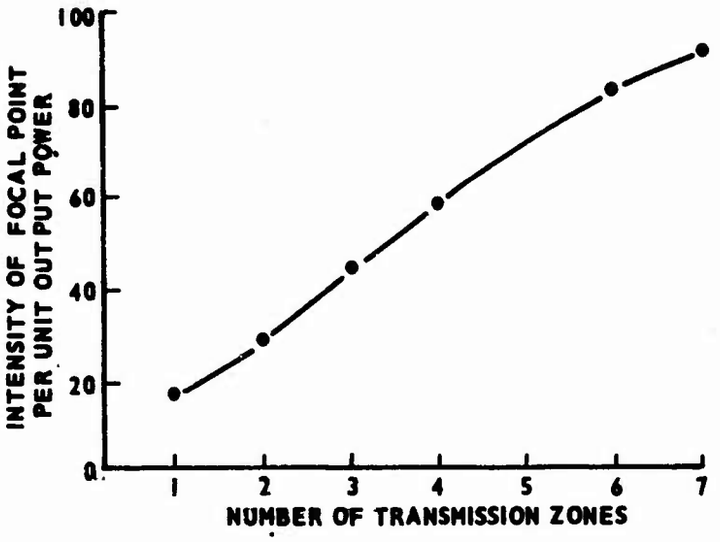

Figure 50. Intensity at Focal Point per Unit Output Power as a Function of Number of Transmission Zones; Resonator Operating in the TEM_{00} Mode, Resonator Fresnel Number = 1.0, Power Reflectivity of Transmission Zones = 0.36

half-period zones. The center zone was a transmission zone. The power reflectivity of the transmission zones was (0.500). Two cases were considered; in the first case all seven of the transmission zones were used, in the second case only the four inner-most transmission zones were used. It was found that by decreasing the number of transmission zones from seven to four that the focused intensity per unit output power decreased by only 22 percent. This small decrease is explained simply by considering the fields in resonators having large Fresnel numbers. These fields have small amplitudes and large phase variations at the outer edge of the mirror. The field for the resonator using all seven transmission zones has been presented previously, and it might be of interest to examine it again. The amplitude of this field on the output mirror is given in Figure 14 and its phase is given in Figure 15.

E. Transmission Zone Area

In the chapter on the zoned mirror (Chapter III) some general conclusions were made concerning the relationship between the focusing properties of the zoned mirror and the transmission zone area. In particular, it was concluded that to maximize the focused intensity, the area of each transmission zone should correspond to the area of a half-period zone. It was also concluded that to maximize the focused intensity per unit output power, the area of each transmission should correspond to about 74 percent of the area of a half-period zone.

In order to verify that these results could be extended to the zoned resonator, the external fields of a zoned resonator were determined for various transmission zone areas. The resonator evaluated had a Fresnel number of (0.1) and it was operated in the TEM_{00} mode. The output mirror had thirteen half-period zones, the transmission zone reflectivity was zero, and there were seven transmission zones on the mirror. Each transmission zone began at the beginning of every odd-numbered half-period zone. All portions of the zoned mirror not transmitting were completely reflecting.

The amplitudes of the transmitted axial fields are shown in Figure 51. These amplitudes are all normalized to the same basis. The transmission zone area for each case is indicated in the figure by a fraction of A; the term A represents the area of a half-period zone. The amplitude at the focal point is a maximum for the case in which each transmission zone area is equal to the area of a half-period zone; therefore, the intensity is also maximum.

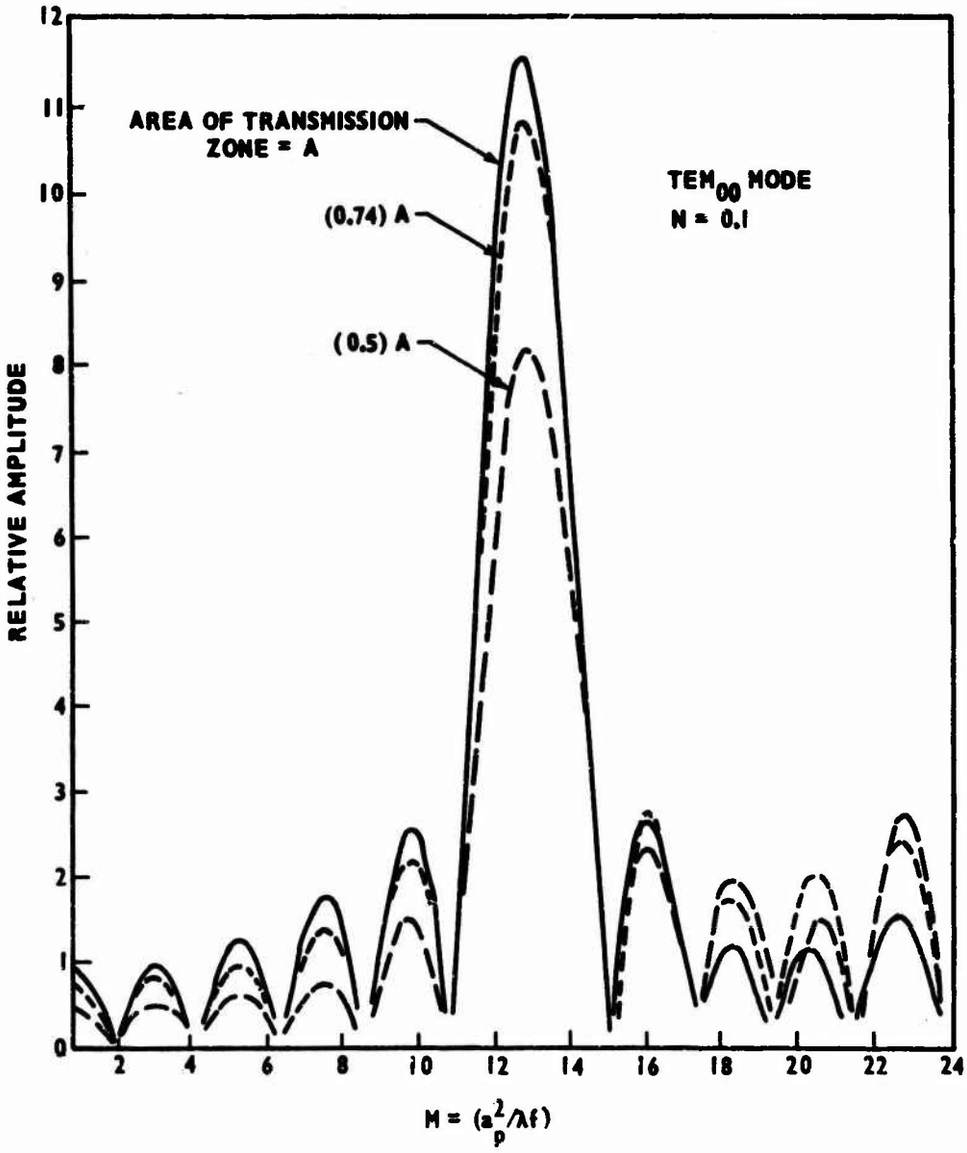

Figure 51. Relative Amplitude of Field Along Resonator Axis for Various Values of Transmission Zone Area; Resonator Mode TEM_{00}; A = Area of Half-Period Zone

The intensity per unit output power was also determined. Normalized to the same basis, the intensities per unit output power for these cases are as follows: For the transmission zone area equal to A the intensity per unit output power was (2.0), for the transmission zone area equal to (0.74) A the intensity per unit output power was (2.3), and for the transmission zone area equal to (0.5) A the intensity per unit output power was (2.0).

As was predicted in Chapter III, maximum focused intensity is achieved when each transmission zone area is equal to the area of a half-period zone, and maximum focused intensity per unit output power is achieved when each transmission zone area is equal to 74 percent of the area of a half-period zone.

For some resonators it may be desirable to reduce the area of the transmission zones for reasons other than maximizing the intensity per unit output power. For instance, decreasing the transmission zone area decreases the perturbation of the zoned mirror on the resonator mode structure. To demonstrate this, the lowest-order mode, for zero angular degeneracy, was determined for a resonator having the following characteristics: resonator Fresnel number equal to eighteen, thirteen, zones on the output mirror, and reflectivity of transmission zones equal to zero.

With each transmission zone having an area equal to the half-period zones, the amplitude of the field on the output mirror is that given in Figure 52. The double pass power loss is 72 percent, and the relative intensity at the focal point is (6.7).

For the next case the same resonator was used except the area of the first three transmission zones was reduced to one-half their original value.

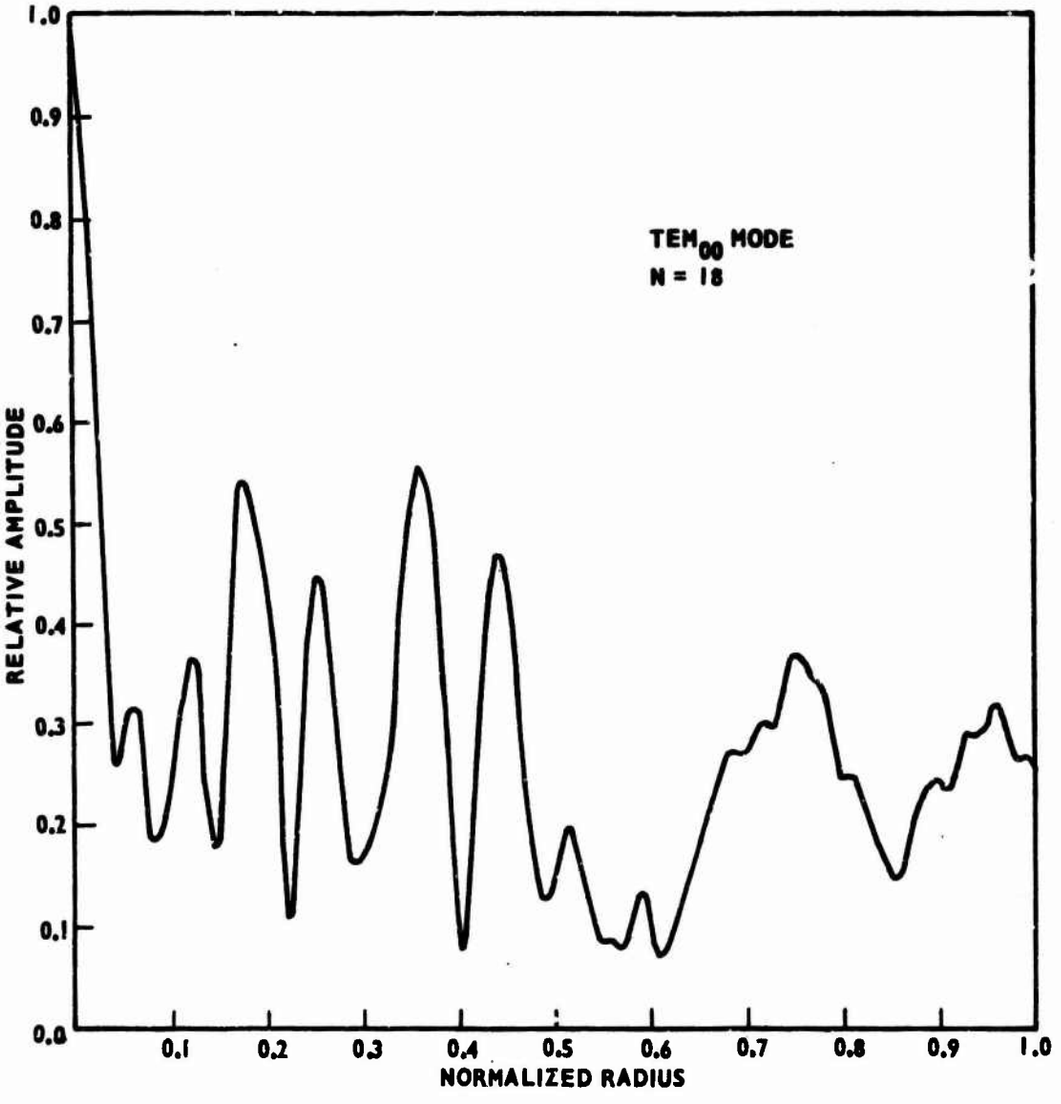

Figure 52. Relative Amplitude of the TEM_{00} Mode on the Output Mirror; Resonator Fresnel Number = 18, Output Mirror Zoned, Reflectivity of Transmission Zones = 0.000 (13 half-period zones, 7 transmission)

The amplitude of the field on the output mirror for this case is given in Figure 53. The double pass power loss for this case is 56 percent, and the relative intensity at the focal point is (7.4). Thus, one sees that reducing the areas of some of the transmission zones resulted in better focusing as well as a decreased power loss.

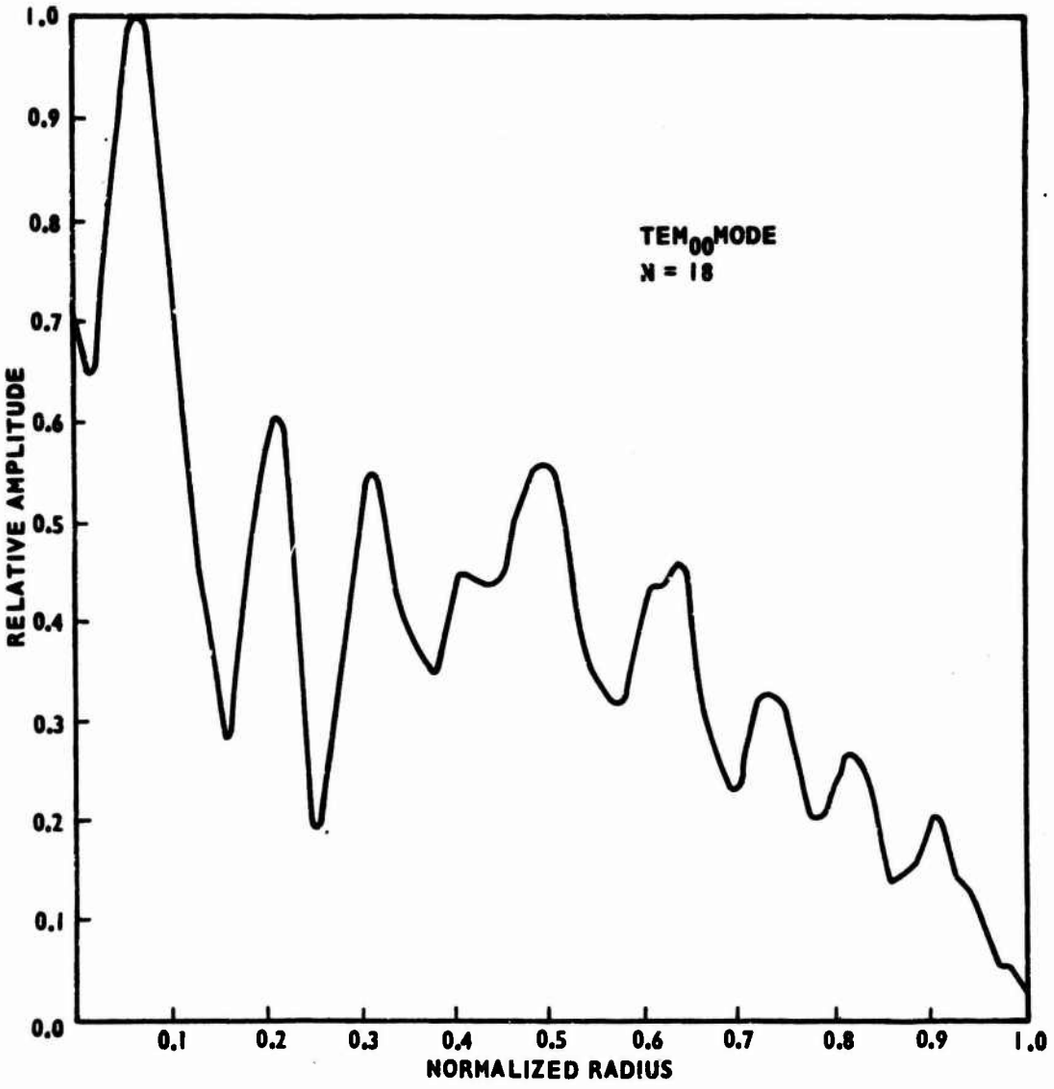

Figure 53. Relative Amplitude of the TEM_{00} Mode on the Output Mirror; Resonator Fresnel Number = 18, Output Mirror Zoned, Reflectivity of Transmission Zones = 0.000 (13 zones of mixed size, 7 transmission)

CHAPTER VII

SUMMARY AND CONCLUSIONS

The zoned mirror selectively reflects incident fields and it tends to distort reflected fields. These effects impart interesting, but limiting, characteristics to the zoned resonator. For instance, the resonator mode having the least loss is often of higher order than the usually dominant TEM_{00} mode. The zoned mirror produces the best focusing for the field configuration which most closely approximates a uniform wave; this, of course, would be the TEM_{00} mode. Thus, if the focusing properties of the zoned resonator were to be realized practically, mode control would be required.

For a zoned resonator in which the output mirror consisted of alternately totally reflecting and totally transmitting zones of equal area the following were observed: When the focal length of the zoned mirror was less than the resonator length, stable resonator modes were obtained and sharp focusing of the output was achieved. When the focal length of the resonator was approximately equal to the resonator length, stable resonator modes were not obtained. When the focal length of the resonator was greater than the resonator length, stable modes were obtained, but sharp focusing of the output could not be achieved. Because of this finding it was concluded that focusing at large distances was not feasible.

The mode structures of zoned resonators were more irregular than the corresponding mode structures of unzoned resonators. It was found that the mode structures of zoned resonators could be made more regular by increasing the reflectivity of the transmission zones and/or decreasing the area of the transmission zones. The irregularity of the resonator fields was more pronounced for resonators having large Fresnel numbers than for those having small Fresnel numbers.

For resonators having small Fresnel numbers, the maximum focused intensity was achieved when the reflectivity of the transmitting zones was zero and the areas of the transmitting and reflecting zones were equal. However, maximum focused intensity per unit output power was achieved when the area of the transmitting zones was reduced and the area of the reflecting zones correspondingly increased. The optimum transmission area was about 74 percent of the area of the half-period zones. Optimum values of reflectivity and area for resonators having large Fresnel numbers are almost impossible to predict; this is because the field structures for these resonators are strongly dependent on the characteristics of the zoned mirror. However, optimum values do exist, and for a given resonator configuration they could be found.

Some of the zoned resonators analyzed had focused intensities several times greater than the maximum intensity of the resonator field. However, the power passing through the main lobe in the focal plane was limited to about 20 percent of the total power transmitted out of the resonator.

BIBLIOGRAPHY

Boyd, G. D., and J. P. Gordon, "Confocal Multimode Resonator for Millimeter Through Optical Wavelength Masers" Bell System Technical Journal, Volume 40, pp. 489-508 (1961).

Boyd, G. D., and H. Kogelnik, "Generalized Confocal Resonator Theory" Bell System Technical Journal, Volume 41, pp. 1347-1369 (1962).

Fox, A. Gardner, and Tingye Li, "Computation of Optical Resonator Modes by the Method of Resonance Excitation" IEEE Journal of Quantum Electronics, Volume QE-4, pp. 460-465 (1968).

Fox, A. G., and Tingye Li, "Resonant Modes in a Maser Interferometer" Bell System Technical Journal, Volume 40, pp. 453-488 (1961).

Fox, A. G., and Tingye Li, "Modes in a Maser Interferometer with Curved and Tilted Mirrors" Proceedings of the IEEE, Volume 51, pp. 80-89 (1963).

Fox, A. G., and Tingye Li, "Effect of Gain Saturation on the Oscillating Modes of Optical Masers" IEEE Journal of Quantum Electronics, Volume QE-2, pp. 774-783 (1966).

Hildebrand, F. B., Methods of Applied Mathematics, Prentice-Hall, Inc., p. 427 (1952).

Jenkins, Francis A., and Harvey E. White, Fundamentals of Optics, McGraw-Hill Book Company, Inc., p. 360 (1957).

Johnston, W. D., Jr., Tingye Li, and P. W. Smith, Journal of Quantum Electronics, Volume QE-4, pp. 469-471 (1968).

Kogelnik, H., and W. W. Rigrod, "Visual Display of Isolated Optical-Resonator Modes" Proceedings of the IRE, Volume 50, p. 220 (1962).

Li, Tingye, "Diffraction Loss and Selection of Modes in Maser Resonators with Circular Mirrors," Bell System Technical Journal, Volume 44, pp. 917-932 (1965).

Li, Tingye, and J. G. Skinner, "Oscillating Modes in Ruby Lasers with Nonuniform Energy Distributions" Journal of Applied Physics, Volume 36, pp. 2595-2596 (1965).

Li, Tingye, and H. Zucker, "Modes of a Fabry-Perot Laser Resonator with Output Coupling Apertures" Journal of the Optical Society of America, Volume 57, pp. 984-986 (1967).

McNice, Garner T., and Vernon E. Derr, "Analysis of the Cylindrical Confocal Laser Resonator Having a Single Circular Coupling Aperture" IEEE Journal of Quantum Electronics, Volume QE-5, pp. 569-575 (1969).

Rosenberger, D., "Mode Spectrum in the He-Ne Maser" Quantum Electronics — Paris 1963 Conference, by P. Grivet and N. Bloembergen, Volume 2, Columbia University Press, pp. 1301-1304 (1964).

Scarborough, J. B., Numerical Mathematical Analysis, Fourth Edition, The Johns Hopkins Press, pp. 178-179 (1958).

Silver, Samuel, Microwave Antenna Theory and Design, McGraw-Hill Book Company, Inc., New York, p. 167 (1949).

Stratton, J. A., Electromagnetic Theory, McGraw-Hill Book Company, Inc., New York, p. 373 (1941).

Statz, H., and C. L. Tang, "Problem of Mode Deformation in Optical Resonators" Journal of Applied Physics, Volume 36, pp. 1816-1819 (1965).

Wells, W. H., IEEE Journal of Quantum Electronics, Volume QE-2, pp. 94-102 (1966).

UNCLASSIFIED

Security Classification

DOCUMENT CONTROL DATA - R & D

(Security classification of title, body of abstract and indexing annotation must be entered when the overall report is classified)

1. ORIGINATING ACTIVITY (Corporate author) Physical Sciences Laboratory Research and Engineering Directorate U.S. Army Missile Command Redstone Arsenal, Alabama 35809	2a. REPORT SECURITY CLASSIFICATION 2b. GROUP

3. REPORT TITLE

ANALYSIS OF A CYLINDRICAL LASER RESONATOR HAVING A ZONED OUTPUT MIRROR

4. DESCRIPTIVE NOTES (Type of report and inclusive dates)

5. AUTHOR(S) (First name, middle initial, last name)

George A. Emmons

6. REPORT DATE	7a. TOTAL NO. OF PAGES	7b. NO. OF REFS
16 September 1970	169	

8a. CONTRACT OR GRANT NO.	9a. ORIGINATOR'S REPORT NUMBER(S)
b. PROJECT NO. (DA) 1T262303A308	RR-TR-70-22
c. AMC Management Structure Code No. 522C.11.47300 d.	9b. OTHER REPORT NO(S) (Any other numbers that may be assigned this report) AD_____

10. DISTRIBUTION STATEMENT

This document has been approved for public release and sale; its distribution is unlimited.

11. SUPPLEMENTARY NOTES	12. SPONSORING MILITARY ACTIVITY
	Same as No. 1

13. ABSTRACT

A theoretical analysis was performed on a zoned resonator to determine whether both resonator feedback and a focused output could be achieved with a single optical element. It was found that under certain conditions that well-defined modes do exist and that a focused output could be obtained.

This resonator was formed by two parallel mirrors (circular, plane, and equal sized) symmetrically placed about a common axis. One mirror had a uniform reflectivity of unity. The other mirror was zoned. It consisted of alternately transmitting and totally reflecting concentric zones. The reflecting zones provided the resonator feedback and the transmitting zones provided the output coupling. The transmission zones were arranged in a manner similar to the transmission zones on a Freznel zone plate. Thus, the zoned mirror tended to focus the field coupled out of the resonator.

For a zoned resonator in which the output mirror consisted of alternately totally reflecting and totally transmitting zones of equal area the following results were obtained:

1) When the focal length of the zoned mirror was less than the resonator length, stable resonator modes were obtained and sharp focusing of the output was achieved.

2) When the focal length was approximately equal to the resonator length, stable resonator modes were not obtained.

3) When the focal length was greater than the resonator length, stable modes were obtained but sharp focusing of the output could not be achieved. (Continued)

DD FORM 1 NOV 68 1473 REPLACES DD FORM 1473, 1 JAN 64, WHICH IS OBSOLETE FOR ARMY USE.

UNCLASSIFIED

Security Classification

14. KEY WORDS	LINK A		LINK B		LINK C	
	ROLE	WT	ROLE	WT	ROLE	WT
Fresnel numbers						
Mirrors						
Focal length						
Resonator						

ABSTRACT (Concluded)

Based on these findings it was concluded that a focused output was possible bu. that focusing at large distances was not feasible.

The mode structures of zoned resonators were more irregular than the corresponding mode structures of unzoned resonators. It was found that the mode structures could be made more regular by increasing the reflectivity of the transmission zones and/or decreasing the area of these zones. The irregularity of these fields was more pronounced for resonators having large Fresnel numbers than for those having small Fresnel numbers.

For resonators having small Fresnel numbers, the maximum focused intensity was achieved when the reflectivity of the transmitting zones was zero and the transmitting and reflecting zones were equal in area. However, maximum focused intensity per unit output power was achieved when the area of the transmitting zones was reduced and the area of the reflection zones correspondingly increased. The optimum transmission area was about 74 percent of the area of the half-period zones. Because their field structures are strongly dependent on the characteristics of the zoned mirror, the optimum values of reflectivity and area for resonators having large Fresnel numbers are almost impossible to predict. However, optimum values do exist, and for a given configuration they could be found.

Some of the zoned resonators analyzed had focused intensities several times greater than the maximum intensity of the resonator field. However, the power passing through the main lobe in the focal plane was only about 20 percent of the total output power.